



UNIVERSITA' DEGLI STUDI DI PADOVA

DIPARTIMENTO DI SCIENZE CHIMICHE

INSTITUT FÜR NATURWISSENSCHAFTEN UN TECHNOLOGIE IN DER KUNST

CORSO DI LAUREA MAGISTRALE IN CHIMICA

TESI DI LAUREA MAGISTRALE

Blended Thitsiol/Urushiol Asian laquers in Cultural Heritage: curing, ageing, and photo-aging study by THM-Py-GC/MS and other techniques

Relatore: Prof. Zoleo Alfonso

Correlatore: Dr. Pintus Valentina, MSc., BSc.

Correlatore: Prof. Nodari Luca

Controrelatore: Prof. Di Marco Valerio

LAUREANDO: Cozzani Carlotta

ANNO ACCADEMICO 2021/2022

Tables of contents

ABSTRACT	III
RIASSUNTO	IV
ZUSAMMENFASSUNG	V
List of abbreviations	VI
Acknowledgments	VII
1. INTRODUCTION	1
2. ASIAN LACQUERS	4
2.1 <i>Thitsiol</i>	4
2.1.1 Drying mechanism	5
2.1.2 Ageing mechanism	7
2.2 <i>Urushiol</i>	9
2.2.1 Drying mechanism	11
2.2.2 Ageing mechanism	13
2.3 Blend of <i>urushiol</i> and <i>thitsiol</i>	13
2.3.1 Drying mechanisms	14
2.3.2 Aging Mechanism	16
3.1 Digital Microscopy	17
3.2 Colorimetry	18
3.3 Fourier Transform Infrared Spectroscopy (FTIR)	22
3.3.1 Transmission mode	24
3.3.2 ATR mode	25
3.4 Thermally assisted Hydrolysis and Methylation of Pyrolysis Gas Chromatography / Mass Spectrometry (THM-Py-GC/MS)	26
3.4.1 Thermally assisted Hydrolysis and Methylation (THM) and Pyrolysis (Py)	27

3.4.2 Gas Chromatography (GC)	29
3.4.3 Mass Spectrometry (MS)	33
3.5 Accelerated artificial daylight aging	36
4. EXPERIMENTAL PART	39
4.1 Mock-ups preparation	39
4.2 Drying procedure	41
4.3 Instruments and parameters	41
5. RESULTS AND DISCUSSION	47
5.1 <i>Thitsiol</i>	47
5.1.1 Digital Microscopy	47
5.1.2 Colorimetry	49
5.1.3 FTIR	53
5.1.4 THM-Py-GC/MS	61
5.2 <i>Urushiol</i>	76
5.2.1 Digital Microscopy	76
5.2.2 Colorimetry	77
5.2.3 FTIR	79
5.2.4 THM-Py-GC/MS	84
5.3 Blend of <i>urushiol</i> and <i>thitsiol</i>	91
5.3.1 Digital Microscopy	91
5.3.2 Colorimetry	94
5.3.3 FTIR	98
5.3.4 THM-Py-GC/MS	105
6. CONCLUSION AND OUTLOOK	120
7. REFERENCES	Errore. Il segnalibro non è definito.

ABSTRACT

Nowadays Western Museums host a variety of precious collection of Asian Lacquers dated since the XV century, exported from Eastern Asia to a West fascinated by exotic objects and furniture. The focus of this research is a blend of two Asian Lacquer types, thitsi and urushi, very common in the West collections due to its cheap price. This special material has been studied for two years, starting from its curing process to the final artificial photo-aging. In order to acquire a deep knowledge of the chemical structure and its degradation process, both chemical and physical approach have been adopted. THM-Py-GC/MS has been used to determine the structures of the blend in comparison with the two pure lacquers, thitsi and urushi, through their typical markers, such as alkyl benzenes and aliphatic hydrocarbons, and oxidation products, such as substituted dimethoxybenzenes and mазzeic acid, and their oxidative reactions after UV exposure. THM-Py-GC/MS was joined by both ATR- and Transmission FTIR techniques, which were used to monitor the changes in the principal and characteristic functional groups of the lacquers, in a destructive (THM-Py-GC/MS) and non-destructive (FTIR) way. In conclusion, these data have been used to explain the images obtained with Digital Microscope during the whole research, in which it is clearly possible to see micro-cracks on the surface of thitsi and the blended lacquer but not of urushi, providing an overview of what kind of reactions could happen during the time, their mechanisms, why they happen and how to prevent them.

RIASSUNTO

Al giorno d'oggi i musei occidentali ospitano una varietà di preziose collezioni di lacche asiatiche datate fin dal XV secolo, importate dall'Oriente verso un Occidente affascinato da oggetti e mobili esotici. Il fulcro di questa ricerca è una miscela di due tipi di lacche asiatiche, thitsi e urushi, molto comune nelle collezioni occidentali dato il suo prezzo economico. Questo materiale molto speciale è stato studiato per due anni, partendo dal processo di asciugatura fino all'invecchiamento accelerato. Per acquisire una profonda conoscenza della struttura chimica e il suo processo di degradazione, è stato adottato sia un approccio chimico sia uno fisico. La THM-Py-GC/MS è stata usata per determinare la struttura della miscela paragonata alle due lacche pure, thitsi e urushi, attraverso i loro marker tipici, come gli alchil benzeni e gli idrocarburi alifatici, e prodotti di ossidazione, come i dimetossi benzeni sostituiti e l'acido mazzeco, e le loro reazioni di ossidazione quando sottoposti a luce UV. La THM-Py-GC/MS è stata affiancata da tecnica FTIR, sia in ATR che in Trasmissione, impiegate per monitorare i cambiamenti dei principali e caratteristici gruppi funzionali delle lacche, per via distruttiva (THM-Py-GC/MS) e non distruttiva (FTIR). Infine, questi dati sono stati utilizzati per spiegare le immagini ottenute con Microscopio Digitale durante l'intera ricerca, in cui è chiaramente possibile notare microfratture sulla superficie del thitsi e della miscela ma non su quella dell'urushi, fornendo una spiegazione di quali reazioni potrebbero avvenire nel corso del tempo, i loro meccanismi, perché avvengono e come prevenirli.

ZUSAMMENFASSUNG

Heutzutage beherbergen westliche Museen eine Vielzahl wertvoller Sammlungen asiatischer Lacke aus dem 15. Jahrhundert, die aus Ostasien in einen Westen exportiert wurden, der von exotischen Objekten und Möbeln fasziniert war. Der Schwerpunkt dieser Arbeit liegt auf einer Mischung aus zwei asiatischen Lackarten, Thitsi und Urushi, die aufgrund ihres günstigen Preises in den westlichen Kollektionen sehr verbreitet waren. Dieses spezielle Material wurde zwei Jahre lang von seinem Aushärtungsprozess bis zur endgültigen künstlichen Lichtalterung untersucht. Um ein tiefes Wissen über die chemische Struktur und ihren Abbauprozess zu erlangen, wurden sowohl chemische als auch physikalische Ansätze gewählt. Mittels THM-Py-GC/MS wurden die Strukturen des Blends im Vergleich zu den beiden reinen Lacken Thitsi und Urushi anhand ihrer typischen Marker wie Alkylbenzole und aliphatische Kohlenwasserstoffe sowie Oxidationsprodukte wie substituierte Dimethoxybenzole und Mazzeic bestimmt Säure und ihre oxidativen Reaktionen nach UV-Exposition. THM-Py-GC/MS wurde durch ATR- und Transmissions-FTIR-Techniken ergänzt, um die Änderungen in den wichtigsten und charakteristischen funktionellen Gruppen der Lacke auf destruktive (THM-Py-GC/MS) und nicht-destruktive (FTIR) Weise zu überwachen. Zusammenfassend wurden diese Daten verwendet, um die Bilder zu erklären, die während der gesamten Untersuchung mit dem Digitalmikroskop erhalten wurden, in denen es deutlich möglich war, Mikrorisse auf der Oberfläche von Thitsi und der Mischung von beiden Lacken, aber nicht von Urushi zu sehen, was einen Überblick darüber gibt, was Art von Reaktionen, die während der Zeit auftreten können, ihre Mechanismen, warum sie auftreten und wie sie verhindert werden können.

List of Abbreviation

ATR-FTIR Attenuated Total Reflection Fourier Transform Infrared Spectroscopy

DG Digital Microscopy

EIC Extracted Ion Chromatogram

FTIR Fourier Transform Infrared Spectroscopy

HMDS Hexamethyldisilazane

GC Gas Chromatography

MS Mass Spectroscopy

Py Pyrolysis

Py-GC/MS Pyrolysis Gas Chromatography/Mass Spectrometry

PHySICAL Profound study of Hydrous and Solvent Interactions in Cleaning Asian Lacquer

RH Relative Humidity

RT Retention Time

TIC Total Ion Chromatogram

THM Thermally assisted Hydrolysis and Methylation

TMAH Tetramethyl Ammonium Hydroxyde

Trans-FTIR Transmission Fourier Transform Infrared Spectroscopy

Acknowledgments

Above all I would like to thank o. Univ. Prof. Dr. Katja Sterflinger, Dipl. Biol., head of the Institute for Natural Science and Technology for Art of the Academy of Fine Arts (Vienna) for the great opportunity to spend my Erasmus+ program in this amazing research lab.

With immense gratitude and devotion, I would like to thank my supervisor, Dr. Valentina Pintus, MSc., BSc. who gave me all her knowledge, her enthusiasm, and her time during the last nine months. I found a mentor but also a friend, thank you.

And thanks to my italian supervisor, Professor Luca Nodari, who kindly followed me during this very intense period of my life.

I thank all the people who made me feel at home in this beautiful city, for every emergency, for every hug when I felt alone, for hosting me when I was homeless and for gave me the opportunity to study and work at the same time.

A great thanks to Manuela Prinetto and Francesco Mizzoni, my dear English professors during high school. You gave me the opportunity to experience and fall in love with theatre. You gave me the best time of my life.

Thanks to all my friend, the new ones but I particular the old ones. Our friendship is the most precious gift I could receive from life. In the good moments and in the bad ones you were there, even if at thousands of kilometers far away. Laura, Marco, Carolina, Greta, Michela, Caterina, Roberto, Nicholas, I love you so much.

Thanks to my entire family, my grandmother Silvana, my uncles and aunts, and my cousins. Thank to you I have happy memories that make me feel better whenever I need.

A special thanks to my brother, Jacopo. Even if we do not have the same blood something more important makes us brother. You are the best part of me, when without you I just feel lost and incomplete.

And then, of course, thanks to my amazing parents. You know, you know. If now I am here is because you gave me hope, love, courage every day of my life. I have been through a lot of bad times in my life, and you helped me to rise again, to learn from them, and to smile because the life is incredibly beautiful. Vi amo da morire mamma e papà.

Finally, with tears in my eyes, I would like to thank a very special person I lost too soon. La mia nonnina. I lost her when I could not realize how much important she was for me. But now I know. Nonna, you gave me everything, your love is always with me, in every moment. I wish you could be here, to see the woman I became. You would be very proud. I really hope to meet you again one day.

1. INTRODUCTION

Asian lacquer represents an important historical material used in East and Southeast Asia for thousands of years as a beautiful and highly durable coating because of its flawless finish and light reflecting qualities. Nowadays, numerous and important western museums host a large number of precious Asian lacquered objects originating from numerous importations facilitated by the opening of maritime roads between Europe and East Asia since the end of the fifteenth century [1]. These were often made by using a blend of the less expensive thitsi-type lacquer (often called Burmese lacquer) and urushi-type one (originated from Japan and China exclusively) due to the Dutch demand for Japanese lacquer at lower costs [2, 3].

Degradation phenomena of Asian lacquers such as dull and faded surface and increase in brittleness are urgent issues requiring the attention of chemists and conservation scientists in close cooperation to restorers, conservators, museum collectors, and art historians [4, 5]. To preserve Asian lacquer-based works of art in good conditions different aspects such as their chemical composition as well as their chemical and physical stability have to be considered. These important and critical topics require a lot of information, which are based on state-of-the-art chemical and physical analyses. The scientific analyses of works of art are of fundamental importance for the better understanding of their state of preservation, their chemical composition and how to prevent their degradation when exposed to various atmospheric conditions. A multi-analytical approach based on the synergetic use of several techniques is generally the preferred way for having as much as more information as possible about the chemical and physical stability on Asian lacquers. Non-invasive (sampling not required from the object) and invasive methods may be combined for this purpose.

Despite the numerous scientific studies done on Asian lacquers so far, the curing, ageing, and degradation processes of Asian lacquers still needs to be explored for adopting optimal conservation-decisions making [4, 5, 6]. Particularly, the stability of the urushi/thitsi blend have not been object of any study so far, regardless its high importance in Cultural heritage. Only few studies mainly dealt with the understanding of degradation processes related to either Asian lacquers-based models or objects-based samples [1, 7, 8]. The importance of studying and preserving such amazing and historical material was the focus of Professor Kumanotani's research during the second half of the 20th century [9, 10, 11]. He has been the pioneer of lacquer chemistry, followed by several research studies and projects all around the world [9].

The Getty Conservative Institute (GCI) (Los Angeles, U.S.A.) has been actively involved in the last decade in the characterisation of Asian and European lacquers by organizing international workshops and publishing books and articles [12, 13, 14, 15, 2]. Moreover, the PHySICAL (Profound study of Hydrous and Solvent Interactions in Cleaning Asian Lacquer) project [16] lead by KIK-IRPA, University of Amsterdam, Ghent University, from 2017 focuses on the scientific study of the interactions of organic solvents with lacquer surfaces to formulate “best practices” for cleaning Asian lacquers. Numerous analytical techniques have been used for determining the chemical composition of Asian lacquers. Among those, the most well-established method for the identification and characterization of Asian lacquers is the Thermally assisted Hydrolysis and Methylation of Gas Chromatography coupled with Mass Spectrometry (THM-GC/MS) as invasive technique, which require only a tiny sample in the order of micrograms. On the other hand, Fourier Transform Infrared Spectroscopy (FTIR) is useful for studying changes in the Asian lacquers at the molecular level and in a non-invasive way. Other information about the stability of Asian lacquers have been obtained for examples by colour measurements for detecting colour changes on the material surface and by optical microscopy for the visualization of micro-cracks possibly formed during ageing.

This works aims to fill the big gap about the chemistry of thitsi and urushi blended lacquer. In order to achieve this goal both lacquer types, pure state and blended, have been characterized and monitored for different steps, starting from the drying process to the final photoaging and degradation mechanisms. Different techniques have been applied, each one chosen to better understand a different aspect of the material. First of all, it has been studied the physical changes of the lacquers through non-invasive approach, using techniques such as the microscopic technique and the colorimetry. Then, to better understand the chemical changes and how they are correlated to the physical ones, a micro-invasive technique such as Infrared Spectroscopy, has been used followed by an invasive technique such as Pyrolysis Gas Chromatography/ Mass Spectrometry. A complete overview of the three lacquer types has been obtained which, together with literature works and data, has led to the characterization of markers typical for fresh and aged blend of urushi and thitsi from a qualitative point of view to determine, in a final step, which kind of lacquer could be present in a unknow sample.

This research has been done at the Institute for Natural Sciences and Technology in the Arts at the Academy of Fine Arts Vienna during 8-months period of ERAMUS+ program. During this period an experimental work, strictly connected with a literature

research work, has been performed and several instruments and analytical techniques have been used with the idea to investigate every single aspect of the final goal. The result is a detail explanation of the physical and chemical behaviour of Asian lacquer and a blend of them through a long time of drying, curing, natural and artificial photoaging.

2. ASIAN LACQUERS

Asian lacquer is a sap harvested from three main tree species from *Anacardiaceae* family: *Toxicodendron (Rhus) vernicifluum*, *Gluta (Melanorrhoea) usitata*, and *Toxicodendron (Rhus) succedaneum* [17]. Each of them grows in a specific area of East Asia and their saps are named according to the production region: urushi from Japan, China and Korea, thitsi from Thailand and Myanmar, and laccol from Vietnam, respectively [17].

Asian lacquer sap, freshly collected, is a water in oil (w/o) emulsion. The water phase consists of a mixture of hydrophilic polysaccharides (5–6%), with branched structures, which increase the durability of the lacquer film once cured; enzymes (1%), like laccase, responsible for the polymerization. The oily fraction is made of 3- and 4-substituted catechol (60–70%), with saturated and unsaturated linear aliphatic side chains (C15 and C17); catechol derivatives with an ω -phenylalkyl chain of 10 or 12 carbon atoms only in the case of *thitsiol*; a small proportion of phenol (3%). The sap also contains water insoluble glycoproteins (2–3%). Both polysaccharide and glycoprotein constituents of the sap are thought to play an important role in the structure of the lacquer matrix [1, 7].

2.1 *Thitsiol*



Figure 1. Bamboo basketwork covered with *thitsi* lacquer in red, yellow, and black layers (XIX century) [18].

Thitsiol (Figure 1, [18]) is the main component of the thitsi sap. It is a mixture of catechols substituted in 3- and 4- position by both C15 and C17 side chains, 3-substituted resorcinols, and 3-substituted phenols (Figure 2, [19]). The three main structures, with an abundance respectively of 36%, 20,5 % and 19,7 %, are the 3-(12-phenyldodecyl) catechol 3-(8Z,11Z-heptadecenyl) catechol, and 4-(8Z,11Z-heptadecenyl) catechol [9].

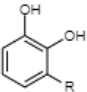
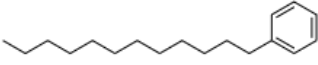

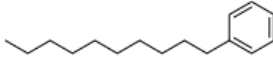

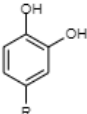

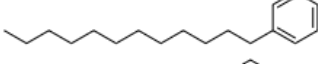
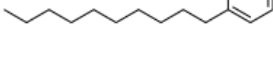


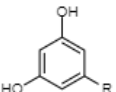
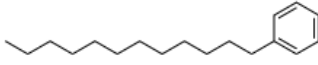
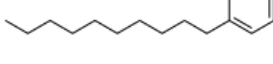
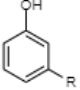
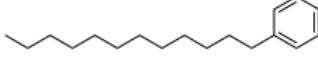
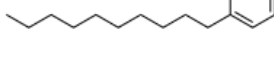
		n°C	MW	%	
a)					} 67,5 %
		C12	354	36	
		C17	344	19,7	
		C10	326	7,9	
		C15	320	3,9	
b)					} 26,6 %
		C17	344	20,5	
		C12	354	3,6	
		C10	326	1,1	
		C17	342	0,7	
		C15	320	0,7	
c)					} 2,8 %
		C12	354	2,1	
		C10	326	0,7	
d)					
		C12	338		
		C10	310	1,4	

Figure 2. Chemical composition of thitsiol after Le Hô [19].

2.1.1 Drying mechanism

The drying process of Asian lacquers is an enzyme-driven polymerization occurring in the presence of high relative humidity (rH %) and moderate temperature (T°C). The

optimum condition for Thailand, Cambodia, and Myanmar lacquer (*thitsi*) is a rH of 90 % and a T °C near to 40 °C [20]. Due to the presence of alkyl benzyl side chains, *thitsi* has a slower drying time than urushi.

As soon as the lacquer sap is tapped from the tree and it comes into contact with the oxygen in the air, the laccase-enzymatic reaction takes place (Figure 3). In this step, laccase oxidizes *thitsiol* to form a radical structure (Figure 3a), which consequentially is converted into semiquinone radicals (Figure 3b).

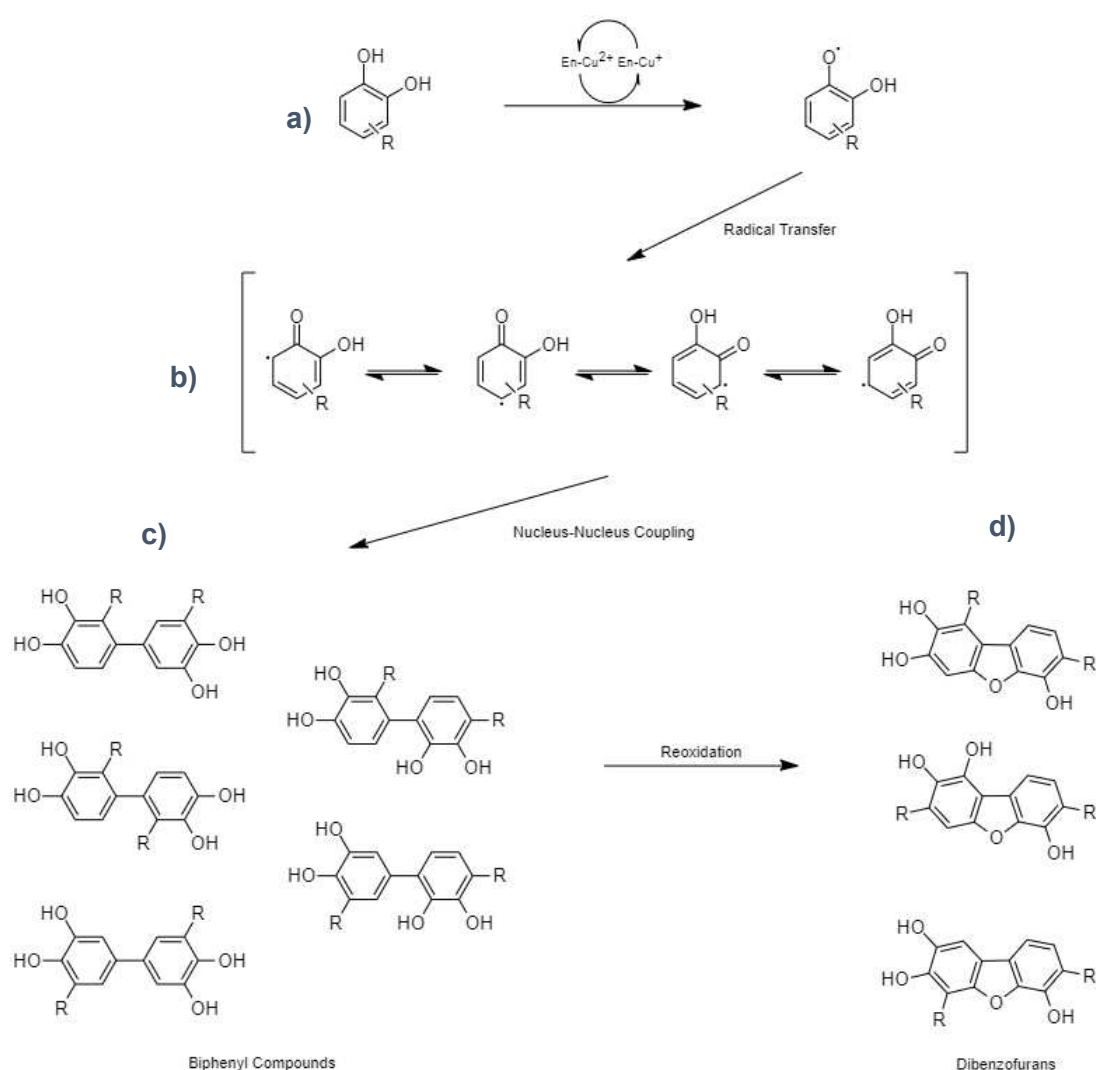


Figure 3. Laccase polymerization of catechol and nucleus-nucleus coupling.

At this point, the following reaction mechanism occurs: the nucleus-nucleus coupling, which leads to the formation of dimers of the biphenyl types (Figure 3c). Successively, the laccase-catalysed oxidation converts some of those biphenyl compounds into

dibenzofurans (Figure 3d) [9, 21, 22]. The presence of a bulky side chain in this molecular composition does not allow a coupling nucleus-side chain. It has been speculated that this could be the reason why the colour of this is blacker than the colour of urushi which follows in his reaction mechanism both nucleus-nucleus coupling and nucleus-side chain coupling [9].

Once the lacquer film is dry, a densely packed grain structure, called the core-shell structure, is present (see paragraph 2.2.2). Each spherical grain (1 to 10 mm in diameter) is composed of a thin shell of polysaccharides (3 to 4 nm of thickness) and glycoproteins as adhesive surrounding the polymerized catechol.

Such a core-shell structure is believed to be responsible for the durability of the lacquer film as long as the polysaccharides shell acts as a high barrier against oxygen [1].

2.1.2 Ageing mechanism

The aging process is a sum of various mechanisms, due, first of all, to a photo-oxidation mechanism. The light exposure causes a damage of the closely packed

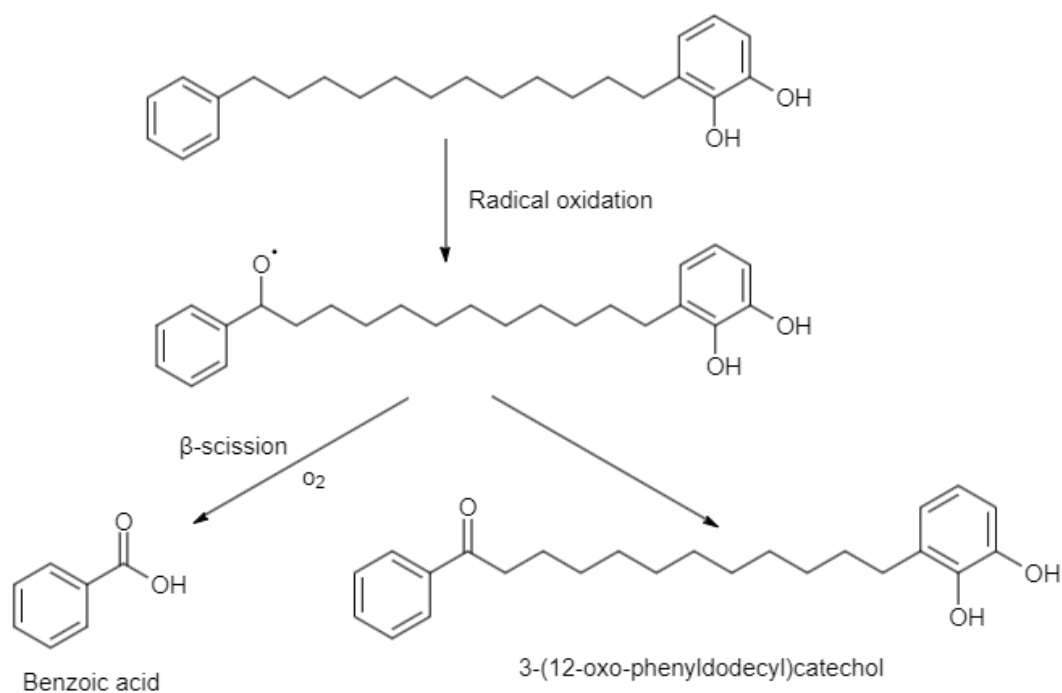


Figure 4. Proposed reaction mechanism of radical oxidation that leads to the formation of benzoic acids and alkylphenylketones as described by Tamburini [7].

shell (polysaccharides–glycoproteins)–core (polymerized catechol) structure of lacquer with the appearance of the polysaccharides, which causes a decrease of the surface brightness [1]. In literature, this degradation process has not been studied for thitsi as well as for urushi. For this reason, it has been chosen to describe it in the 2.2.2 Paragraph.

In Figure 4 is shown the proposed mechanism that leads to the formation of benzoic acid via β -scission reaction and further oxidation and alkylphenylketones, identified as typical oxidation markers of thitsi lacquer [7]. In Figure 5 the mechanisms that leads to the formation of alkylphenylcarboxylic acids and alkyl-oxo-phenylcarboxylic acids is proposed [7].

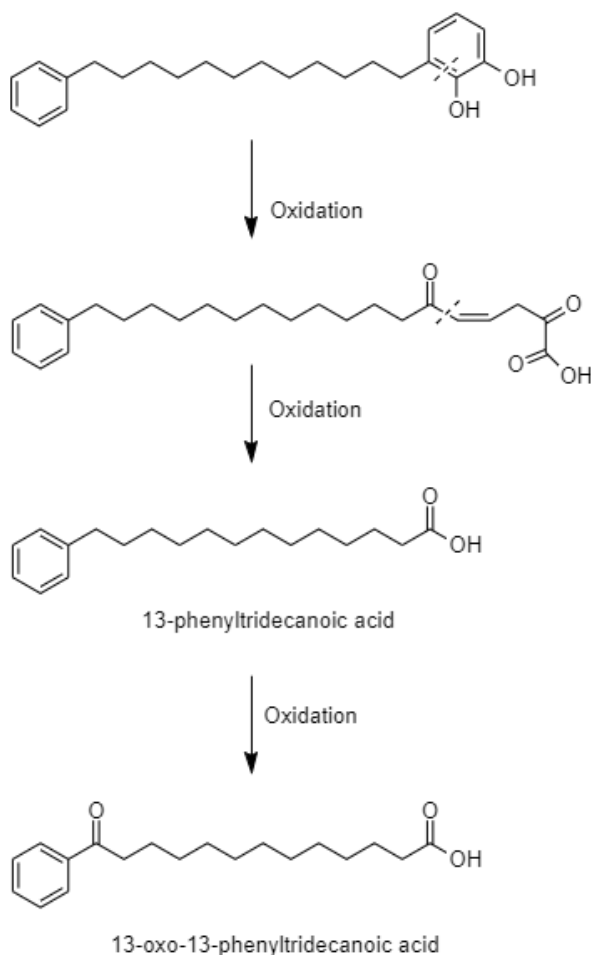


Figure 5. Proposed oxidation mechanism that leads to the formation of alkylphenylcarboxylic acids and alkyl-oxo-phenylcarboxylic acids as described by Tamburini [7].

2.2 Urushiol



Figure 6. Bureau-cabinet, China, ca. 1730 [3].

Urushiol (Figure 6) is the main component of the urushi sap. It is a mixture of catechols substituted at the 3- position by C15 (96,8 %) and C17 (3,3 %) side chains, 4- position by C15 side chains and phenols substituted at the 3- position by C15 side chains

		n ^o C	MW	%	
a)		C15	314	55,5	} 96,8 %
		C15	318	15	
		C15	314	7,4	
		C15	316	6,5	
		C15	320	4,8	
		C15	316	4,4	
		C15	314	1,7	
		C15	318	1,5	
		C15	314		
		C17	344	1,8	
		C17	346	1,5	
		C17	342		
b)		C15	314		
		C15	316		
c)		C15	302		
		C15	302		
		C15	298		
		C15	298		

Figure 7. Chemical composition of urushiol after Le Ho [19]: **a)** 3-alkyl and alkenyl catechols, **b)** 4-alkyl and alkenyl catechols, **c)** 2-alkyl and alkenyl phenols.

(Figure 7). The most abundant structure (55,5%) is the 3-(8Z, 11E, 13Z – pentadecenyl) catechol [9]. Differently from thitsi, urushi has only alkyl side chains (Figure 6). The most abundant structure (55,5%) is the 3-(8Z,11E,13Z-pentadecenyl) catechol [9].

2.2.1 Drying mechanism

The drying process of *urushiol*, is, in the very first step, the same enzyme-driven polymerization of *thitsiol*. The optimum T °C and rH % conditions for *urushiol* are respectively 20–25 °C and 70 % [20], which, correspond to lower severe values in comparison to *thitsiol*.

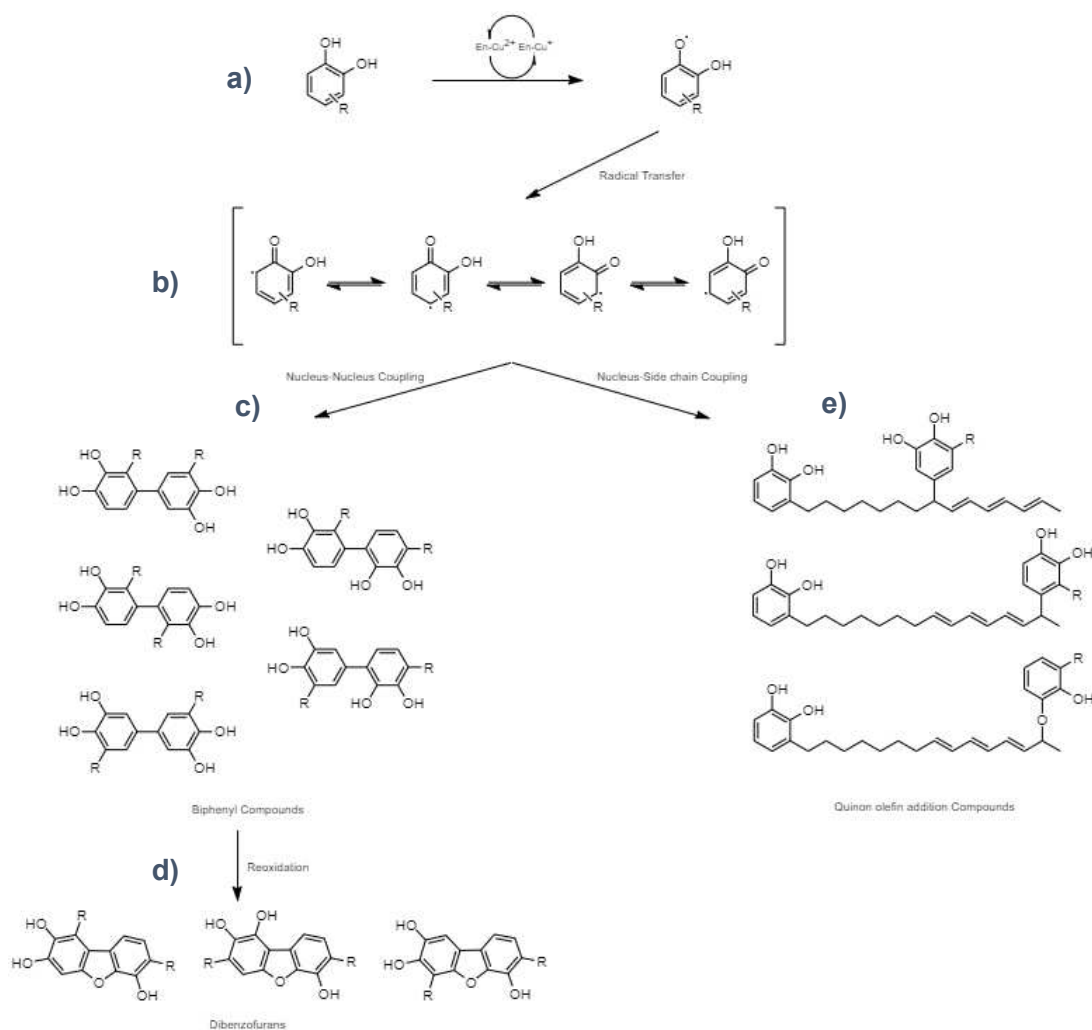


Figure 8. Reaction products of nucleus-nucleus reaction mechanism and nucleus-side chain reaction mechanism.

In contrast to *thitsiol*, after the radical transfer with the consequentially formation of semiquinone radicals, instead of only one mechanism of reaction, two different ones are possible (Figure 8): (c) the nucleus-nucleus (C-C) coupling, which leads to the formation of biphenyl compounds and dibenzofuran compounds (d), thanks to a one more laccase-catalysed oxidation step, and (e) a nucleus-side chain (C-C and C-O) coupling [9, 23]. It has been demonstrated that during the laccase-catalysed

polymerization process, nucleus-nucleus (C–C) and nucleus-side chain (C–C, C–O–C) coupling take place first in *urushiol* derivatives, and subsequently autoxidation of side chain-side chain (C–C) occurs [24]. The main reason why the nuclear-side chain coupling (C–C and C–O) is not predominant in *thitsiol*, is that the side chain in *thitsiol* is longer than the one in *urushiol* [9].

This first step of laccase polymerization is then followed by a second step based on air drying or auto-oxidation of the unsaturated side chains after the *urushiol* decreases to less than 30 % [9]. In this second step the unsaturated chains of the *urushiol* are auto oxidised and peroxides are originated (Figure 9a). These peroxides can react either with the catechol-core or with the unsaturated side chains of the *urushiol*. Consequently, the side chains will cross link (Figure 9b), forming C–O–O–C, C–O–C, or side chain-side chain cross link.

The auto-oxidation reactions start generally after the enzymatic polymerization due to the high content of phenolic hydroxyl groups of *urushiol*, which acts as antioxidants [9]. Both enzymatic reaction and auto-oxidation take place multiple times thus resulting in a durable network polymeric structure.

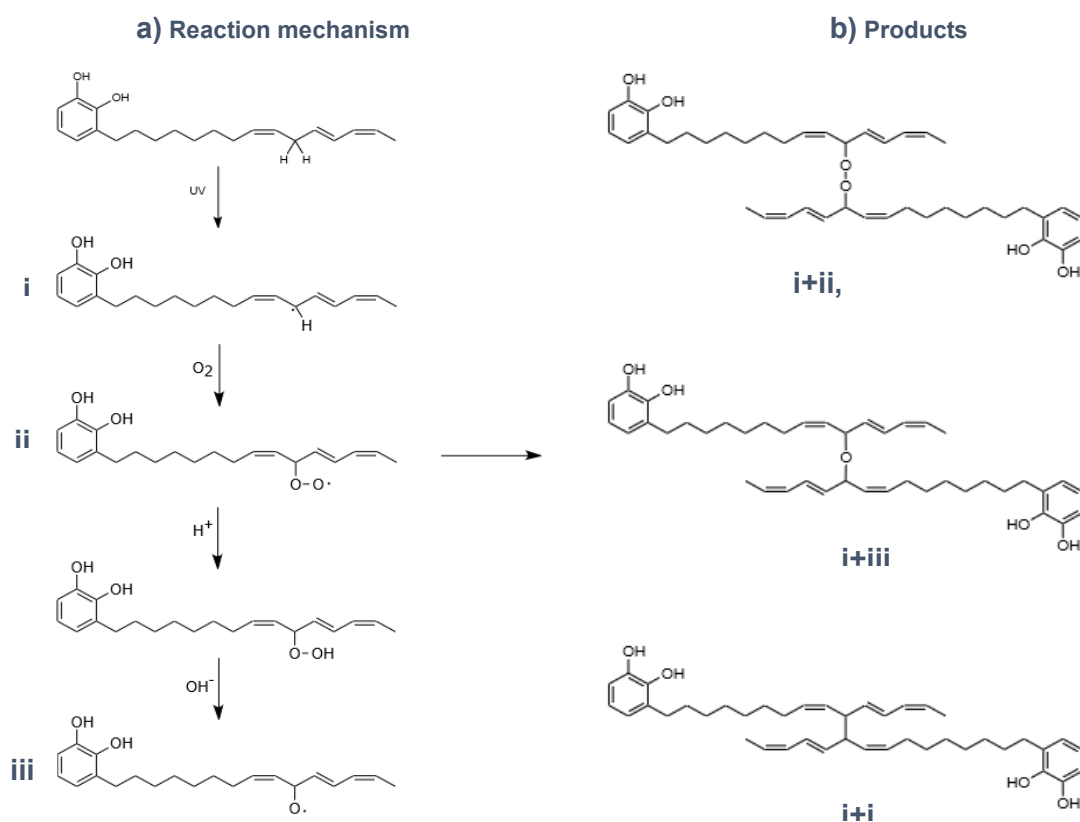


Figure 9. Reaction mechanism and products of *urushi* autoxidation reaction.

2.2.2 Ageing mechanism

The ageing mechanism of urushi has been studied [1] and it has been detected, after light exposure, a structural damage of the lacquer involving the packed shell-core made of polysaccharides and proteins typical of polymerized catechol structure of lacquer (Figure 10). Furthermore, the light-degraded layer swells and shrinks at a different rate to the undamaged surface beneath, and the differential tension that is created as result is relieved by the formation of cracks [25, 26]. From a chemical point of view, the alteration leads to the oxidation of the conjugated side chain of catechol and subsequently to the formation of aldehyde, ketone and carboxylic acid, to a loss of hydroxyl groups on the catechol ring and finally, in the most advanced degradation state, to the decomposition of the polymerized lacquer network [1].

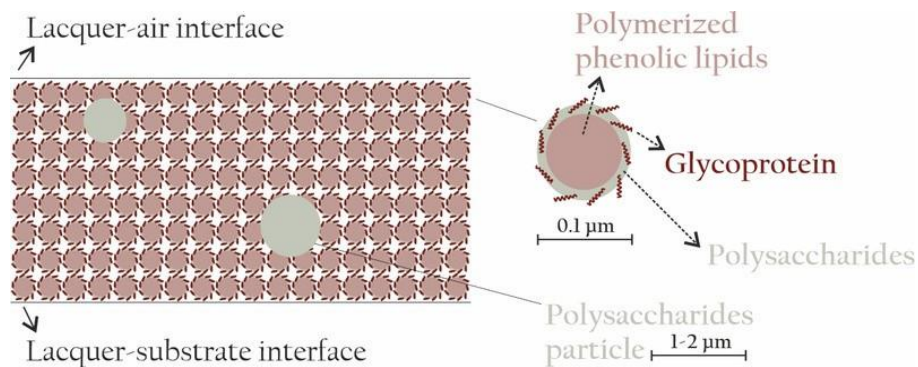


Figure 10. The core-shell structure of a polymerized lacquer film after Le Hô.

In the last ten years of research [1, 7, 13], oxidation products have been found and studied in order to determine which oxidation mechanisms lead to the formation of them. The reaction mechanism proposed in the Paragraph 2.1.2 are supposed to be the same oxidation mechanism that happen to urushi lacquer.

2.3 Blend of *urushiol* and *thitsiol*

The blend of *urushiol* and *thitsiol* (Figure 11) started to be exported during the seventeen and the eighteen centuries as a cheaper lacquer, due to the high demand of oriental lacquers from Europe [15, 2].



Figure 11. Commode à vantaux, French (Paris), ca. 1737 [2].

The thitsi sap has a slower drying time and requires more severe drying conditions than urushi which produces a smoother and glossier film surface. These reasons explain why in the Japanese market urushi costs about 9.000 yen/kg more than thitsi, which corresponds, according to the yen-euro exchange rate of 2022, to a difference of about 65€ [27].

2.3.1 Drying mechanisms

Despite to the abundance of urushi/thitsi blended lacquer-based objects in western museum collections, few researchers focused their works on it [15]. Different properties of blended lacquers have been studied, and in conclusion, it has been found that a blend with about 30 wt % of *thitsiol* to *urushiol* dried quickly and had a good viscosity near that of the mother lacquer *urushiol* [27]. The blended lacquer film also has a higher gloss and UV light resistance compared with the China lacquer film [27].

Regarding the drying reaction mechanisms (Figure 12), it has been demonstrated [28] that the laccase-catalysed dehydrogenative formation of phenoxy radicals firstly occurs on *urushiol* (Figure 10a), then *thitsiol* radicals are produced from *thitsiol* with

phenoxy radicals of *urushiol* by a radical transfer reaction (Figure 10b), and then a coupling reaction between these two radical species occurs to form dimers (Figure 10c). In the propagation step, the dimeric products would further undergo both radical transfer reactions and dehydrogenative oxidation by laccase under presence of dioxygen in the atmosphere [27].

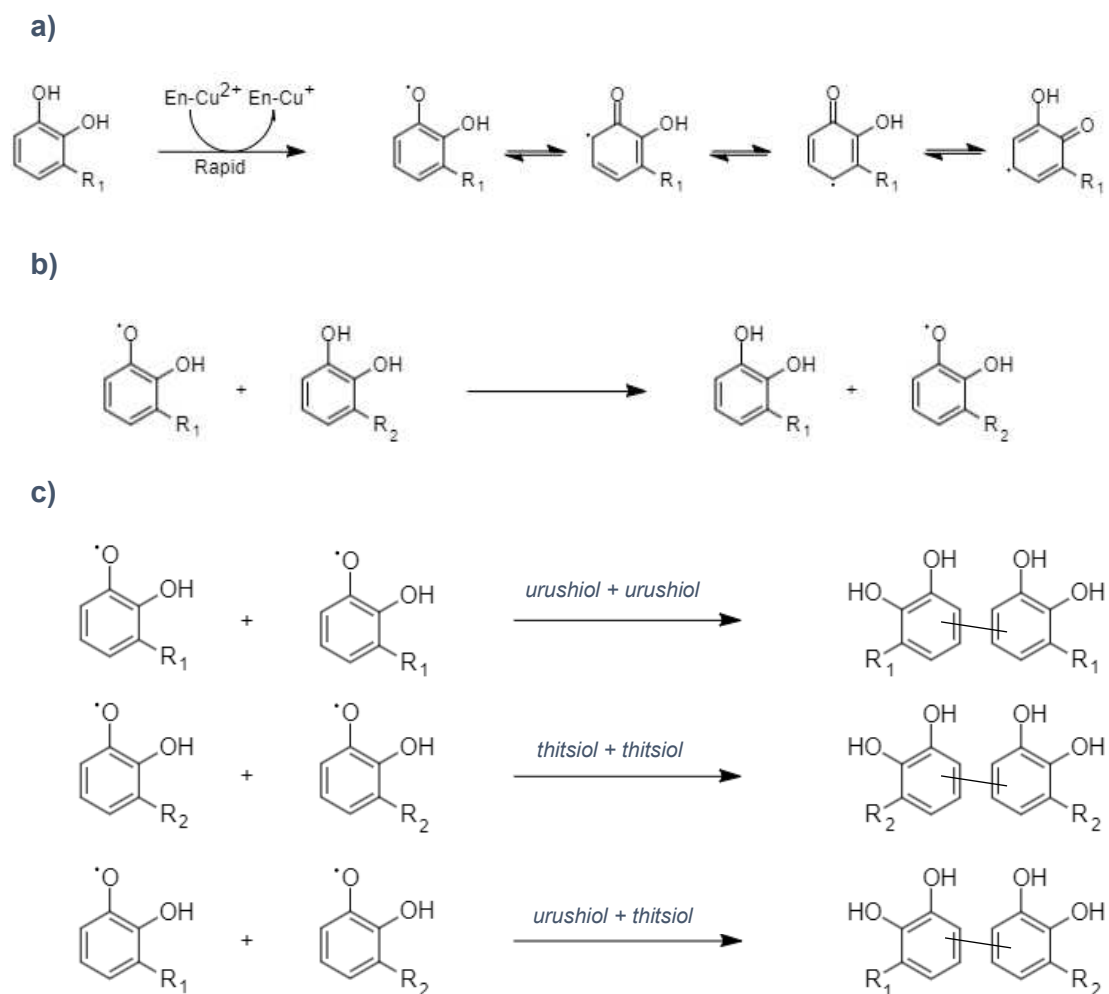


Figure 12. Reaction mechanism of a blend of *urushiol* and *thitsiol*.

2.3.2 Aging Mechanism

The aging and degradation mechanisms of the thitsi and urushi blended lacquer has not been studied yet. In the last decades the research treated about blended lacquers on very few occasions. Its interest focused predominantly on the characterization and drying/aging mechanisms of pure lacquers. About blend of Asian lacquers there are sometimes case studies of ancient blend lacquered objects or lab samples studies aimed at a chemical characterization and a proposed drying mechanism, but never an aging mechanism has been proposed. The most innovative aim of this research is the understanding of aging and degradation processes of a blend of urushi and thitsi comparing the data with the pure ones.

3. ANALYTICAL METHODS AND ACCELERATED ARTIFICIAL DAYLIGHT AGING

In this section the analytical and aging methods are presented. Each of them has been chosen following specific criteria and goals, and together they are thought in order to explain in the most complete and successful way the material, from different point of view. Some techniques have been used for their ability of describing the aspect and the physical changes of the surface and the colour, such as Digital Microscopy and Colorimetry; other to investigate the chemical structure and its aging processes through the time. Furthermore, these techniques have been selected because they represent both side of the invasive and non-invasive approach investigation. This aspect is often very critical in the Cultural Heritage Science because it is not always possible or allowed to take a sample, even if a few micrograms, from an artwork. Invasive and non-invasive techniques give usually different but also complementary information, and this is the reason why it is very important to find a correlation between them that could be useful whenever not all techniques are available.

3.1 Digital Microscopy

A digital microscope (Figure 13) is a variation of a traditional optical microscope that uses optics and a digital camera to output an image to a monitor. It has a digital camera which is the detector and the image output device. The display of the image is done on a computer screen or monitor, defining the microscope's digital scope. This microscope's light source is an inbuilt LED source as compared to the optical microscope, whose light source is accessed from outside the microscope through an eyepiece. Therefore, in the digital microscope, human optics access is eliminated since the entire apparatus has an image monitoring system [29].

A primary difference between a stereo microscope and a digital microscope is the magnification. With a stereo microscope, the magnification is determined by multiplying the eyepiece magnification times the objective magnification. Since the digital microscope does not have an eyepiece, the magnification cannot be found using this method. Instead, the magnification for a digital microscope was originally determined by how many times larger the sample was reproduced on a monitor. The average difference in magnification between an optical microscope and a digital

microscope is about 40%. Thus, the magnification number of a stereomicroscope is usually 40% less than the magnification number of a digital microscope [30].



Figure 13. Keyence Digital Microscopy.

The digital microscope is made of two major parts, which represent two of its major functions: the hardware and the software. The hardware is the analogic part of the microscope, with a light source, the analogic microscope, a camera, and the camera components. The Camera replaces the eyepiece of the traditional microscope [31].

The digital microscope has several advantages: for example, it provides high-resolution magnification of the images in pixels and 2D and 3D image measurements. It can also store huge amounts of data, through imaging and recording movable and unmovable specimens and provide an output of the images through the computer monitors [31].

3.2 Colorimetry

Colorimetry is the science of the measurement of colour. When light strikes an object, electromagnetic radiations interact with matter. Light is partly absorbed, partly transmitted, and partly reflected. The object exhibits the colour of the reflected

radiation. For this reason, colorimetry measures the reflectance (ρ), which is defined as the reflecting power of an object subjected to irradiation [32, 33].

The sum of reflectance (ρ), absorbance (α) and transmittance (τ) is always 1 for the energy conservation law, as shown in (1):

$$\rho + \alpha + \tau = 1 \quad (1)$$

and the reflectance could be calculated as the ratio between the reflected ray (I_r) and incident ray (I_0) as follows (2):

$$\rho = \frac{I_r}{I_0} \quad (2)$$

If light is fully absorbed, the object looks black; if it is fully reflected, the object is white. The colour of a substance depends on the wavelengths of light it absorbs. The perceived colour is the complementary one (Table 1), as light reaching the eye lacks the absorbed colour. What colour is absorbed depends on the chemical nature of the substance [34].

Wavelength (nm)	Colour	Complementary colour
400-435	Violet	Greenish Yellow
435-480	Blue	Yellow
480-490	Greenish Blue	Orange
490-500	Bluish Green	Red
500-560	Green	Purple
560-580	Yellowish Green	Violet
580-595	Yellow	Blue
595-605	Orange	Greenish Blue
605-750	Red	Bluish Green

Table 1. Colours absorbed and their perceived complementary colours depending on the wavelength (nm).

Each colour of the colour spectrum has a different wavelength. Different spectrally pure colours are said to have different hues. A spectrally pure or monochromatic colour can be produced by a single wavelength [34].

However, the same colour can be produced with a combination of two light beams. In fact, not all colours in nature are spectrally pure. Colours obtained by mixing a spectrally pure colour with white are said to have the same hue but different saturation, which can go from a value of 100% (pure original colour) to 0% (white) [34]. The degree of saturation is called the chroma. The relative amounts of a mixture of white and a spectrally pure colour determine the colour saturation, or chroma. Furthermore, comparing identical samples of the same spectrally pure colour, if one of them is strongly illuminated and the other is almost in darkness, the two colours look quite different. The difference between the colour samples is described by its lightness. Therefore, any colour has to be specified by three parameters: hue, saturation (or chroma), and luminance [33, 34].

In 1976 the $L^* a^* b^*$ colour space was proposed based on the opponent theory of colour vision, developed by Hering. This theory describes the unicity of the red, green, yellow and blue hues and together with white and black, they form a group of six basic colour properties that can be grouped into three opponent pairs, white/black, red/green and yellow/blue. The concept of opponency arises from the observation that no colour could be described as having attributes of both redness and greenness, or of both yellowness and blueness. These three opponent pairs were then associated with the three axes of a three-dimensional colour space. In 1976 CIE (Commission International de l'Éclairage) proposed the $L^* a^* b^*$ colour space (Figure 14) using three terms L^* , a^* and b^* to represent colour [32, 33, 34], as follows:

- L^* is the vertical axis and represents lightness: 100 represents a perfect white sample and 0 a perfect black.
- a^* is the axis in the plane normal to L^* and represents the redness–greenness quality of the colour: positive values denote redness and negative values denote greenness.
- b^* is the axis normal to both L^* and a^* and represents the yellowness–blueness quality of the colour: positive values denote yellowness and negative values denote blueness.

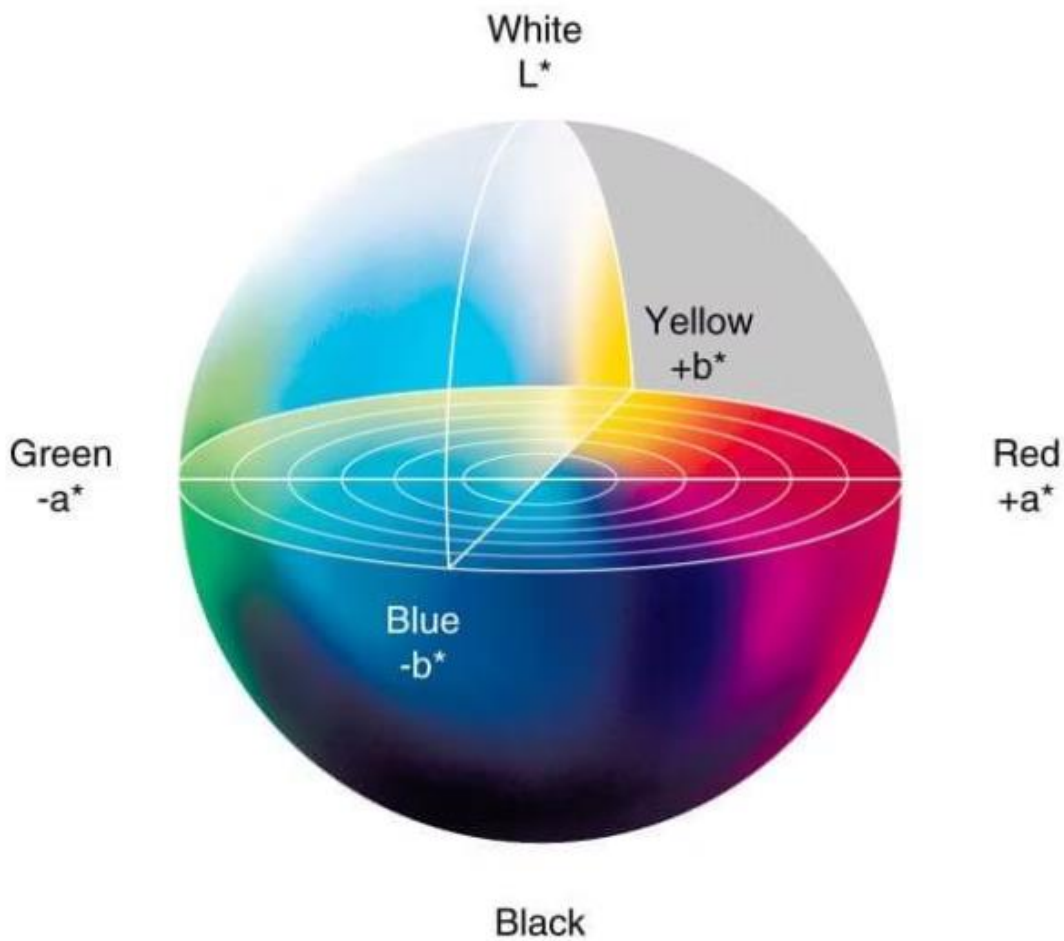


Figure 14. $L^*a^*b^*$ colour space proposed by CIE in 1976.

The total colour difference is the distance between the two points representing those colours in the colour space. The distance, expressed as ΔE^* , is determined using the laws of right-angle triangles [32, 33, 34], as follows (3):

$$\Delta E^* = \sqrt{\Delta L^{*2} + \Delta a^{*2} + \Delta b^{*2}} \quad (3)$$

where ΔL^{*2} , Δa^{*2} and Δb^{*2} are respectively the difference between the $L^* a^* b^*$ values of two trials or a trial and a standard.

The dependence of human eyes colour perception on ΔE^* is shown in Table 2 [35, 36].

ΔE^*	Perception
$\leq 1,0$	Not perceptible by human eyes
1-2	Perceptible through close observation
2-10	Perceptible at a glance
11-49	Colours are more similar than opposite
100	Colours are exact opposite

Table 2. The dependence of human eyes colour perception on ΔE^* .

3.3 Fourier Transform Infrared Spectroscopy (FTIR)

Infrared Spectroscopy is certainly one of the most important analytical techniques available to today's scientists [37, 38]. One of the great advantages of Infrared Spectroscopy is that virtually any sample in virtually any state may be studied, at a high scanning speed. The purchase and use of Infrared (IR) spectrometers in art conservation labs have grown more than tenfold in the last decade [27, 38]. This expansion can be traced to decreased instrument costs, enhanced interest in organic materials in art and archaeological objects, and increased requests for scientific analyses by conservators and curators. In the specific case of Asian Lacquer, FTIR is particularly useful for examining the behaviour of the enzymatic dehydro-genative polymerization of lacquers during a drying or aging process [27, 38]. It is a technique based on the vibrations of the atoms of a molecule. An infrared spectrum is commonly obtained by passing infrared radiation through a sample and determining what fraction of the incident radiation is absorbed at a particular energy. The energy at which any peak in an absorption spectrum appears corresponds to the frequency of a vibration of a part of a sample molecule.

The energy of electromagnetic radiation is expressed by the following equation (4):

$$E = \frac{hc}{\lambda} = h\nu \quad ; \quad \nu = \frac{c}{\lambda} \quad (4)$$

where λ is the wavelength (cm), c is the velocity of light (3.0×10^{10} cm/sec), h is the Planck's Constant (6.63×10^{-34} J sec) and ν is the frequency (sec^{-1}).

Specific wavelengths of energy correspond to all molecular transitions or motions: electronic, translational, rotational, and vibrational. Every molecular transition can be represented in terms of quantized discrete energy. Bond vibrations occur at quantized frequencies, only certain vibrational energy levels are allowed. Whenever a molecule

interacts with radiation, a quantum of energy (photon) is either emitted or absorbed [39, 40].

Since molecule movements are unique to its structure, the measurement of these transitions makes FTIR a powerful tool for compound characterization. There are several types of molecule movements (Figure 15), consisting of asymmetrical and symmetrical stretching vibrations as well as in-plane and out-of-plane bending modes; all are referred to as fundamental vibrations. Stretching vibrations involve motions by atoms in the direction of the bond, whereas bending vibrations (or deformations) involve motions resulting in corresponding changes in the bond angle [39, 40].

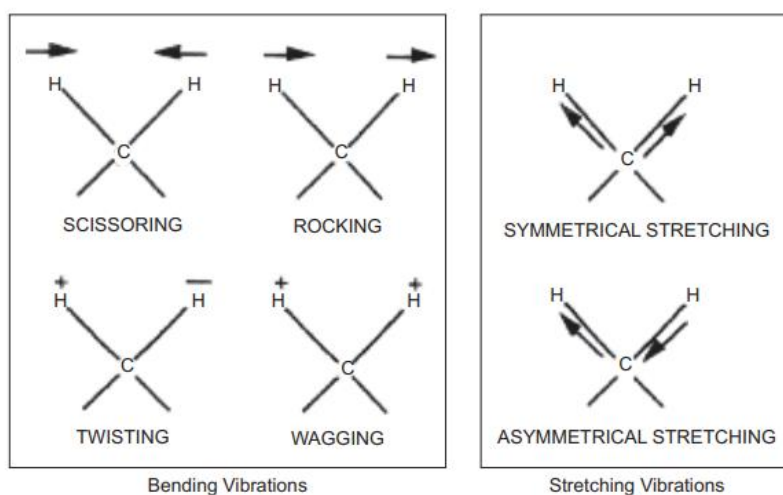


Figure 15. Representation of stretching and bending molecular vibrations.

Within any molecule, a given functional group (a combination of atoms such as a carbonyl group or an amide group) is responsible for infrared absorptions and vibrational frequencies are characteristic of that group. These characteristic vibrations are termed group frequencies and are used for the identification of materials and for the determination of structure in an unknown pure compound. In molecules consisting of multiple groups of atoms, the energy of a vibration and, thus, the position of the band in the IR spectrum are sometimes influenced by the atoms surrounding the vibrational group [39, 40].

When the molecule in the sample compartment of the spectrometer is exposed to a source of continuous IR radiation, called incident radiation (I_0), the photons of discrete energy units that are absorbed by the molecule do not reach the detector. Photons that are not absorbed by the sample are transmitted to the detector essentially

unaltered and are called transmitted radiation (I_t). The ratio between these two quantities per cent is called percent transmittance (%T) [37, 39, 40], as follows (5):

$$T = \frac{I_t}{I_0} \times 100 \quad (5)$$

However, an IR spectrum usually displays detector response as Absorbance (A or Abs) on the y-axis, and IR frequency in terms of wavenumber (cm^{-1}) on the x-axis. Absorbance is inversely related to percent transmittance, as shown in (6) [39, 40]:

$$A = -\log T = \log I_0 - \log I_t \quad (6)$$

The detector response indicates the resultant intensity of IR radiation that reaches the detector after passing through the sample and the IR spectrum reveals these missing photons, or absorptions, as a series of well-defined, characteristic, and reproducible absorption bands [39, 40].

3.3.1 Transmission mode

Transmission Spectroscopy is the oldest and most straightforward infrared method. This technique is based upon the absorption of infrared radiation at specific wavelengths as it passes through a sample. It is possible to analyse samples in the liquid, solid or gaseous forms when using this approach. One advantage of Transmission analysis is that the total sample absorption is proportional to the thickness of the sample (pathlength) and its concentration [37, 39, 40]. Also, because of high energy throughput, Transmission analysis methods have greater sensitivity

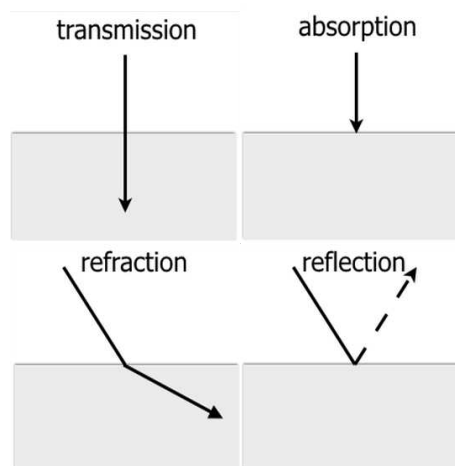


Figure 16. Representation of four possible interaction between light and an object.

than reflection analysis. The character of a Transmission spectrum is dependent on sample preparation, particle size, and absorptivity. For example, spectral distortions, such as band broadening, occur when the transmitted beam is partially reflected or refracted (Figure 16). Additionally, whenever another material is added to the sample, either to dilute it or to support it, there is an added risk of contamination, which can result in spurious absorption bands [37, 39, 40].

For Transmission analysis, the sample can be placed freestanding in the IR beam, or it may be held in place by a supporting material. Ideally, the supporting material would not absorb any of the IR radiation. For this purpose, two materials, potassium bromide (KBr) and barium fluoride (BaF_2), are commonly used as IR windows in the mid-IR region [39, 40].

3.3.2 ATR mode

The technique of Internal Reflection Spectroscopy (IRS), also called Attenuated Total Reflection (ATR), was introduced in the early 1960s and quickly became popular, since almost any material—solid, powder, or liquid—could be easily and non-destructively analysed [39, 40]. The fact that this method is non-destructive (possibly non-invasive) and provides surface information, makes it a suitable tool for the study of cultural heritage and surface degradation phenomena such as photodegradation [38]. The analyses are performed placing the sample in intimate contact with the

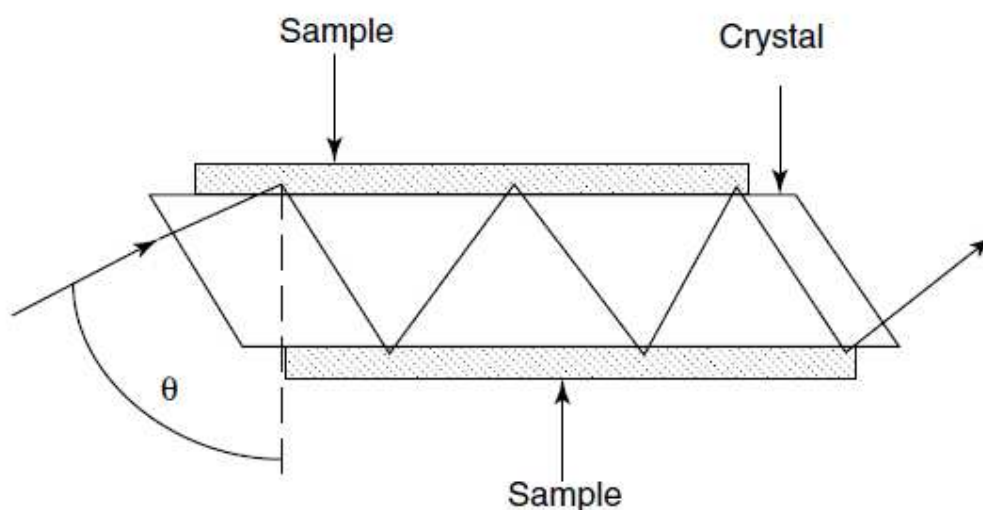


Figure 17. Representation of the evanescent wave created by infrared radiation entering an ATR crystal with an angle θ .

surface of a transparent material with significantly higher refractive index (n) than the sample itself [39, 40].

When infrared radiation enters certain crystalline materials, usually called IRS element (Internal Reflection Element) with high refractive indices (such as ZnSe and Ge), the radiation is totally internally reflected. In addition, the internal reflectance creates a wave called an evanescent wave that extended slightly beyond the surface of the ATR crystal (Figure 17). If a sample material is placed in contact with the ATR crystal, the evanescent wave penetrates the sample to a very small depth, producing an infrared spectrum at the surface of the sample material. The fact that the evanescent wave decays exponentially with distance from the surface of the ATR crystal is crucial to the ATR technique. This characteristic makes the ATR technique insensitive to the thickness of the sample. The total internal reflection occurs when the angle of incidence at the interface between the sample and crystal is greater than the critical angle (θ_c). The resultant attenuated radiation is measured and plotted as a function of wavelength by the spectrometer and gives rise to the absorption spectral characteristics of the sample [39, 40].

3.4 Thermally assisted Hydrolysis and Methylation of Pyrolysis Gas Chromatography / Mass Spectrometry (THM-Py-GC/MS)

Thermally assisted Hydrolysis and Methylation Pyrolysis Gas Chromatography / Mass Spectrometry (THM-Py-GC/MS) is considered the most suitable analytical technique for comprehensive characterization of organic materials in Asian lacquers. It provides the most detailed compositional information about the catechol-rich saps [13]. The potential to analyse non-volatile and insoluble complex materials, and the small quantity of sample required makes this technique very attractive in the cultural heritage field and has been widely applied to the characterization of many organic materials found in artworks [41]. THM-Py-GC/MS is a method of chemical analysis that consists in a first derivatisation, usually with Tetramethyl Ammonium Hydroxide $N(CH_3)_4^+OH^-$ (TMAH), and then thermally degrades the sample to produce smaller and more analytically useful fragments that can be separated on a GC column and detected with an MS instrument.

3.4.1 Thermally assisted Hydrolysis and Methylation (THM) and Pyrolysis (Py)

Thermally assisted Hydrolysis and Methylation (THM) of pyrolysis (Py) (Figure 18) is a process of derivatisation occurring at high temperature conditions inside the furnace of the Pyrolyzer. It is performed in order to reduce the polarity of certain components [24] (i.e. hydroxyl moieties (-OH), carboxylic acids (COOH), and amino groups (NH₂)), thus converting them in volatile compounds, which can be exposed to high temperatures and analysed. THM of Py combines the use of a derivatising agent with the high temperature conditions of the pyrolyzer.

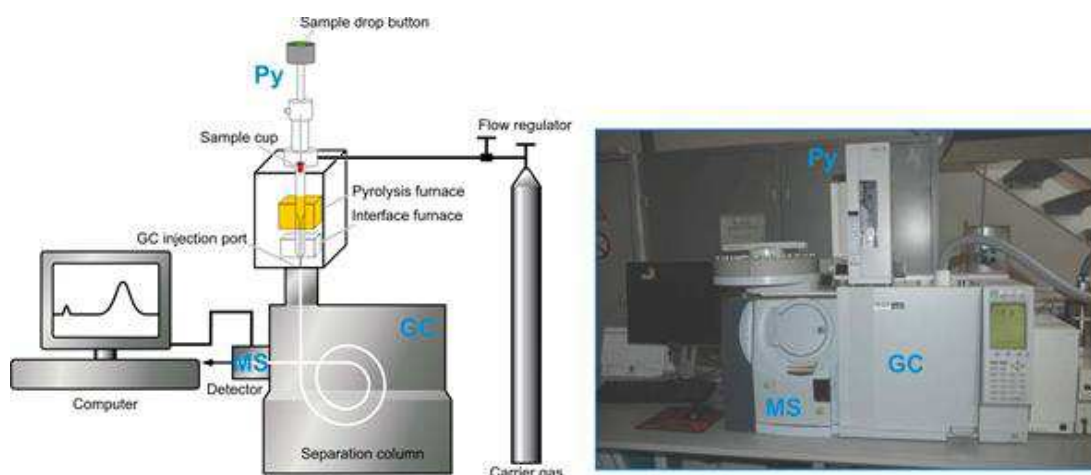


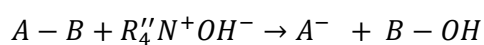
Figure 18. Schematic representation of the Pyrolysis – Gas Chromatography / Mass Spectrometry (Py-GC/MS) instrument used for this Master's thesis at the Institute for Natural Sciences and Technology in the Arts, at the Academy of Fine Arts Vienna

Derivatising agents such as Tetramethyl Ammonium Hydroxide $N(CH_3)_4^+OH^-$ (TMAH) reacts with molecules having polar functional groups by substituting the H atom with less polar groups, such as methyl (CH_3) ones. In case of the Asian lacquers, their most significant pyrolysis products as alkylcatechols and alkylphenols are polar due to their two and one hydroxyl groups (-OH), respectively. The use of Pyrolyzer without the THM allows to detect a phenol structure with one hydroxyl group on the benzene ring (108 m/z) and a catechol tropylium ion (123 m/z). The phenol product is formed because when lacquer hardens, the hydroxyl group is involved in the polymerization reaction, and the -OH bond is easily broken during pyrolysis. In general, the thermal decomposition reaction progresses more easily on the phenol structure than on the catechol one. On the other hand, THM of Py serves to enhance the volatility of the alkylphenols and alkylcatechols as well as of their oxidation products, and thus their detection and identification.

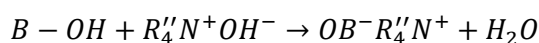
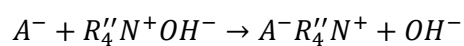
Pyrolysis (from greek *pyros* – fire, and *lysis* – separating) is a thermal method of derivatisation of high molecular weight compounds such as polymers and oils, which are less volatile. It is based on a rapid thermal decomposition of few milligrams of a sample in absence of oxygen. Among different typologies of pyrolizers, the furnace is the most commonly used for the investigation of Asian lacquers. The pyrolizer consists of a furnace that includes a glass insert tube, where the capsule containing the sample moves gravitationally downwards and is heated up at desiderated temperatures steps up to 1000 °C. It is connected to the Gas Chromatograph (GC) by an interface in which the thermal decomposed sample materials pass into with the aid of a carrier gas and reach the separation column of the gas chromatograph. The furnace increases rapidly the temperature of the sample to the desired pyrolysis temperature.

Generally, few microliters of TMAH are added into the lacquer sample material contained in a tiny metallic cup and left to react for approximately one hour in order to achieve a good impregnation and contact with the specimen. Successively, the sample cup is then inserted into the pyrolizer and heated up at 500 °C in absence of oxygen for less than 20 msec. The mechanism for this in-situ-(trans) methylation takes place in a first hydrolysis step (in case of ester and ether bonds) at high temperature conditions, as the name THM implies, with the consequent formation of Tetraalkylammonium (TMA) salts. This is followed by the methylation with trimethylamine as a by-product after heating the salt with TMAH. The following series of reactions outlines the mechanism of thermally assisted hydrolysis and methylation [42, 43]:

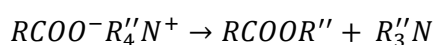
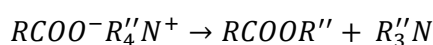
Hydrolysis:



Formation of TMA salts:



Thermal dissociation to alkyl derivatives:



In case of Asian Lacquers, the THM process is mostly based on the deprotonation of hydroxyl moieties followed by methylation, as shown in Figure 19:

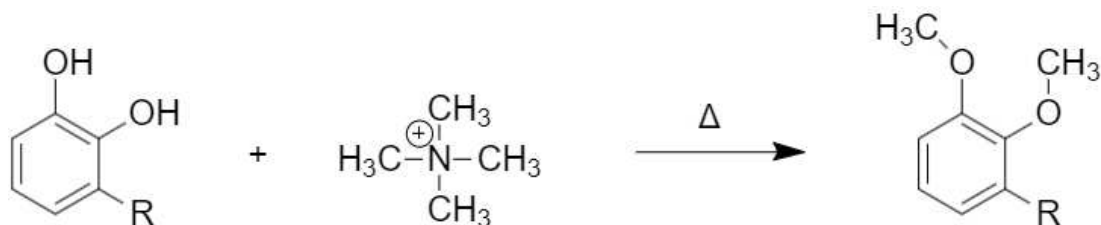


Figure 19. Catechol methylation reaction with Tetramethyl Ammonium Hydroxide (TMAH).

After being heated to a high temperature, the sample becomes vaporized, the gas products are analysed, and the sample structure can be inferred (Figure 20) [24].

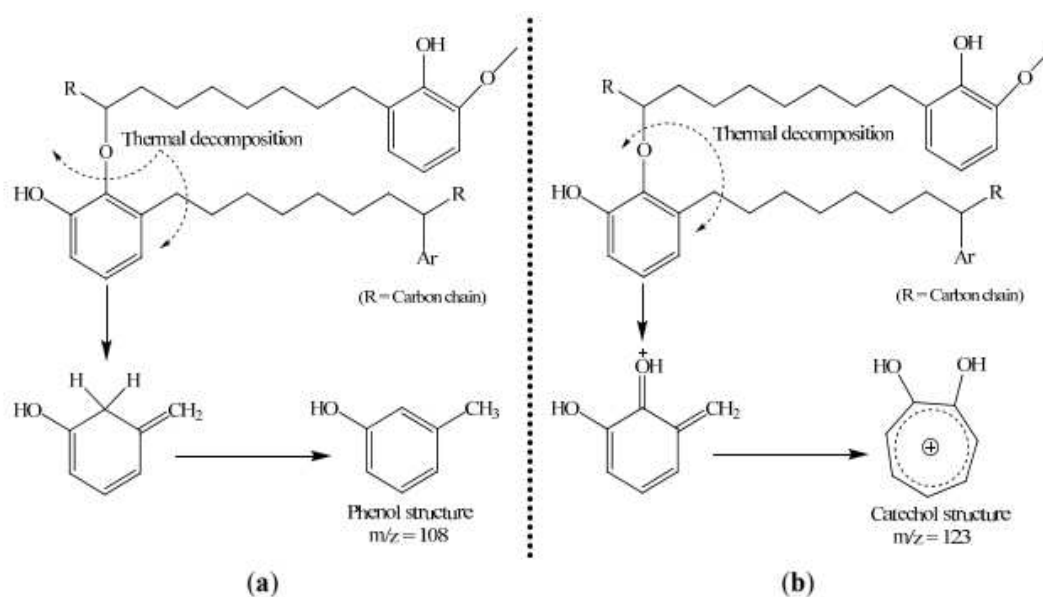


Figure 20. Reaction mechanisms of the two major pyrolysis products of Asian lacquers without the Thermally assisted Hydrolysis and Methylation (THM): a) the formation of phenol structure ($m/z=108$); b) the formation of catechol structure ($m/z=123$).

3.4.2 Gas Chromatography (GC)

Nowadays, chromatography is one of the most important analytical techniques. Chromatographic techniques are used for separating the components, or solutes, of a mixture on the basis of the relative amounts of each solute distributed between a

moving fluid stream, called the mobile phase, and a contiguous stationary phase. The stationary phase can be either a solid or a liquid, the mobile phase is a liquid, a gas, or a supercritical fluid. Both phases must be able to interact physically or chemically with the sample molecules. When the mobile phase is flowing through or over the stationary phase the analytes in the sample mixture undergo characteristic partition between the two phases. The mobile phase transports, the stationary phase retains. If, for a particular solute, the distribution favours the moving fluid, the molecules will spend most of their time migrating with the stream and will be transported away from other species whose molecules are retained longer by the stationary phase. For a given species, the ratio of the times spent in the moving and stationary regions is equal to the ratio of its concentrations in these regions, known as the partition coefficient (K), as shown in (7) [44, 45, 46]:

$$K = \frac{C_S}{C_M} \quad (7)$$

C_S and C_M being the concentration of the analyte in the stationary and mobile phases, respectively, at equilibrium.

The driving force for solute migration is the moving fluid, and the resistive force is the solute affinity for the stationary phase. This affinity depends on the physical and chemical interactions molecules could have differently with the two phases. If a molecule has a strong interaction with the stationary phase, like in case of organic compounds with an apolar stationary phase or cationic molecules with an anionic stationary phase and vice versa, the partition coefficient K will be > 1 and the stronger the interaction, the bigger K will be. At the contrary, molecules with weaker interactions with stationary phase or stronger interactions with mobile phase, will have a $K < 1$ and the weaker the interaction, the smaller K will be. As a direct consequence, substances with the biggest K will stop soon in the chromatography column and will take more time to be eluted, being the last to be detected; while substances with the smallest K will not interact with the stationary phase and they will be eluted first. If $K = \infty$ the compound is totally adsorbed by the stationary phase and will not be transported through the chromatographic bed. If $K = 0$ no retention takes place and the residence time in the column will be minimal [44, 45, 46].

The recording of the detected signal as a function of elution time is called chromatogram, and the elution bands are called peaks. The time-dependent concentration profile has a characteristic bell shape and can be described in close approximation by a Gaussian curve [44, 45, 46].

Having a tight peak means, consequently, having a lower standard deviation (σ). The peak shape depends on three parameters A , B and C (Figure 21) describing the flow distribution, the longitudinal diffusion and the resistance to mass transfer between the mobile and stationary phase, respectively. A depends on the irregularity of the column packing and the average particle diameter. B depends on the diffusion coefficient in the mobile phase. C depends on the retention factor, on the average film thickness of the stationary phase on the support material and on the diffusion coefficient of the analyte in the liquid stationary phase.

The terms B and C follow different trends: on one hand increasing the linear velocity (flow rate) of the mobile phase decreases the effect of diffusion (hence the plate height), on the other hand it increases mass transfer effects, which increase plate height. A certain time is required for the mass transfer between phases [44, 45, 46].

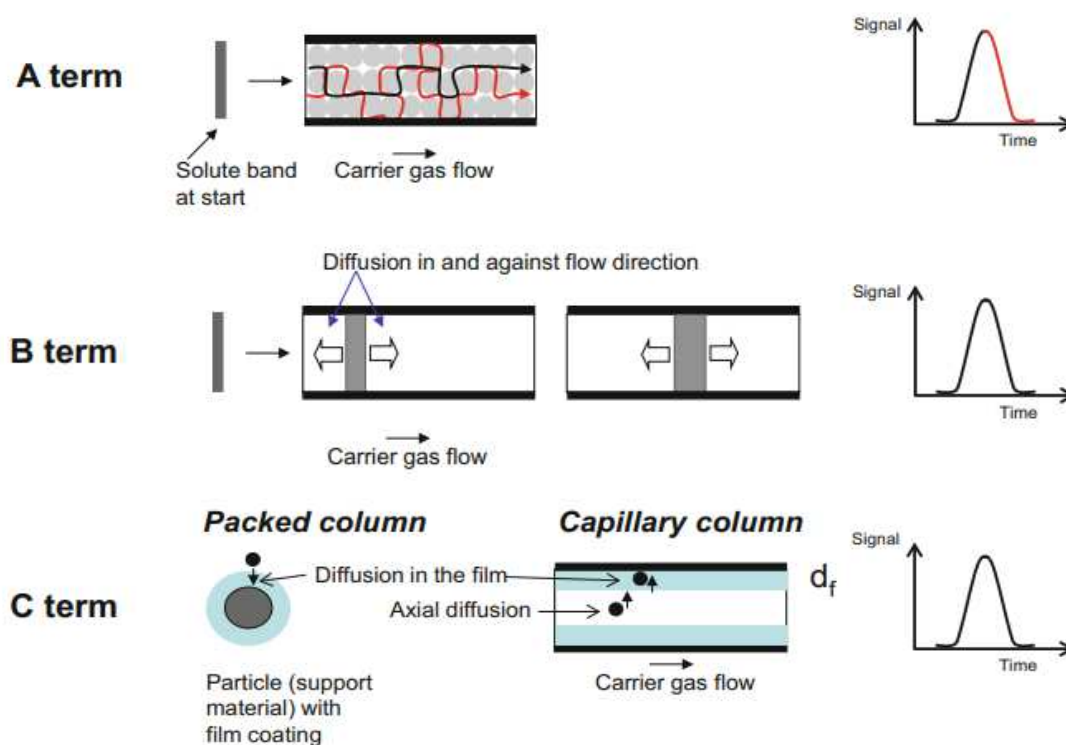


Figure 21. Representation of A , B and C parameters describing the flow distribution, the longitudinal diffusion, and the resistance to mass transfer between the mobile and stationary phase, respectively.

Chromatography also aims to separate the components of mixtures into individual signals. The parameter that describes the separation for an adjacent peak pair is the resolution (R_s). There are two general options to increase the resolution of an

incompletely separated peak pair: by the improvement of the column efficiency or by an increase of the selectivity.

The efficiency can be increased using longer columns, but concomitantly, the column head pressure and the analysis time increase with increasing column length. On the other hand, selectivity has a strong influence on the resolution. It can be influenced by changes in column temperature or by selecting a different stationary phase [44, 45, 46].

Gas chromatography (GC), in particular, involves volatilization of the sample in a heated inlet or injector of a gas chromatograph, followed by separation of the components of the mixture in a chromatographic column. Only those compounds that can be vaporized without decomposition are suitable for GC analysis. A carrier gas (sometimes referred to as the mobile phase but which the analyte does not interact with), usually hydrogen or helium, is used to transfer the sample from the injector, through the column, and into a final detector. Detectors are dedicated tools designed specifically for use on a gas chromatograph; examples are thermal conductivity (TCD), flame ionization (FID), nitrogen–phosphorus (NPD), flame photometric (FPD), and electron capture (ECD). A Mass Spectrometer (MS) could be coupled with gas chromatographic device and used as detector too [44, 45, 46].

The separation along the column and the separation efficiency (resolution) in Gas Chromatography is strongly dependent on the vapour pressure of the compounds and the degree of interaction with the stationary phase. The column is placed in an oven, where temperature programs are selected, in order to separate the maximum amounts of components in a mixture depending on their respective boiling points. Possibilities include an isothermal run where the temperature remains constant, a temperature-programmed run where the temperature is increased at a constant rate, and a multilevel run where the temperature rate is increased at different rates at different times during the GC run. Finally, the temperature may be held constant for various periods of time: at the beginning, in the middle of a temperature program, or at the end of the analysis. Generally, isothermal conditions are used when only a few compounds are in the sample, and these compounds are similar in boiling point and polarity. When the sample contains many compounds of a wide boiling-point range, temperature programming is necessary to separate all of the components of the mixture. With a temperature program all of the peaks are usually separated in a reasonable time, and they all have an excellent signal-to-noise ratio [44, 45, 46].

The initial temperature of the analytical run depends on the temperature at which the first compound of interest elutes, the solvent used to dissolve the analytes, and the injection mode. Temperature program rates are usually 4–20 °C/min; the actual rate depends on the number of analytes and how closely they elute. In a multilevel temperature program, the temperature program should be relatively slow to separate compounds with similar boiling points that near one another; then the rate of programming should be increased when only a few compounds with widely different boiling points are expected to elute. When all of the compounds of interest have eluted, it is common practice to rapidly increase the temperature program rate to around 50 °C/min to just below the column limit. The purpose of this is to elute extraneous high-boiling compounds from the sample or from other sources such as the septum. If there are no high-boiling impurities in the sample or in the column, then the final temperature can be that at which the last analyte elutes.

Qualitative information about the analytes can be gained from the peaks' position in a chromatogram, whereas quantitative information is obtained by evaluating peak height and area [44, 45, 46].

3.4.3 Mass Spectrometry (MS)

Mass spectrometry (MS) is an indispensable analytical tool to identify a compound from the molecular or atomic mass(es) of its constituents (Figure 22). A mass

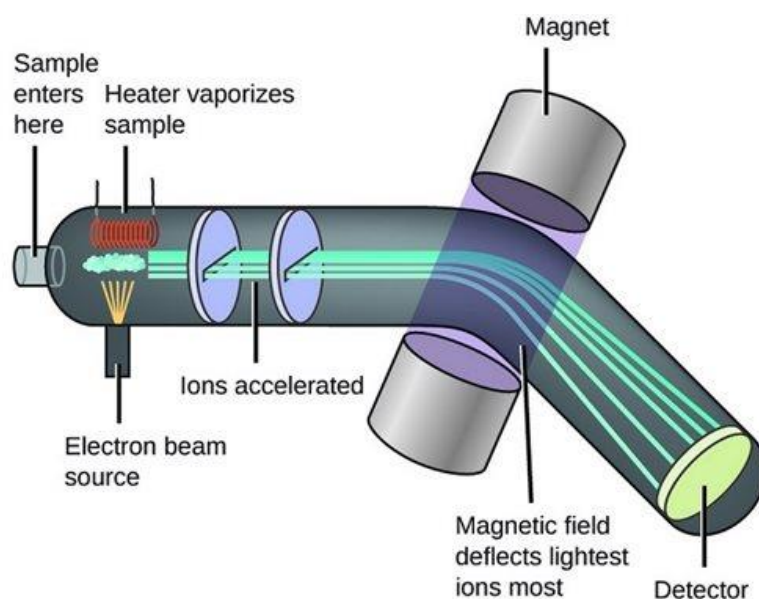
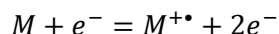


Figure 22. Schematic representation of a mass spectrometer.

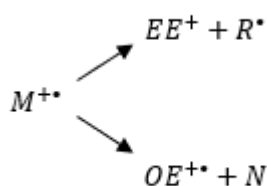
spectrometer consists of an ion source, a mass analyser, and a detector which are operated under high vacuum conditions [47].

Mass spectrometers are designed to create ions from neutrals in order to be able to accelerate and to force them into direction-controlled motion with the aim to ultimately achieve m/z analysis of these ions. The mass analyser of any mass spectrometer handles only charged species, ions that have been created from atoms or molecules. It is the task of the ion source to perform this crucial step and there is a wide range of ionization methods in use to achieve this goal for the whole variety of analytes, often divided in two categories: hard and soft ionization methods. The classical procedure of ionization involves shooting energetic electrons on a gaseous neutral. This is called electron ionization (EI). When a neutral is hit by an energetic electron source, typically a resistively heated tungsten filament, carrying several tens of electron volts (eV) of kinetic energy, some of the energy of the electron is transferred to the neutral. If the electron, in terms of energy transfer, collides very effectively with the neutral, the energy transferred can exceed the ionization energy (IE) of the neutral. Then ionization by ejection of one electron generating a molecular ion, a positive radical ion, occurs [47]:



For EI, the neutral analytes previously must have been transferred into the highly diluted gas phase, which is done by means of any sample inlet system suitable for the evaporation of the respective compound. In the case the mass spectrometer is coupled with a gas chromatograph the neutral analytes enter the system already diluted in a gas phase, that is the carrier gas [47].

This molecular ion normally undergoes fragmentations. Because it is a radical cation with an odd number of electrons, it can fragment to give either a radical (R^{\bullet}) and an ion with an even number of electrons (EE^{+}), or a neutral molecule (N) and a new radical cation ($OE^{+\bullet}$):



All these ions are separated in the mass spectrometer according to their mass-to-charge ratio and are detected in proportion to their abundance. A mass spectrum of the molecule is thus produced. It provides this result as a plot of ion abundance versus mass-to-charge ratio. The most intense peak is called the base peak and is arbitrarily assigned the relative abundance of 100 %. The abundances of all the other peaks are given their proportionate values, as percentages of the base peak. Ions provide information concerning the nature and the structure of their precursor molecule. In the spectrum of a pure compound, the molecular ion, if present, appears at the highest value of m/z (followed by ions containing heavier isotopes) and gives the molecular mass of the compound.

Electron ionization is a hard ionization technique because it leads to a high fragmentation of the molecular ion, which sometimes prevents its detection. Other useful ionization methods are the soft ones, such as Chemical Ionization (CI), Electron Spray Ionization (ESI) or Matrix-Assisted Laser Desorption Ionization (MALDI). Each of these techniques presents the advantage of yielding a spectrum with less fragmentation in which the molecular ion is easily recognized [47].

Once the gas-phase ions have been produced, they need to be separated according to their masses and detected. Several analysers are employed nowadays for this purpose. The five main characteristics for measuring the performance of a mass analyser are the mass range limit, the analysis speed, the transmission, the mass accuracy, and the resolution. The mass range determines the limit of m/z over which the mass analyser can measure ions. The analysis speed, also called the scan speed, is the rate at which the analyser measures over a particular mass range. The transmission is the ratio of the number of ions reaching the detector and the number of ions entering the mass analyser. Mass accuracy indicates the accuracy of the m/z provided by the mass analyser, such as the difference that is observed between the theoretical m/z and the measured m/z . Resolution or resolving power is the ability of a mass analyser to yield distinct signals for two ions with a small m/z difference [47].

The analyser used in this research is a quadrupole analyser. A quadrupole analyser is a device which uses the stability of the trajectories in oscillating electric fields to separate ions according to their m/z ratios. A linear quadrupole mass analyser consists of four hyperbolically or cylindrically shaped rod electrodes extending in the z -direction and mounted in a square configuration (xy -plane). The pairs of opposite rods are each held at the same potential. The ions accelerated along the z axis enter the space between the quadrupole rods and maintain their velocity along this axis,

but they are also submitted to forces induced by the electric fields along x and y axis. The trajectory of an ion will be stable if the values of x and y never reach the half distance between two opposite rods, thus if it never hits the rods. If ion discharges itself against a rod this is not detected [47].

In the end, the ions able to pass the quadrupole without touching the rods pass through the mass analyser and are then detected and transformed into a usable signal by a detector. Detectors are able to generate from the incident ions an electric current that is proportional to their abundance. Because the number of ions leaving the mass analyser at a particular instant is generally quite small, significant amplification by a conventional electronic amplifier is often necessary to obtain a usable signal [47].

3.5 Accelerated artificial daylight aging

Accelerated ageing is a technique widely used in the field of Culture Heritage for three main reasons. The first is to establish in a convenient short time the state of materials considering their chemical stability and physical durability over time. The stability is defined as the resistance of a material to environmental factors, such as oxygen, ozone, moisture, heat, and light, which primarily bring about chemical changes, while the durability is mainly intended as the physical resistance to changes related to the stress and strain of use. The second goal is to estimate potential long-term behaviours of the material systems under expected conditions. Finally, processes of deterioration are speeded up in the laboratory in order to achieve a better understanding of the chemical reactions involved for example in the degradation and its physical consequences [48, 49].

The goal of the aging tests is usually to create degraded conditions inducing an alteration of sample under light exposure and usually it is necessary to reproduce a "simplified" environment. It should be a too complex and illusive undertaking to reproduce the degradation of a sample resulting from a long period of undefined burial (in terms of temperature, relative humidity, and interactions with its environment) [1]. Furthermore, it must not be forgotten that all predictions of long-term behaviour are essentially educated guesses. Fundamentally, accelerated-aging tests simply rank materials and systems regarding their stability relative to one another under a given set of conditions. This because there are difficulties in the prediction of the correlation between natural and artificial aging and in many cases, there is no correlation, or it is not possible to deduce it. It is nonetheless useful to review the approaches that

chemists and engineers have regularly employed in the effort to meet the objective of predicting long-term behaviour and time to failure. Sometimes, when there is doubt as to how well the conditions used in an accelerated-aging test will lead to a duplication of the results observable under ordinary conditions of usage, it is useful to include controls in a testing program, materials whose behaviour and effective lifetime under normal conditions of usage is reasonably well known [49].

In accelerated aging tests the most customary method of monitoring the changes that occur is to measure some chemical property, because it is realized that changes in physical properties are generally and fundamentally influenced by the chemical changes that occur with age.

Heavy reliance on the measurement of chemical properties comes about for at least two practical reasons: such measurements can usually be made with conveniently small samples and with considerable speed, sensitivity, and precision. In addition, changes in chemical properties can often be detected in advance of an obvious change in physical property. Moreover, the research investigators understand physical properties such as brittleness, tensile strength, and folding endurance are difficult to measure with precision. Consequently, most discussions regarding the theory and practice of accelerated-aging tests deal primarily with the chemical changes that materials undergo and how these changes may be interpreted to explain and compare the chemical and physical stability of a material [49].

For studying the photostability, defined as the resistance to photooxidative degradation, materials are exposed to accelerated and controlled light conditions. Thus, selecting the range of wavelength to be adopted for the ageing test is crucial. Regarding art objects, they are naturally exposed to different light conditions depending on their use and display. Objects kept indoor and part of museum collections are exposed to a light with wavelength under 280-315 nm, whereas objects exposed outdoor, as for street art and open-air museums of contemporary art, the exposure range is wider and includes UV-A and UV-B radiations, much more energetic and dangerous for the stability of the materials. In the present work the attention is focused on the stability of Asian Lacquers exposed to indoor conditions.

Electromagnetic radiation of shorter and longer wavelengths causes different reactions: short induces mainly photolytic deterioration, while longer ones induce photochemical processes. The energy of photons in the infrared range (long wavelength, low frequency) is seldom sufficiently great to induce the chemical reactions that are normally encountered in photochemical deterioration. However, as

the wavelength of radiation gets shorter and shorter, through the blue and violet region of the visible and into the ultraviolet, the photons possess an increasing amount of energy and are capable of inducing significant photochemical changes.

Although it is necessary to check each case, the wisest procedure for those interested in the behaviour of materials under museum conditions is to rarely if ever use radiation that does not pass-through ordinary window glass, nominally below 310 to 315 nm. In some research it has been demonstrated that wavelengths much below 315 nm could indeed lead to “unnatural” photochemical deterioration reactions, as written by Bauer, Peck, and Carter [50].

Many elaborate mathematical treatments have been applied to determining how well the results of accelerated aging tests correspond with the behaviour of materials during outdoor aging [51]. However, examples of extensive data on indoor aging under normal museum conditions with which to correlate with accelerated tests are extremely rare.

4. EXPERIMENTAL PART

This research began in January 2020 (Figure 23) with the preparation of Asian lacquer mock-ups, which had been subsequently monitor in their drying and curing processes for eight months. During this period of time, due to the liquid and semiliquid conditions of the samples, only FTIR Spectroscopy in Transmission mode and THM-GC/MS techniques have been used for the characterization of the materials. After 2 years of natural aging, in March 2022 the mock-ups have been analysed again. This time, thanks to the solid state achieved, it has been possible to analyse the samples with a broader spectrum of techniques. Attenuated Total Reflection (ATR) mode has been performed in addition to the Transmission mode, and both Colorimetry and Digital Microscopy has been added to the techniques.

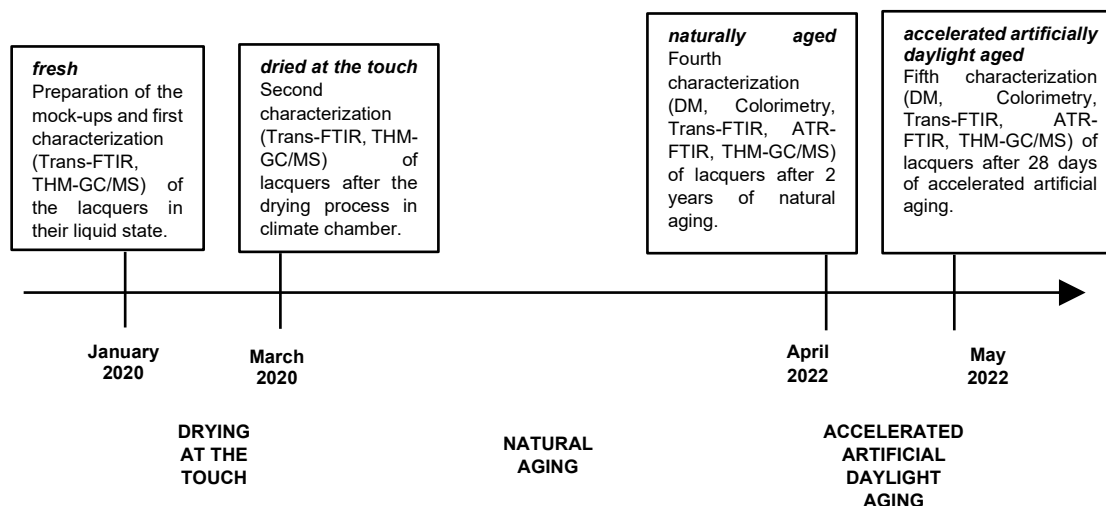


Figure 23. Timeline of the analytical methods used to characterize Asian lacquer-based samples and their correspondent physical state.

4.1 Mock-ups preparation

Seven different lacquer samples had been prepared, two years ago by another student. Each one had been prepared in four repetitions for a total of 28 mock-ups. For thitsi-based mock-ups, a pure Thitsi (Royal Forest Department of Thailand, Bangkok, Thailand) has been used: the first set has been made of pure thitsi itself, the second set has been made of pure thitsi subsequently filtered, and the third set has been made of pure thitsi subsequently filtered and added with 10% of Essential Oil (Gurjun Balsam, Mystic Moments, Hampshire, U.K). For urushi-based mock-ups a pure Urushi (Kremer, Germany) has been used. In the end three blended lacquers have been prepared: pure Urushi added with filtered Thitsi in a 1:1 ration; pure Urushi

added with filtered Thitsi in a 1:4 ration and pure urushi added with 10% essential oil filtered thitsi. The summary of the seven mock-up types is shown in Table 3 and a photo of them is shown in Figure 24:

Labelled number	Asian lacquer type
1	Thitsi pure
2	Thitsi filtered
3	Thitsi filtered + 10 % Essential Oil
4	Urushi pure
5	Urushi + Thitsi filtered (1:1)
6	Urushi + Thitsi filtered (1:4)
7	Urushi + Thitsi filtered + 10% Oil

Table 3. Summary of the seven mock-up types.

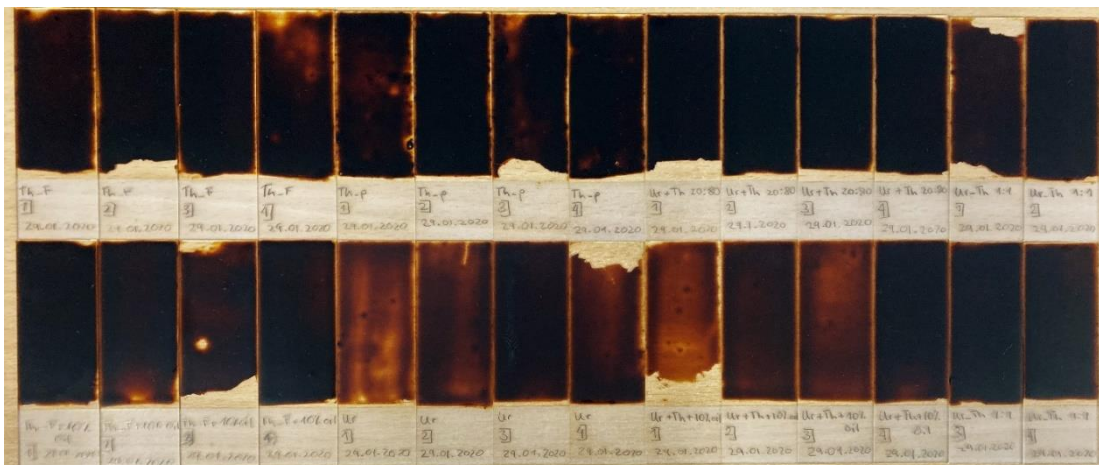


Figure 24. Photograph acquired by iPhone SE 2020 camera of the 28 mock-ups at the begin of the Erasmus+ program (March 2022), after 2 year of natural aging and before the 28-day accelerated artificial daylight aging.

The lacquer films (pure or combined) had been applied with a plastic spatula on microscope glass slides. To achieve a standardized thickness of the lacquer-layers, one glass slide had been placed between two other glass slides covered with melinex (Hostaphanfolie RN 75, 105 g/m², Deffner und Johann). The average thickness of the lacquer-specimens, therefore, has approximately the same thickness than the melinex (75µm). The pure thitsi samples had showed several lumps within the film surface, which could have not been avoided. To eliminate the lumps formation the thitsi lacquer had been filtered through a paper tissue.

4.2 Drying procedure

In order to allow the mock-ups to completely dry at their most favourable environmental conditions, each set of samples had been placed in a climate chamber at 20 °C and 80 % rH for 8 weeks, between February 2020 and March 2020, by another student. The climate chamber had been connected with tubes to distilled water and synthetic air to reach and keep constant relative humidity.

The set of pure urushi completely had dried within two weeks, while the thitsi samples (pure, filtered and mixed) had needed a longer period for drying. To reach a fully dried stage some of the samples had needed up to eight weeks. The determination of the total dryness of the specimens had been performed by examining their surface and by slightly scratching the surface with a needle under the optical microscope. Once dry the surface was not viscous and sticky anymore but solid and glassy instead.

4.3 Instruments and parameters

Digital Microscopy

Microscopic visual changes on the samples surface have been regularly documented every week during the 28 days of accelerated artificial daylight aging (between April and May 2022) by taking photos with a digital microscope Keyence VHX-6000. The digital microscope (RZ 100x-1000x objective - VH-Z100R Keyence) was equipped with a LED (Light Emitting Diode) light source with a colour temperature of 5700 K and with a LCD monitor. The images of the sample were acquired by a CMOS camera equipped with a 1/1.8-inch CMOS image sensor (virtual pixels: 1600 (H) × 1200 (V)).

In order to collect always photos approximately of the same areas of the mock-up's surface, a paper mask has been created and superimposed every time on the mock-up's surface (Figure 25).

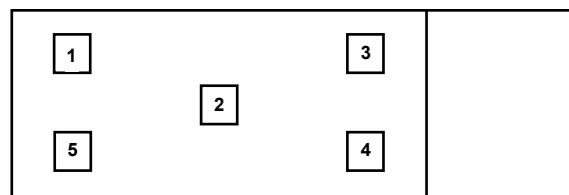


Figure 25. Representation of the paper mask used to collect photographs with Digital Microscopy.

Each area has been photographed every week with three different magnifications: 100x, 500x and 1000x. With 100x magnification a lateral light set up has been used in order to better see the roughness of the surface, while with 500x and 1000x magnification a normal perpendicular light set up has been used.

Colorimetry

For the colorimetric investigations a X-Rite Spectro Eye (Switzerland) has been employed to acquire reflection spectra of the lacquers. The instrument is equipped with a D65 illuminant (defined by the CIE, having a spectral power distribution comparable to daylight and a 6500 K colour temperature, usually obtained with a Tungsten halogen lamps), range 380-730 nm, 10° Standard Observer, and 45°/0° geometry.

The colorimetric analysis has been performed regularly every week during the 28 days of accelerated artificial daylight aging in order to monitor the colour changes of the samples. Measurement firstly took place with the acquirement of the baseline with a white reference, and then five random spots have been measured on the mock-ups surface. Differently from Digital Microscopy and FTIR Spectroscopy random spots have been chosen in order to reduce bias and to obtain a more complete representativity of the sample. However, due to the high heterogeneity of the sample layer on the mock-ups and to the low number of measurements performed on each sample, the deviation standard associated to the averaged a^* , b^* and L^* values is very high.

The data have been finally averaged and plotted using Microsoft Excel software in order to obtain both $L^*a^*b^*$ space graphs and Reflectance (ρ) against Wavelength (nm) spectra.

Fourier Transform Infrared (FTIR) Spectroscopy

FTIR analysis have been obtained in Transmission and Attenuated Total Reflection (ATR) mode with a LUMOS Standalone FTIR microscope (Bruker Optics GmbH) equipped with a Globar thermal light source, a RockSolid™ interferometer, and a liquid nitrogen cooled mid-band 100 x 100 μm^2 Photoconductive Mercury Cadmium Telluride (PC-MCT) detector. The instrument is equipped with a XYZ motorized sample stage, which allows to select digitally the area of interest. All the optics and

beam splitter were made of zinc selenide (ZnSe). Spectra has been acquired in the spectral range between 4000 and 450 cm^{-1} , performing 64 scans at 4 cm^{-1} resolution.

Attenuated Total Reflection (ATR) mode has been performed in April 2022 and May 2022 in order to characterize the material before and after the accelerated artificial daylight aging. It has not been considered for the first and second characterization in 2020 due to the liquid and semiliquid conditions of the samples from their preparation stage until the final drying stage: the tip of the crystal implemented in ATR mode and in contact with the liquid sample surface would have caused the contamination of one spot measurement to the other. In April and May 2022 five measurements for each sample have been registered and the software has been set up in order to register always the same five points of the mock-up's surface.

On the contrary, Transmission mode has been performed since the beginning of this research. In this case the sample needed to be powdered before the measurement: tiny samples have been taken from the mock-ups and placed in a diamond cell, in which were pressed prior the analyses for achieving an optimal contact with the cell. Then, between 5 and 9 measurements for each sample have been randomly registered. In both ATR and Transmission mode the resulting spectra have been collected and evaluated with the spectrum software OPUS-IRTM (Bruker Optics GmbH, Version 8.0). The collected spectra of each sample have been baselining corrected, normalized with a min-max normalization, and averaged using OPUS software.

Thermally assisted Hydrolysis and Methylation – Gas Chromatography / Mass Spectrometry (THM-GC/MS)

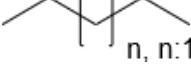
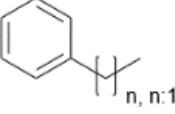
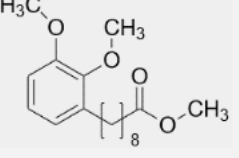
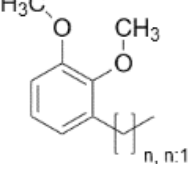
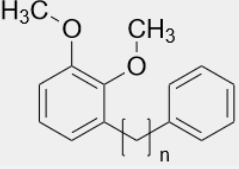
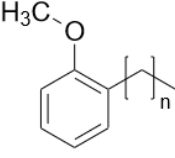
For the THM-GC/MS investigations the PY-2020iD (Frontier Lab, Japan) pyrolyzer unit combined with a GCMS-QP2010 Plus (Shimadzu, Japan) has been employed. The GC/MS unit was equipped with a capillary column SLB-5ms Supelco, U.S.A. (30 m length x 0.25 mm internal diameter x 0.25 μm film thickness) using bonded and highly cross-linked 5% diphenyl / 95% dimethyl siloxane. The capillary column was connected with a deactivated silica pre-column Rxi Guard Column Restek, U.S.A. (5 m length x 0.32 mm internal diameter). For the THM/GC-MS analysis, the pyrolysis temperature was set to 500 $^{\circ}\text{C}$, while the pyrolysis interface and the injector temperature were set to 280 $^{\circ}\text{C}$ and 250 $^{\circ}\text{C}$, respectively.

The sample preparation followed a strict procedure: a fraction of the lacquer sample was taken and weighed (about 200-300 μg) with a digital analytic balance, subsequently it was put in a sample cup (ECO-CUP Frontier Lab, Japan) and added with 2 μl of TMAH methylating reagent (25 wt% aqueous solution of TMAH, Sigma-Aldrich, USA). After approximately one hour, the THM-GC/MS analysis were performed.

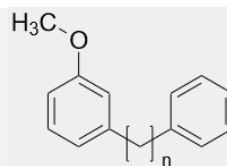
The GC column temperature conditions have been set as follows: initial temperature 40 $^{\circ}\text{C}$, held for 2 minutes and followed by a temperature increase of 6 $^{\circ}\text{C}/\text{min}$ to 300 $^{\circ}\text{C}$ and held for 20 minutes. The helium gas flow was set to 1 mL/min and the electronic pressure control was set to a constant flow of 31.7 ml/min, in split mode at a 1:50 ratio. The mass spectra were recorded under electron impact (EI) ionization in positive mode at 70 eV and the temperature of the MS interface and the ion source were 280 $^{\circ}\text{C}$ and 200 $^{\circ}\text{C}$, respectively. The mass spectrometer was scanned from m/z 50 to m/z 750. For the THM-GC/MS a solvent cut time of 5 min by turning off the filament in the ion source was used. This mode prevents the sharp decrease of the vacuum inside the ion source due to the entrance of the TMAH reagent, which has a detrimental effect on the filament and other components.

The processing and evaluation of the results have been performed thank to SHIMADZU GCMS Postrun Software and a data comparison with literature data. Unfortunately, most of the literature conducted the pyrolysis GC/MS analysis without performing the Thermally assisted Hydrolysis and Methylation with TMAH reagent [52, 53, 54, 55] or sometimes samples have been treated with different derivatising reagent, such as Hexamethyldisilazane (HMDS) [7, 56, 57]. In both cases fragments are different from the ones obtained with TMAH reagent. In the case of simple pyrolysis-GC/MS the typical Extracted Ion Chromatograms are the $m/z=108$ and $m/z=123$, showing substituted phenols and catechols, respectively. In the second case the derivatization with HMDS is a silylation reaction whose fragments have different typical EIC for the trimethylsilyl derivatives [7]. In case of TMAH derivatising reaction obtained fragments have methylated phenols and catechols and the characteristic EIC chromatograms are the $m/z=57$, showing alkyl and alkenyl hydrocarbons due to the fragmentation of aliphatic side chain (in both thitsi and urushi), and $m/z=91$, showing alkyl and alkenyl benzenes due to the fragmentation of alkylphenyl side chain (in case of thitsi), dimethoxy alkyl and phenyl benzenes (substituted methylated catechols) and anisoles. Furthermore, some oxidation products have been detected: the methyl 8-(2,3-dimethoxyphenyl) octanoate (Mazzeic acid), belonging to the acid catechols group often detected in aged lacquers,

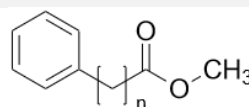
can be found in the $m/z=91$ EIC together with methyl-n-phenyl alkanoates (Körberic, Watanabic, Szelewskic and Keulenic acid) while the group of phenyl ketones can be found at $m/z=120$. In Table 4 a summury of the detected markers is shown.

EIC $m/z=57$	Chemical structure
Alkyl and alkenyl hydrocarbons	
EIC $m/z=91$	Chemical structure
Alkyl and alkenyl benzenes	
Mazzeic acid	
1,2 - Dimethoxy - alkyl and alkenyl benzenes	
1,2 - Dimethoxy - phenyl benzenes	
Alkyl anisoles	

Phenyl anisoles



Methyl-n-phenyl-alcanoates:



EIC $m/z=120$

Chemical structure

Alkylphenyl ketones

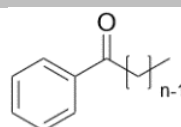


Table 4. THM-Py-GC/MS markers of Asian lacquers found in Extracted Ion Chromatograms (EIC) at: $m/z=57$, $m/z=91$ and $m/z=120$.

Accelerated artificial daylight aging

Accelerated artificial daylight aging has been performed in the period of time between April and May 2022 for 28 days starting from the *naturally aged* samples. It has been used a Daylight accelerated ageing chamber: UVACUBE SOL 500 RF2 (Dr. 2 Hönle, Germany) (460 W/m nominal irradiance) equipped with a filter glass H1, which provides radiation with wavelengths from 320 nm, thus allowing sun-glass filtered simulation.

5. RESULTS AND DISCUSSION

5.1 *Thitsiol*

5.1.1 Digital Microscopy

The images obtained with Keyence Digital Microscopy in three different magnifications (100x, 500x, 1000x) of thitsi pure, thitsi filtered and thitsi filtered with 10% oil are shown in Figure 26, 27 and 28, respectively.

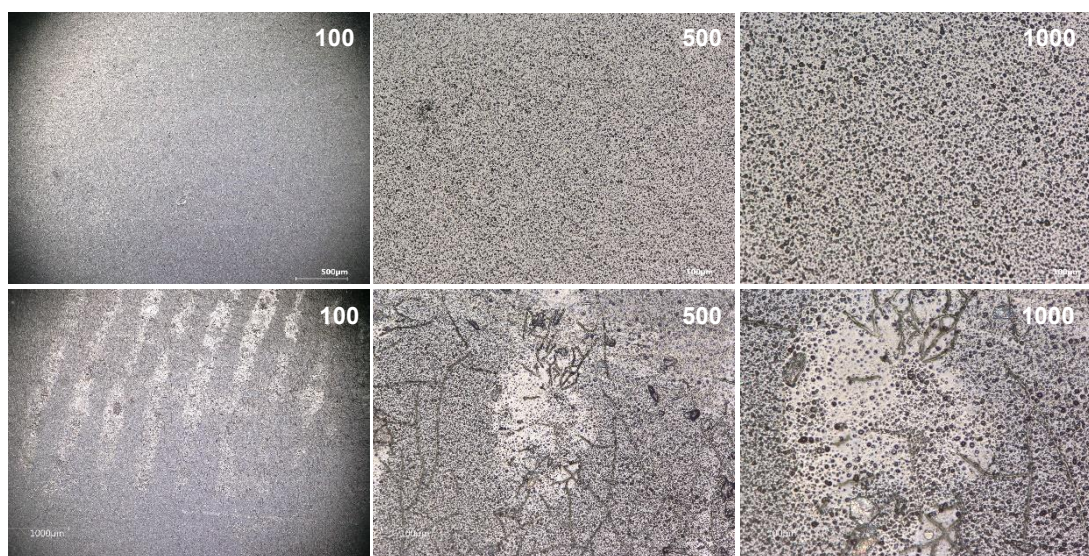


Figure 26. Pre (up) and post (down) accelerated artificial daylight aging images of thitsi pure acquired by digital microscopy in three different magnifications: 100x (left), 500x (middle), 1000x (right).

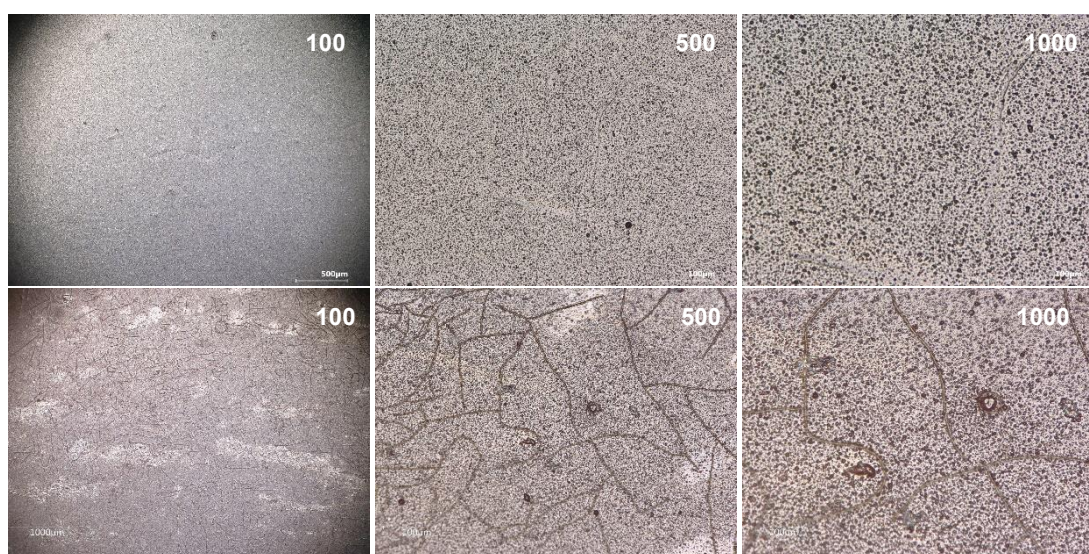


Figure 27. Pre (up) and post (down) accelerated artificial daylight aging images of thitsi filtered acquired by digital microscopy in three different magnifications: 100x (left), 500x (middle), 1000x (right).

Digital Microscopy investigation on thitsi lacquer gave interesting results about the resistance of the material and the physical changes in its surface when subjected to accelerated artificial daylight aging. After 28 days in UV chamber thitsi-based samples showed several geometric cracks all along the surface of the materials. The cracks network seems to be thicker and more geometric for thitsi filtered and thitsi filtered added with 10% of essential oil, while in thitsi pure images the cracks network is more irregular.

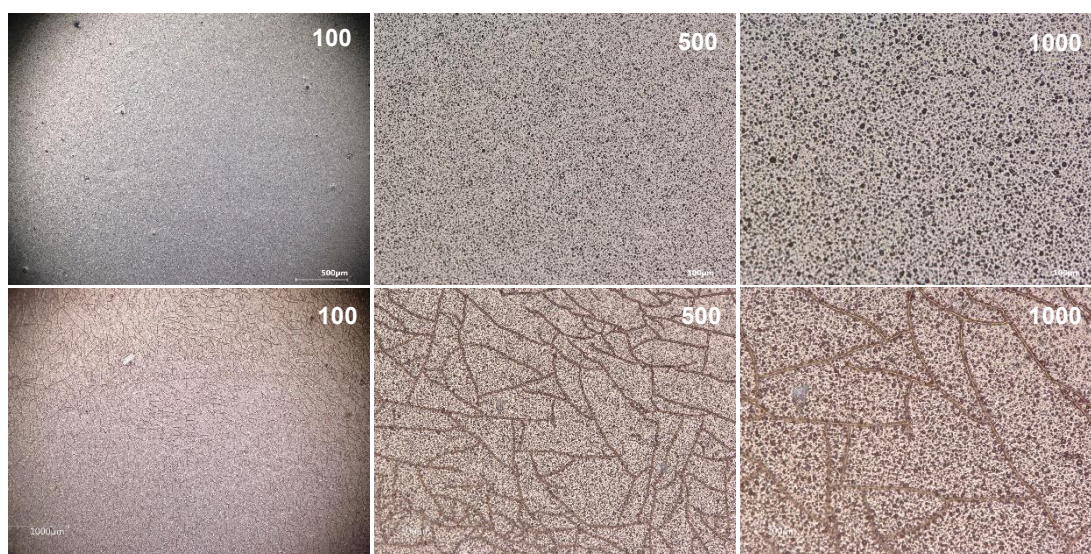


Figure 28. Pre (up) and post (down) accelerated artificial daylight aging images of thitsi filtered with 10% oil acquired by digital microscopy in three different magnifications: 100x (left), 500x (middle), 1000x (right).

This network of cracks is the physical evidence that an oxidation process has happened. According to the literature, this process begins on the surface of the material and with the occurring of the oxidation process the cracks become deeper and deeper [1]. As reported in paragraph 2.1.2 the oxidation process leads to the oxidation of the conjugated side chain of catechol and subsequently to the formation of a series of oxidation products which, in the end, leads to the decomposition of the polymerized lacquer network [1]. Furthermore, the light-degraded layer swells and shrinks at a different rate to the undamaged surface beneath, and the differential tension that is created as result is relieved by the formation of cracks [25].

Another important phenomenon detected in thitsi-based samples' surface is the appearance of some circular and dark spots after 28 days of accelerated artificial daylight aging. They could be interpreted as the of the dispersed polysaccharide particles in the surface layer, due to the UV exposure. In fact, under light exposure,

the core-shell structure, composed of a thin shell of polysaccharides and glycoproteins and surrounding the polymerized catechols, is damaged. This fact has been detected in the literature [1] with the appearance of circular spots in the surface of some artificially aged Asian lacquer samples.

The black small and circular spots in the background are the marks of waterdrops in the lacquer sap [58]. No significant qualitative changes during the 28 days of accelerated artificial daylight aging have been detected.

5.1.2 Colorimetry

Colorimetry investigation on thitsi lacquer gave different information useful for the understanding of the material colour and reflectance behaviour during the 28 days of accelerated artificial daylight aging.

The reflectance spectra of thitsi pure, thitsi filtered and thitsi filtered with 10% oil are shown in Figure 29, 30 and 31, respectively. In all three spectra it is easily possible to notice a shift to higher reflectance number from the pre aging (blue) to the post aging (orange). This means that thitsi lacquer type tends to increase its reflecting power after an aging process.

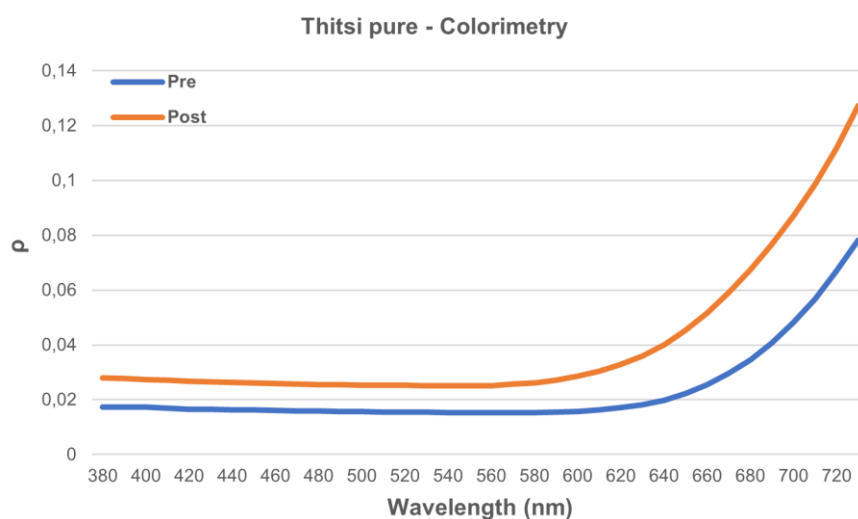


Figure 29. Reflectance spectrum of thitsi pure pre (blue) and post (orange) accelerated artificial daylight aging.

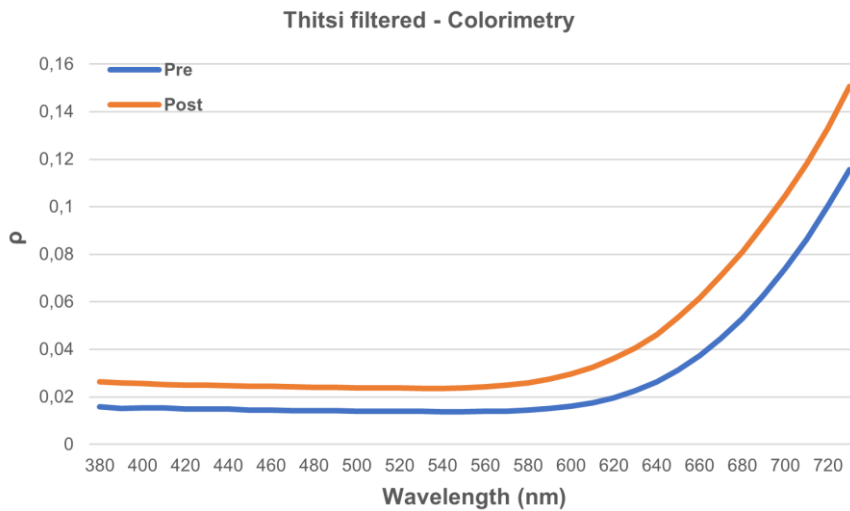


Figure 30. Reflectance spectrum of thitsi filtered pre (blue) and post (orange) accelerated artificial daylight aging.

The $L^*a^*b^*$ space graphic representations of thitsi pure, thitsi filtered and thitsi filtered with 10% oil, are shown in Figure 32, 33 and 34, respectively while the measured values are shown in Table 5 together with their standard deviations. The high heterogeneity of the sample layer on the mock-ups and the low number of measurements performed on each sample determined a very high standard deviation for L^* , a^* and b^* values. In each image it is represented the variation of colour depending on the three L^* , a^* and b^* coordinates of the $L^*a^*b^*$ space with two separate graphs: to the left it is shown the a^* against b^* graph which demonstrates

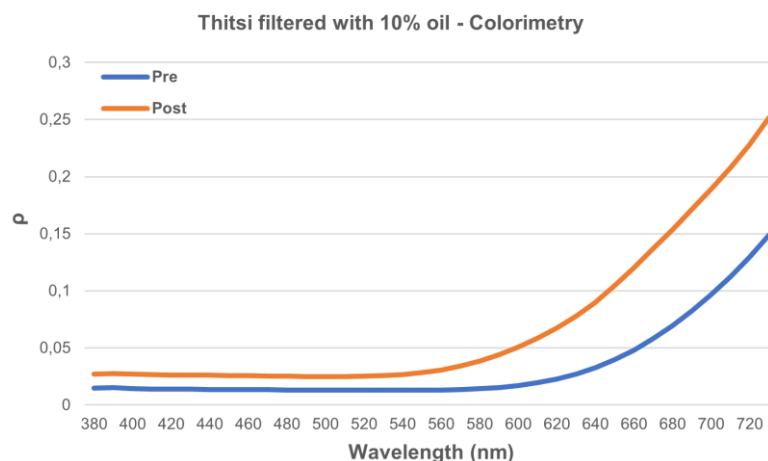


Figure 31. Reflectance spectrum of thitsi filtered with 10% oil pre (blue) and post (orange) accelerated artificial daylight aging.

that thitsi lacquer type is subjected to a common shift to a^{*+} coordinate (red in the red/green axis) and b^{*+} coordinate (yellow in the yellow/blue axis). This means that the colour of this material has changed to more red and more yellow hues during the 28 days of accelerated artificial daylight aging. Interesting is the fact that among the three thitsi-based samples the one with a higher yellowing (Δb^{*}) is thitsi with 10% of essential oil. This could be due to the presence of the oil, which is known to shift to more yellow hue with aging [59].

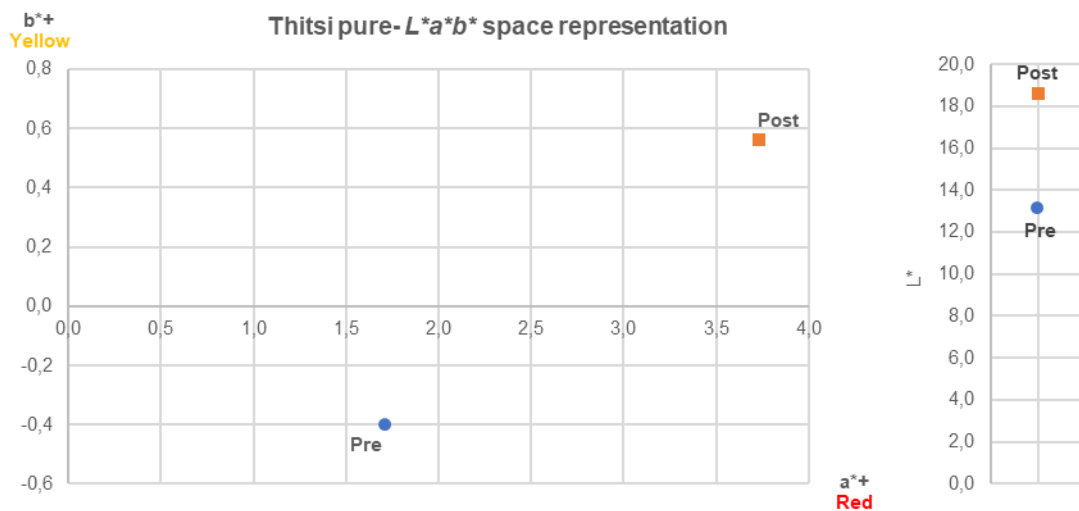


Figure 32. $L^*a^*b^*$ space representation of thitsi pure pre (blue) and post (orange) accelerated artificial daylight aging: a^*b^* graph (left) and L^* graph (right).

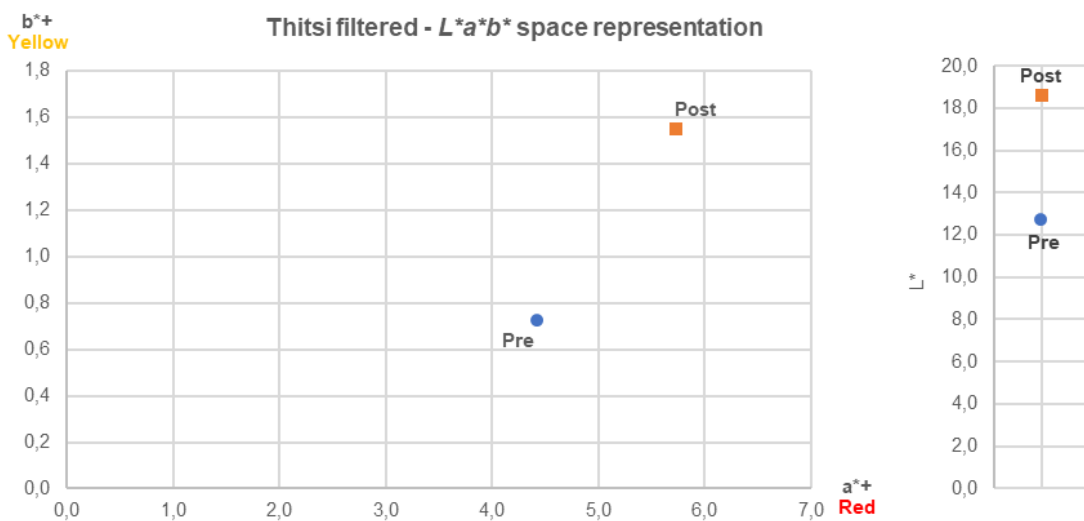


Figure 34. $L^*a^*b^*$ space representation of thitsi filtered pre (blue) and post (orange) accelerated artificial daylight aging: a^*b^* graph (left) and L^* graph (right).

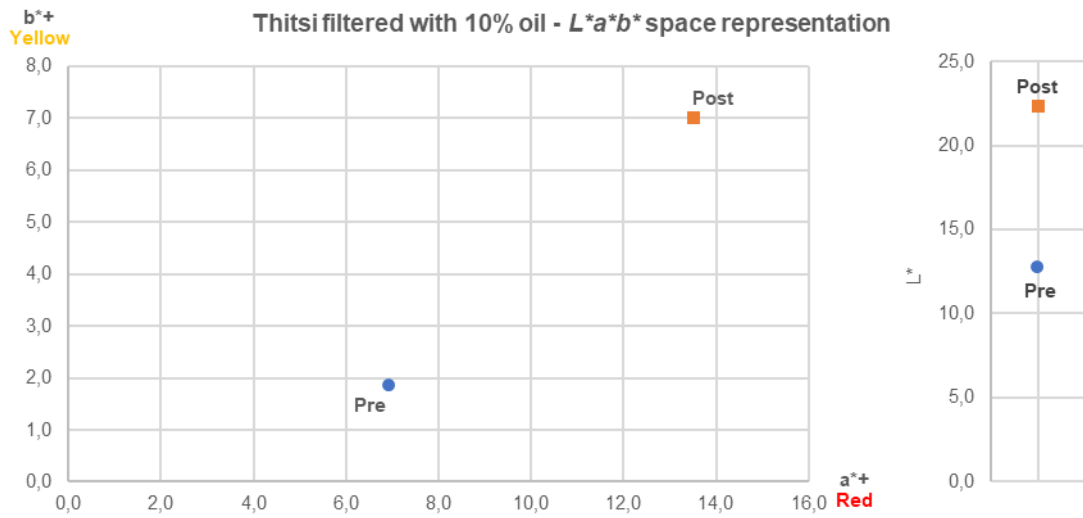


Figure 33. $L^*a^*b^*$ space representation of thitsi filtered with 10% oil pre (blue) and post (orange) accelerated artificial daylight aging: a^*b^* graph (left) and L^* graph (right).

More important is the variation of the L^* coordinate. Each thitsi sample shows an increase of L^* values which means a common tendency to shift to brighter colour. Since the white and black components are correlated to a higher and lower reflectance, respectively, (if light is fully absorbed, the object looks black; if it is fully reflected, the object is white) it is possible to deduce that this material tends to increase its reflecting power. Therefore, both colorimetric measurements gave the same result: thitsi lacquer type subjected to an accelerated artificial daylight aging shows an increase in reflectance.

The calculated ΔE^* values are shown in Table 5: the higher the increase of this number, the higher the total colour change of the material. Comparing thitsi pure, filtered and filtered added with 10% oil it has been found that thitsi filtered with 10% oil has the higher increase of ΔE^* number, due to the high contribution of b^* . This is due to the presence of essential oil and its tendency to yellowing as already said. Furthermore, according with Table 2, thitsi pure and thitsi filtered ΔE^* mean that the colour change is “perceptible at a glance” while thitsi filtered with 10% oil ΔE^* means that “colours are more similar then opposite”.

	L*	s _x (L*)	a*	s _x (a*)	b*	s _x (b*)	ΔE*
Thitsi pure Pre	13,1	0,2	1,7	2,0	-0,4	0,7	
Thitsi pure Post	18,6	2,5	3,7	2,8	0,6	1,1	5,9
Thitsi filtered Pre	12,7	0,6	4,4	3,2	0,7	1,4	
Thitsi filtered Post	18,6	0,9	5,7	4,1	1,5	2,0	6,1
Thitsi filtered with 10% oil Pre	12,7	0,4	6,9	2,0	1,9	0,9	
Thitsi filtered with 10% oil Post	22,3	2,1	13,5	4,6	7,0	5,1	12,7

Table 5. L*, a* and b* values and their standard deviations measured for thitsi pure, thitsi filtered and thitsi filtered with 10% oil before (pre) and after (post) accelerated artificial daylight aging and the calculated ΔE*.

5.1.3 FTIR

In the following section Transmission mode FTIR spectra and Attenuated Total Reflection mode (ATR) FTIR spectra of thitsi pure, thitsi filtered and thitsi filtered with oil, are shown. As described in the timeline scheme (Figure 23), Transmission spectra have been registered since the mock-ups preparation when the material was still in a liquid state (*fresh*) and then in every step of their physical state change: after the drying in climate chamber (*dried at the touch*), after 2 years of natural aging (*naturally aged*), and after 28 days of accelerated artificial daylight aging (*accelerated artificially daylight aged*). ATR spectra have been registered only for *naturally aged* and accelerated artificial aged thitsi-based samples, due to liquid and semiliquid state of the material in the first two steps.

Transmission mode

The Transmission Spectra of thitsi pure, thitsi filtered and thitsi filtered with 10% oil are shown in Figure 34, 35 and 36, respectively. The complete peaks assignment is shown in Table 6.

The spectra show the changes of functional groups in thitsi-based samples during the drying, natural aging and accelerated artificial daylight aging process. The series of absorption between 3100-3000 cm⁻¹ have been assigned to C-H stretching of cis double bonds in the different side chains of *thitsiol* (Figure 2). The one at 3024 cm⁻¹, assigned to C-H stretching of double bonds in the side chain, is the most intense in the spectrum registered when the mock-ups were still *fresh*, but it decreases after eight weeks of drying in climate chamber.

Absorptions at 2924 and 2853 cm^{-1} have been assigned to asymmetric and symmetric C-H in the side chain, respectively, and no significant changes in their intensity ratio has been observed, in agreement with the literature [1]. The most significant variation in terms of intensities ratio has been detected for the peaks around 1715 and 1595 cm^{-1} , assigned to carbonyl in the oxidation products, and C=C stretching of the aromatic ring skeletal vibrations of the polymerized catechol derivatives, respectively. In the spectrum registered with *fresh* urushi, the peak at 1595 cm^{-1} is higher than the one at 1725 cm^{-1} . After 8 weeks of drying in climate chamber, the carbonyl absorption slightly increases in intensity, but the predominant absorption is still the C=C ring absorption. After 2 years of natural aging, the carbonyl absorption increases in

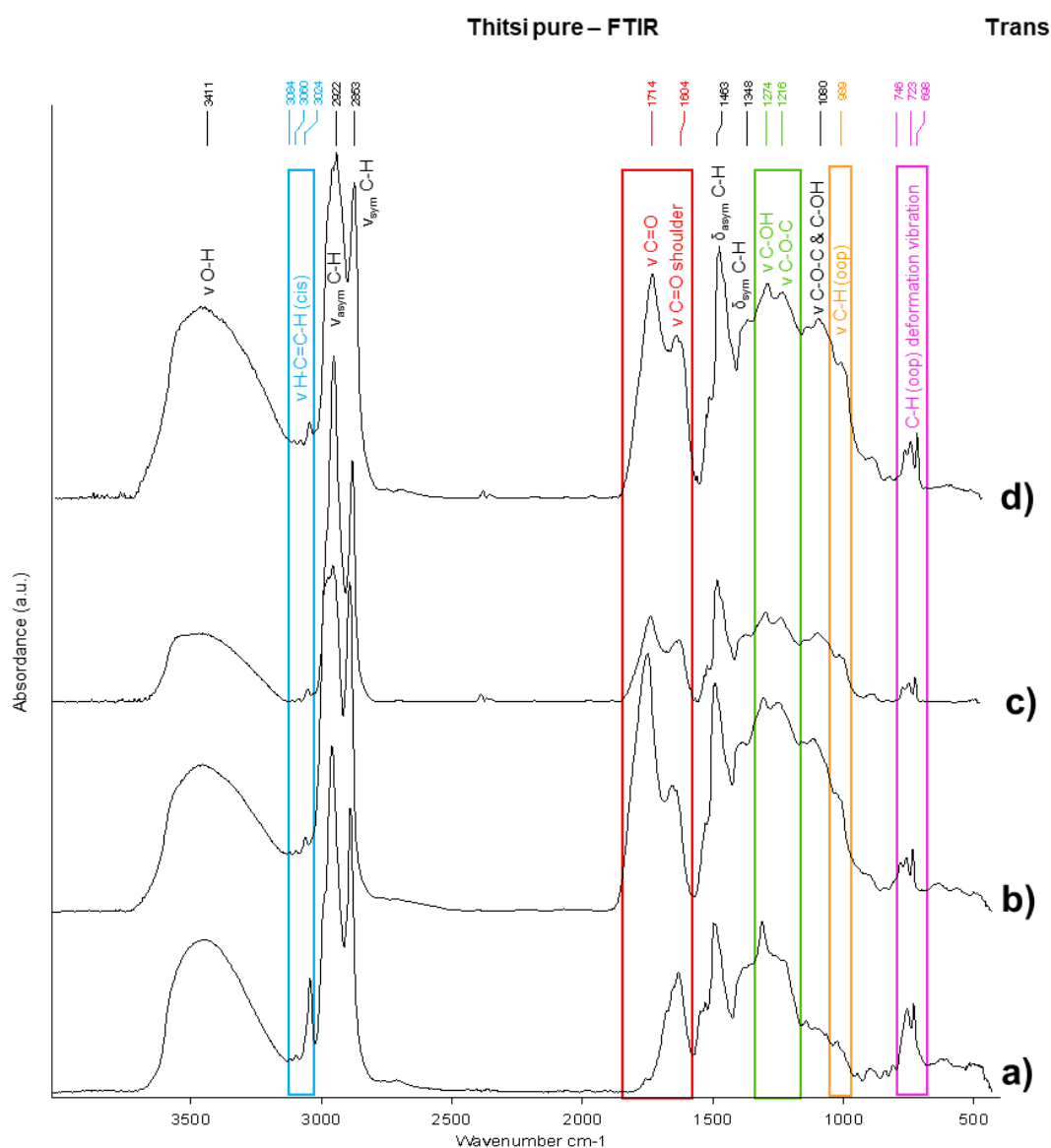


Figure 34. Transmission FTIR spectra of *thitsi pure*: **a)** fresh, **b)** dried at the touch (8 weeks), **c)** naturally aged (2 years) and **d)** accelerated artificially daylight aged (28 days, starting from the naturally aged samples set).

intensity and shifts towards lower wavenumber, at 1715 cm^{-1} , due to the oxidation products formation. The increase in the intensity of the carbonyl peak continued after 28 days of accelerated artificial aging and it has been associated to the progressing of oxidation process [17].

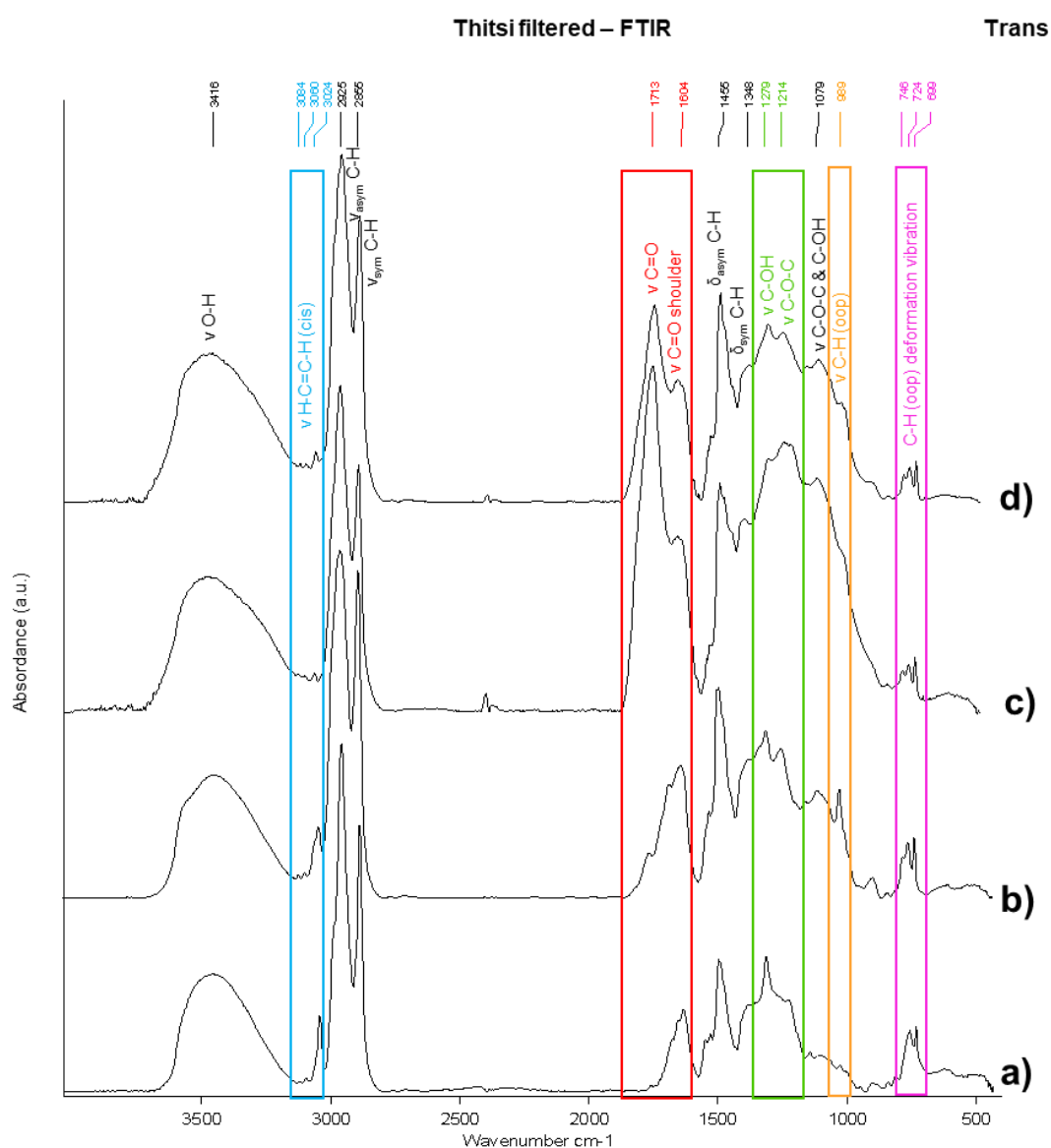


Figure 35. Transmission FTIR spectra of thitsi filtered: **a)** fresh, **b)** dried at the touch (8 weeks), **c)** naturally aged (2 years) and **d)** accelerated artificially daylight aged (28 days, starting from the naturally aged samples set).

It is interesting to point out the progressive decreasing of the peak at 1274 cm^{-1} , assigned to C-OH stretching in catechols and phenols. Its decrease is representative of the lacquer photo-oxidation, that also leads to a loss of hydroxyl functions on the catechol ring [1] and that the hydroxyl groups in the catechol monomer polymerized

in nucleus-nucleus and nucleus-side chain coupling as the laccase polymerization advanced [20, 27]. In general, the region 1300-1000 cm^{-1} is assigned to C–O stretching vibrations that have different contributions from different functional groups to their intensities, namely C–OH groups: ether groups formed during the oxidative polymerization of lacquer and C–O–C glycosidic groups from the lacquer polysaccharides [41].

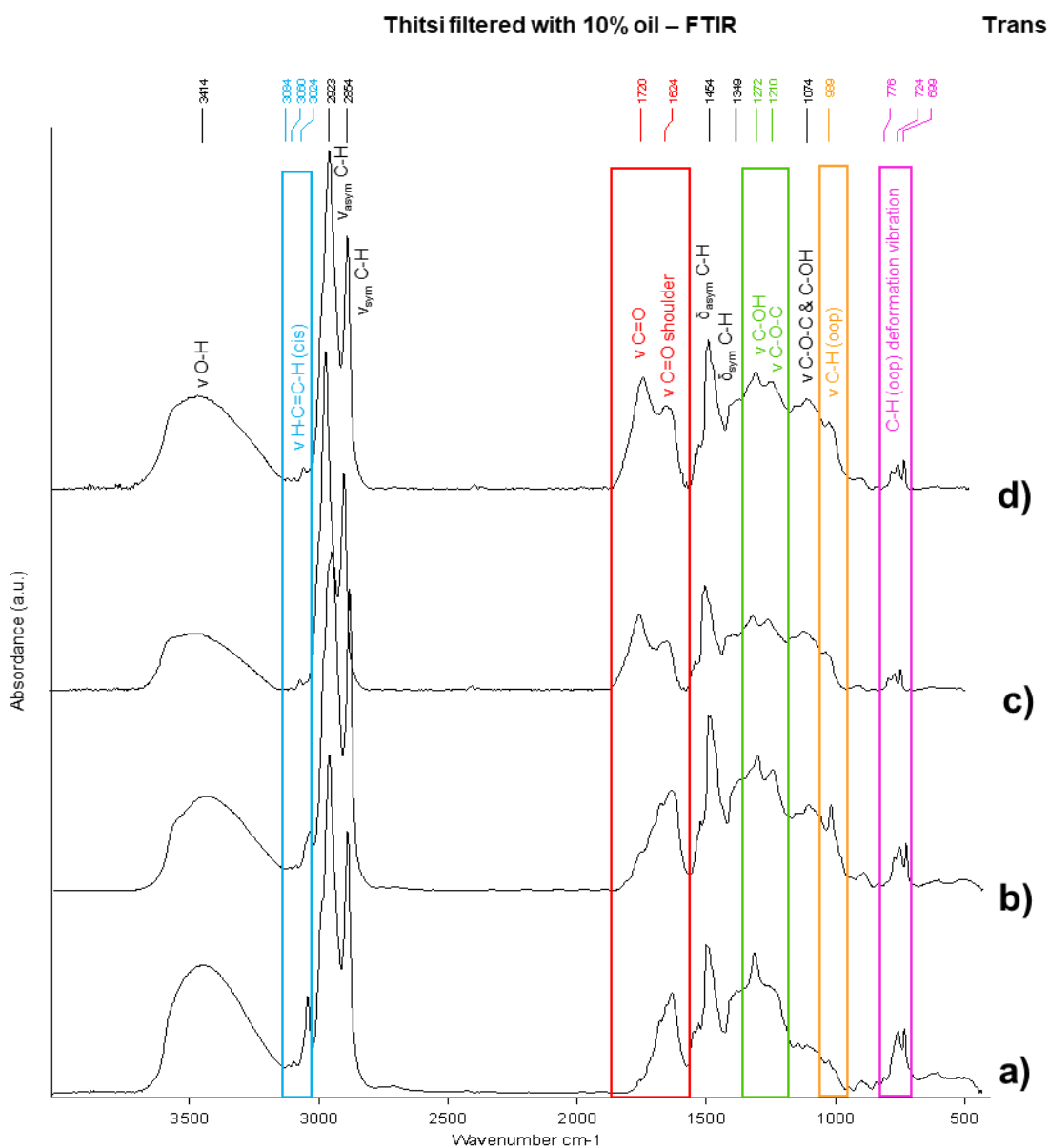


Figure 36. Transmission FTIR spectra of thitsi filtered with 10% oil: **a)** fresh, **b)** dried at the touch (8 weeks), **c)** naturally aged (2 years) and **d)** accelerated artificially daylight aged (28 days, starting from the naturally aged samples set).

A significant transformation induced by the aging is the decreasing in intensity of the absorption centred at 993 cm^{-1} , assigned to C-H out of plane stretching of conjugated

trienes in the side chain. Its decrease has been interpreted as a decrease in the number of unsaturated side chains, as the polymerization occurs [1]. Finally, the three peaks around 776, 731 and 699 cm^{-1} have been assigned to C-H deformation vibrations out-of-plane. The 731 cm^{-1} one, in particular, is assigned to the catechol group in the monomer and its decrease suggests that the enzyme polymerization had occur [20].

Thitsi pure (cm^{-1})	Thitsi filtered (cm^{-1})	Thitsi filtered+ 10% oil (cm^{-1})	Peaks Assignment
3411	3416	3414	O-H stretching of catechol ring or polysaccharide [9, 20, 27, 41]
3084 – 3060 - 3024	3084 – 3060 - 3024	3084 – 3060 - 3024	H-C=C-H stretching of the different substituted catechols, phenols and aromatic side chains in <i>thitsiol</i> [60]
2922	2925	2923	C-H stretching asymmetric of CH_2 and CH_3 of the side chain [9, 17, 41]
2853	2855	2854	C-H stretching symmetric of CH_2 and CH_3 of the side chain [9, 27, 41]
1714	1713	1720	C=O stretching [9, 17, 41]
1604	1604	1624	C=C stretching (C=O shoulder) of the aromatic ring skeletal vibrations of the polymerized catechol derivatives [41]
1463	1465	1454	C-H bending (asymmetric) of side chain [17, 41]
1348	1348	1349	CH_3 bending (symmetric) [9]
1274	1279	1272	C-OH stretching of phenol [41]
1216	1214	1210	C-O-C glycosidic group [1, 41]
1080	1079	1074	C-O-C of sugar units [61] or C-OH stretching of polysaccharides [41]
989	989	989	C-H out of plane stretching of conjugated trienes in the side chain [9, 20]
746	746	776	C-H deformation vibration out-of-plane [41]
723	724	724	C-H deformation vibration out-of-plane [41] due to catechol in the monomer [20]
699	699	699	C-H deformation vibration out-of-plane [41] due to catechol in the monomer [20]

Table 6. Transmission FTIR peaks and their assignment for *thitsi* pure, *thitsi* filtered and *thitsi* filtered with 10% oil.

ATR mode

The ATR Spectra of thitsi pure, thitsi filtered and thitsi with 10% oil are shown in Figure 37, 38 and 39, respectively.

The complete peaks assignment is shown in Table 7.

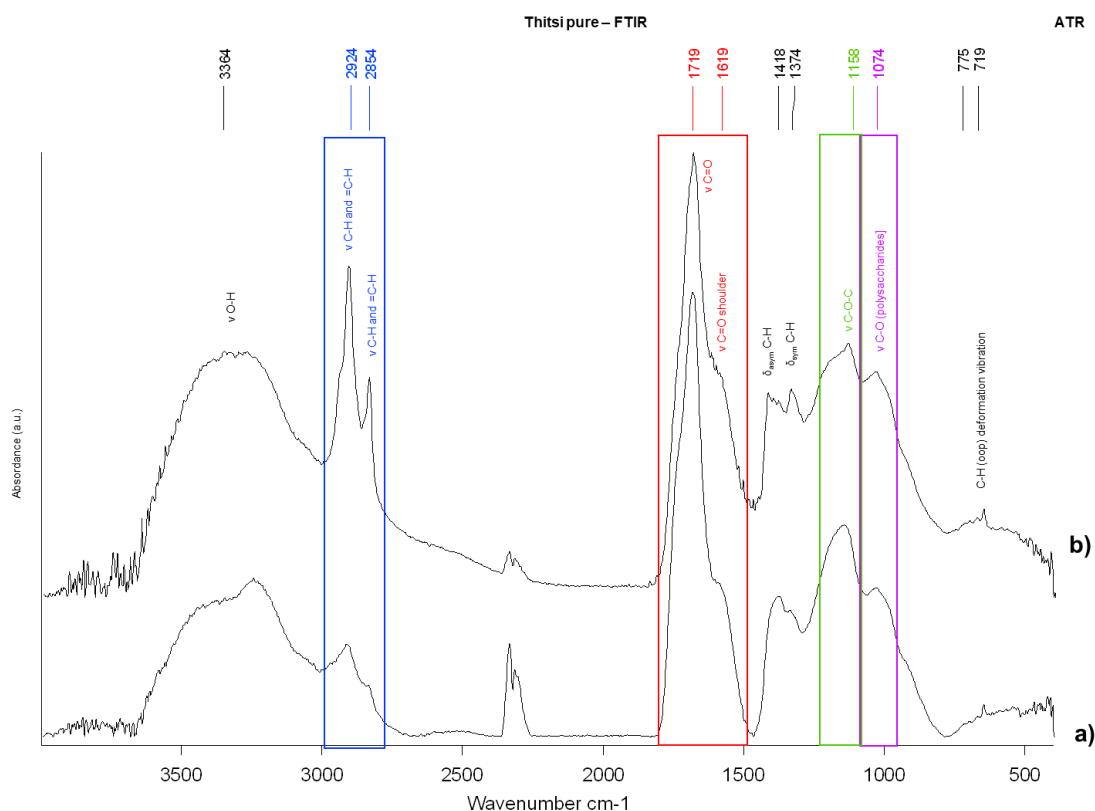


Figure 37. Attenuated Total Reflection FTIR spectra of thitsi pure: **a)** naturally aged (2 years) and **b)** accelerated artificially daylight aged (28 days, starting from the naturally aged samples set).

The spectra show the changes of functional groups in thitsi-based samples' surface after the natural aging and accelerated artificial daylight aging processes. It is possible to notice that ATR spectra profile is different from Transmission spectra profile and some typical peaks, for examples the characteristic peak at 3100-3000 cm^{-1} detected Transmission spectra are not present in the ATR one. This is probably due to the higher signal/noise ratio registered in ATR spectra. The ATR mode works with the surface of materials and its performing depends on the physical state of the material and on the pressure of the interaction between the crystal and the material. So, the sensibility of the ATR mode is intrinsic lower than Transmission mode and the detection of mild peaks such as the ones between 3100-3000 cm^{-1} is lost.

The peaks at 2924 and 2854 cm^{-1} , assigned to C-H stretching in the side chain, have been detected in ATR spectra too. However, in ATR spectra an increase in the relative intensity of the peak at 2924 cm^{-1} have been detected, differently from Transmission spectra where the 2924/2854 ratio was constant with the passage of the time. This is due to the fact that after 28 days of accelerated artificial daylight aging the oxidation process led to the formation of oxidation products and to the disintegration of the polymerized network, included the aliphatic chains. However, this disintegration mechanism begins from the surface of the material and not from the bulk: this is the reason why the decrease of absorption at 2924 and 2854 cm^{-1} has been detected with ATR and not with Transmission mode.

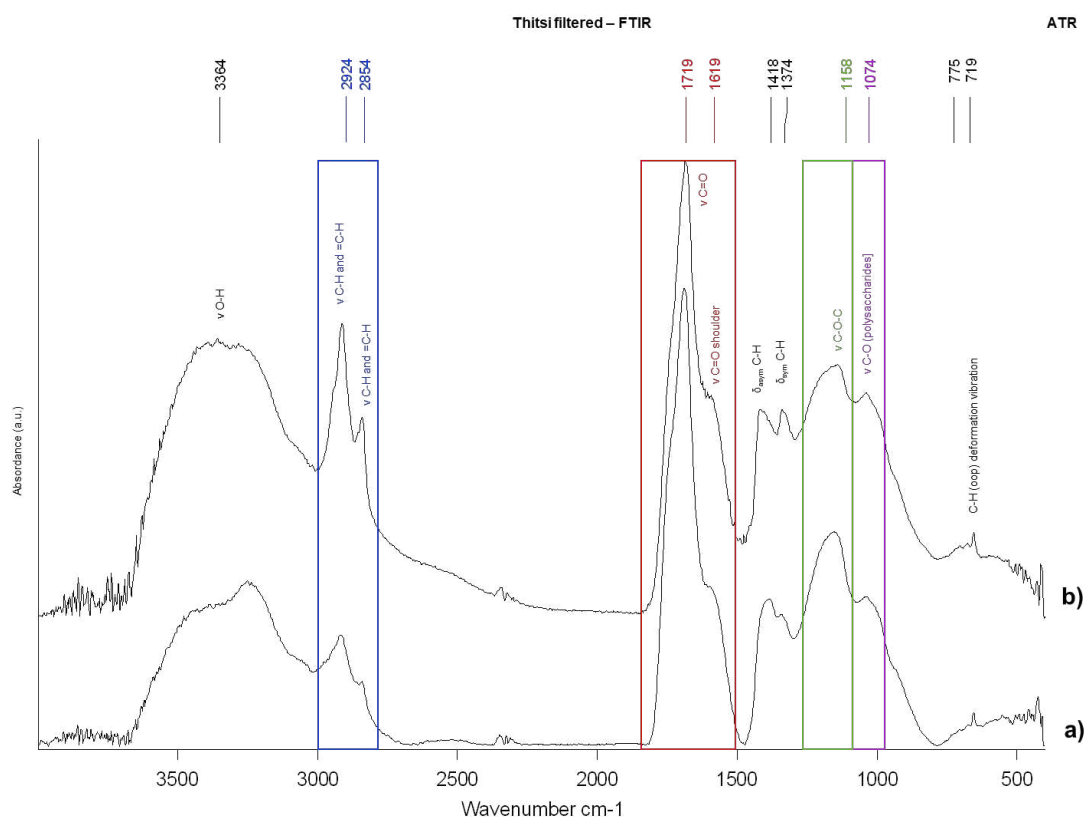


Figure 38. Attenuated Total Reflection FTIR spectra of thitsi filtered: **a)** naturally aged (2 years) and **b)** accelerated artificially daylight aged (28 days, starting from the naturally aged samples set).

The carbonyl and aromatic C=C stretching absorption in the ATR spectra does not show significant variations in comparison with the ones collected in Transmission mode. This is because ATR mode spectra have been registered only with 2-year naturally aged thitsi-based lacquers (a) and 28-days artificially accelerated daylight

aged thitsi-based lacquer (b)) and at this stage of the aging process oxidation products, responsible for the absorption at 1719 and 1619 cm^{-1} , have already been formed.

The absorption centred at 1158 cm^{-1} has been assigned to the C-O stretching in the phenol groups [41, 62] while the one at 1074 cm^{-1} has been assigned to the polysaccharide component. The latter slightly increases during the 28 days of accelerated artificial daylight aging as consequence of the breaking of the core-shell structure of polysaccharides and glycoproteins, described in paragraph 2.2.2. According with literature [1], the UV exposure allows the surface release of polysaccharide units, so this evidence is particularly evident in the ATR spectrum. On the contrary, the spectra collected in Transmission mode do not show any increasing, because of the predominance of the bulk contribution.

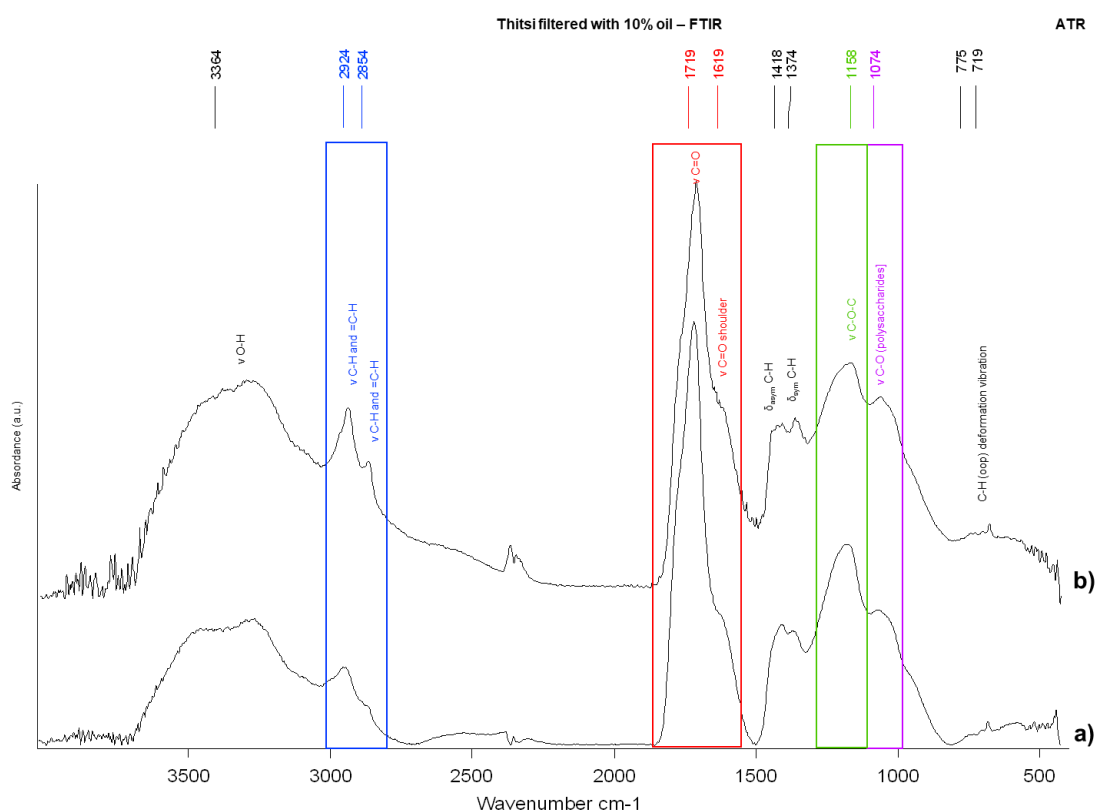


Figure 39. Attenuated Total Reflection FTIR spectra of thitsi filtered with 10% oil: **a)** naturally aged (2 years) and **b)** accelerated artificially daylight aged (28 days, starting from the naturally aged samples set).

Wavenumber (cm ⁻¹)	Peaks Assignment
3364	O-H stretching of catechol ring or polysaccharides [9, 20, 27, 41]
2924	C-H and H-C=C-H stretching [62]
2854	C-H and H-C=C-H stretching
1719	C=O stretching [62]
1619	C=C stretching (C=O shoulder) of the aromatic ring skeletal vibrations of the polymerized catechol derivatives [62]
1418	C-H bending (asymmetric) of side chain [17, 41]
1374	CH ₃ bending (symmetric) [9]
1158	C-O-C stretching [62]
1074	C-O stretching in polysaccharides [1, 41]
775 - 719	C-H deformation vibration out-of-plane [62]

Table 7. ATR FTIR peaks and their assignment for thitsi pure, thitsi filtered and thitsi filtered with 10% oil.

5.1.4 THM-Py-GC/MS

In the following section Total Ion Chromatograms (TIC) and the most significant Extracted Ion Chromatograms (EICs) of thitsi filtered, thitsi pure, and thitsi filtered with 10% oil are shown. As described in the timeline scheme (Figure 23), these chromatograms were registered at different timing, starting when the lacquers were freshly applied on the glass-slides and in a liquid state (*fresh*), followed by different and consequent periods of time corresponding to their chemical-physical change: after the drying in climate chamber (*dried at the touch*), after 2 years of natural aging (*naturally aged*), and finally after 28 days of accelerated artificial daylight aging (*accelerated artificially daylight aged*).

TIC

Total Ion Chromatograms (TIC) of thitsi pure, thitsi filtered and thitsi filtered with 10% oil, are shown in Figure 40, 41 and 42, respectively.

The TIC profile of the thitsi-based Asian lacquer models shows two main groups of peaks: the first, between 5-33 minutes of retention time (RT), shows an irregular shape which becomes thicker with the time and which is characterized by the most intense peak of the series around 30,100 RT; the second, between 40-48 minutes of

retention time (RT), is a set of peaks assigned to dimethoxy alkyl and phenyl benzenes, due to the methylation of catechols with the TMAH derivatising reagent. This last series of peaks decreases after 8 weeks of drying process in climate chamber, and it could be due to the nucleus-nucleus coupling occurring during laccase polymerization. This type of coupling involves catechol hydroxyl groups in the formation of polymerized network and, as a consequence, less hydroxyl groups are available for the methylation with the passage of time.

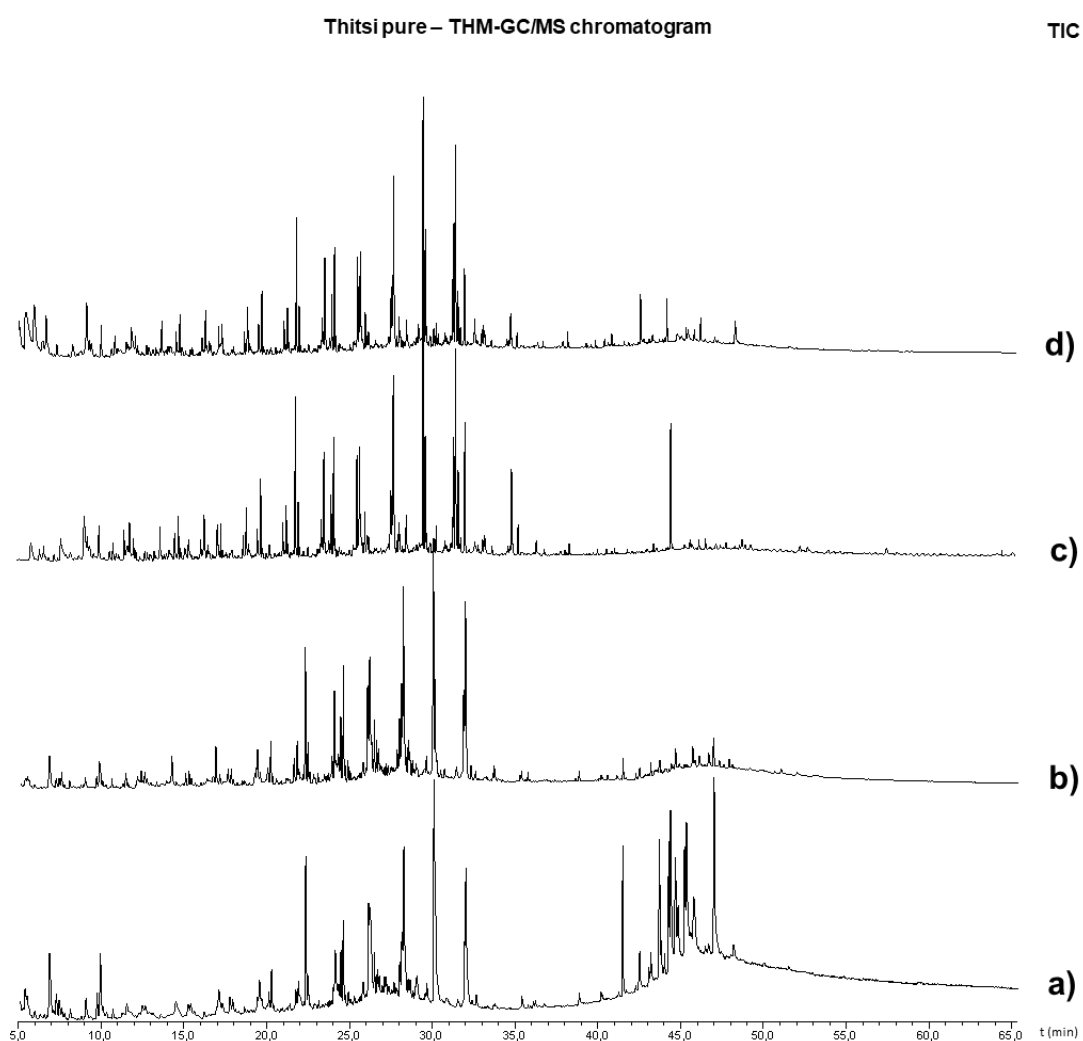


Figure 40. Total ion chromatograms (TIC) of thitsi pure acquired by THM-GC/MS: **a)** fresh, **b)** dried at the touch (8 weeks), **c)** naturally aged (2 years), and **d)** accelerated artificially daylight aged (28 days, starting from the naturally aged samples set).

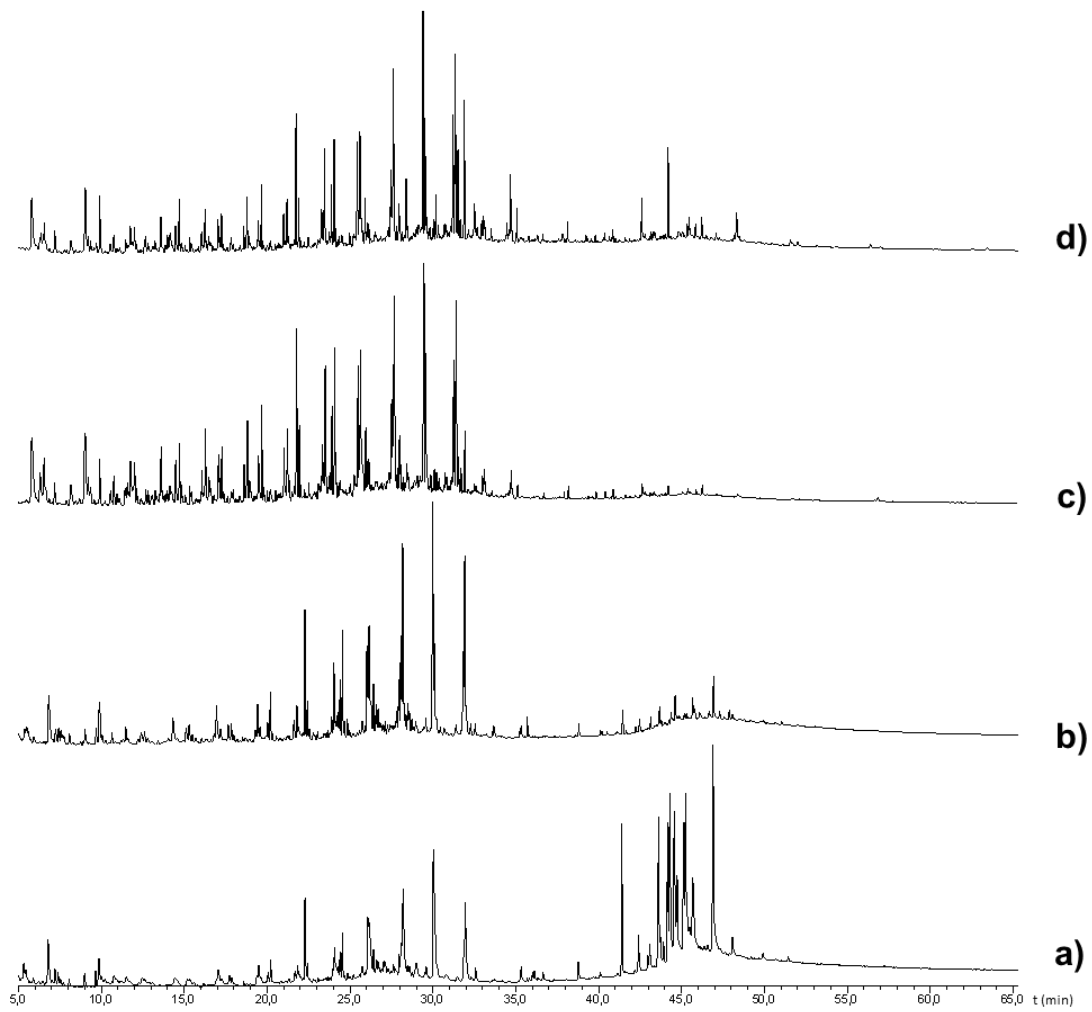


Figure 41. Total Ion Chromatograms (TIC) of thitsi filtered acquired by THM-GC/MS: **a)** fresh, **b)** dried at the touch (8 weeks), **c)** naturally aged (2 years) and **d)** accelerated artificially daylight aged (28 days, starting from the naturally aged samples set).

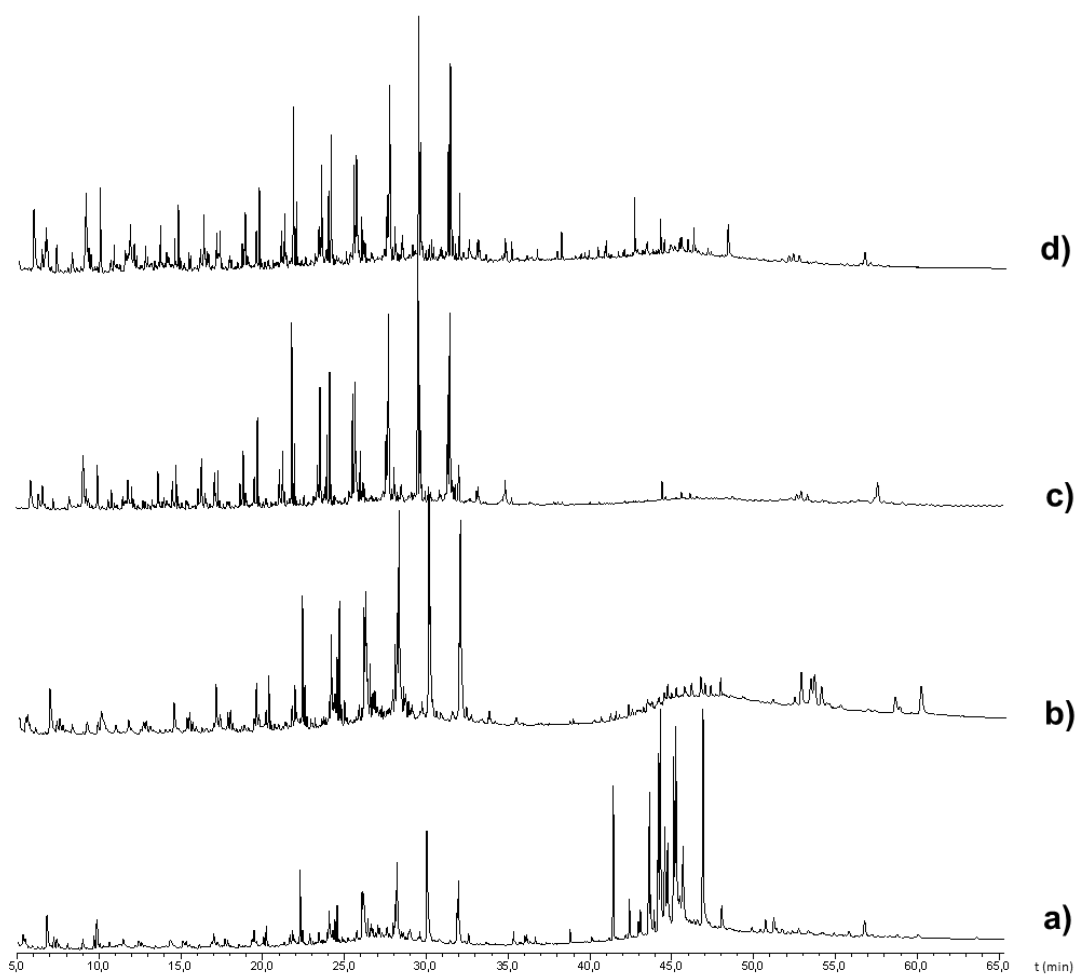


Figure 42. Total Ion Chromatograms (TIC) of thitsi filtered with 10% oil acquired by THM-GC/MS: **a)** fresh, **b)** dried at the touch (8 weeks), **c)** naturally aged (2 years) and **d)** accelerated artificially daylight aged (28 days, starting from the naturally aged samples set).

$m/z=57$ – alkanes and alkenes

Extracted Ion Chromatograms (EIC) at $m/z=57$ of thitsi pure, thitsi filtered, and thitsi filtered with 10% oil, are shown in Figure 43, 44, and 45, respectively.

These EICs show alkyl ($m/z=57$ as base peak) and alkenyl ($m/z=55$ as base peak) hydrocarbons fragments which are the pyrolytic products produced by the cleavage of the linear saturated and unsaturated side chain hydrocarbon on the aromatic ring of catechol such as on the 3- and 4-alkylcatechols in *thitsiol* (Figure 2) [19, 56].

By looking at the the pyrolytic profiles of the EICs at m/z 57 registered for the *fresh* (a) and *dried-at-the-touch* (b) thitsi it is possible to notice a flat-shape between RT 10 and 18 minutes (A9-A12), with A9 as the most intense peak. This changes to a bell-

shape in the EICs registered after the 2 years of natural aging, with A11 as the most intense peak. This could be due to the shift of double bonds in *thitsiol* side chain, due to the several nucleus-side chain and/or side chain-side chain couplings that occurs with polymerization. The pyrolytic fragmentation could, in this way, change its preferential positions along the side chain. The accelerated artificial daylight ageing did not influence any change in this chromatographic range.

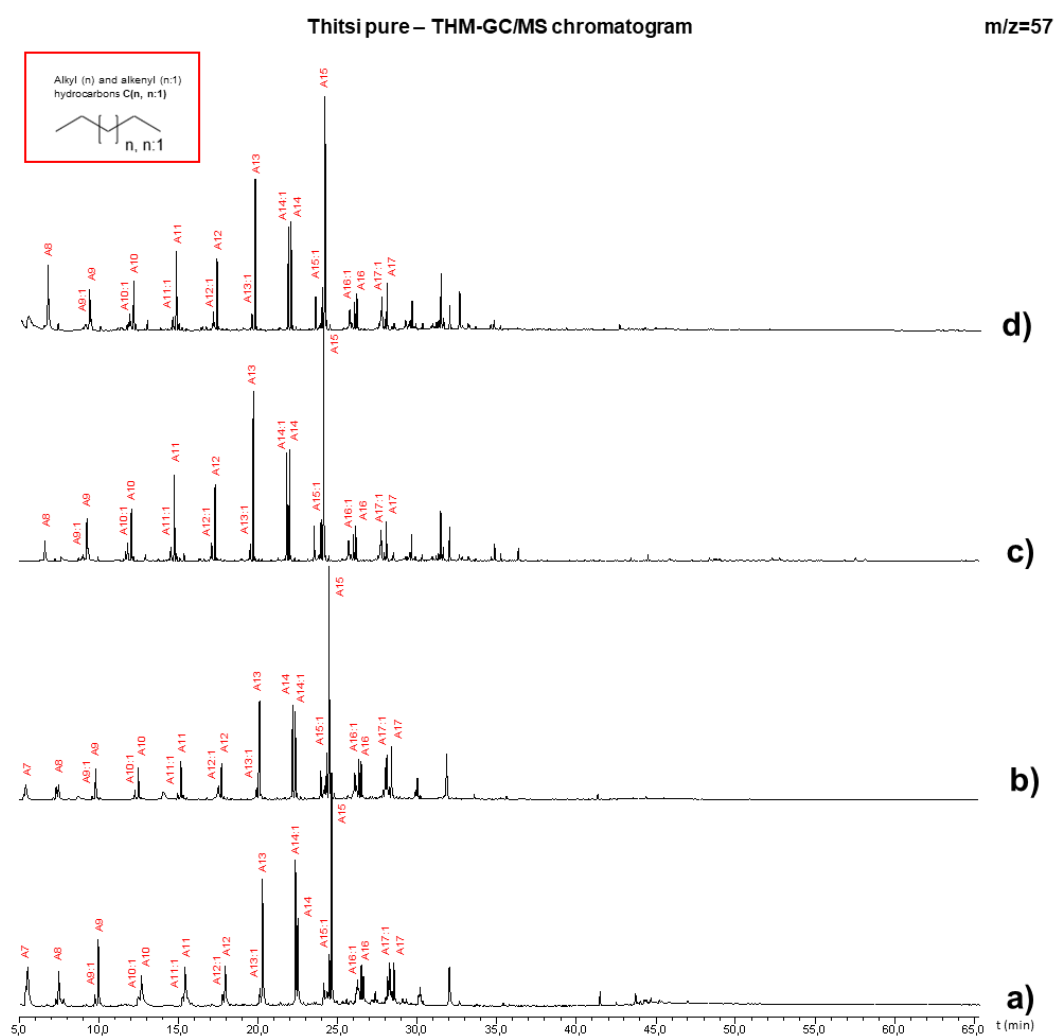


Figure 43. Extracted Ion Chromatograms (EIC) of *thitsi* pure acquired by THM-GC/MS and obtained by plotting single ion mass profile at $m/z=57$: **a)** fresh, **b)** dried at the touch (8 weeks), **c)** naturally aged (2 years) and **d)** accelerated artificially daylight aged (28 days, starting from the naturally aged samples set).

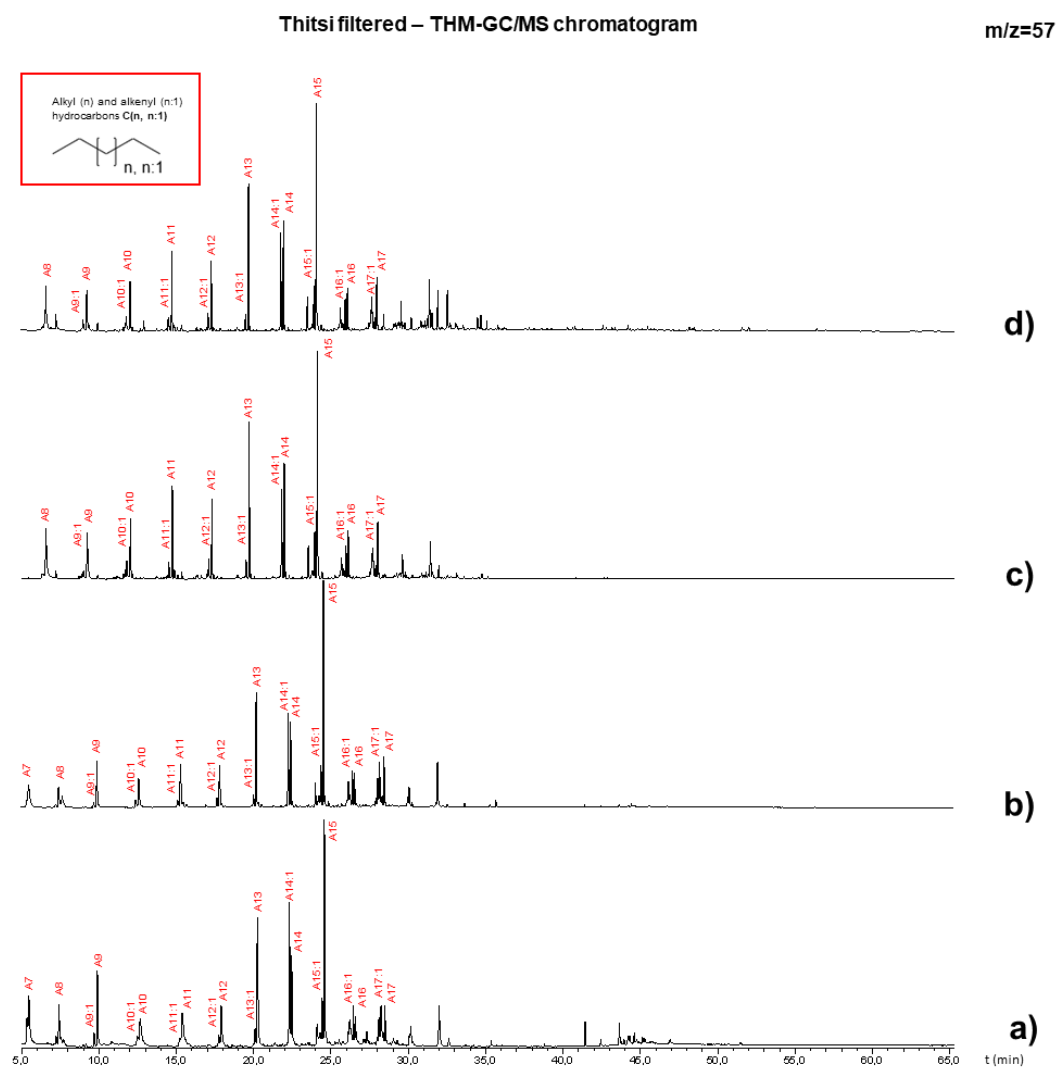


Figure 44. Extracted Ion Chromatograms (EIC) of thitsi filtered acquired by THM-GC/MS and obtained by plotting single ion mass profile at $m/z=57$: **a)** fresh, **b)** dried at the touch (8 weeks), **c)** naturally aged (2 years) and **d)** accelerated artificially daylight aged (28 days, starting from the naturally aged samples set).

Generally, for all recorded EICs at m/z 57 of thitsi-based model samples, the series of alkyl and alkenyl starts with heptane (A7) and ends with heptadecane (A17). The most abundant aliphatic hydrocarbon in all the EICs is pentadecane (A15) and followed by tridecane (A13) and tetradecane (A14) as the further most abundant alkanes, also in accordance with the literature [7, 19, 56, 60]. In the literature a similar EIC at $m/z=57$ for thitsi acquired by THM-GC/MS has been obtained by Le Hô: the most abundant alkanes have been assigned to pentadecane and tridecane while the most abundant alkene has been assigned to tetradecene [19].

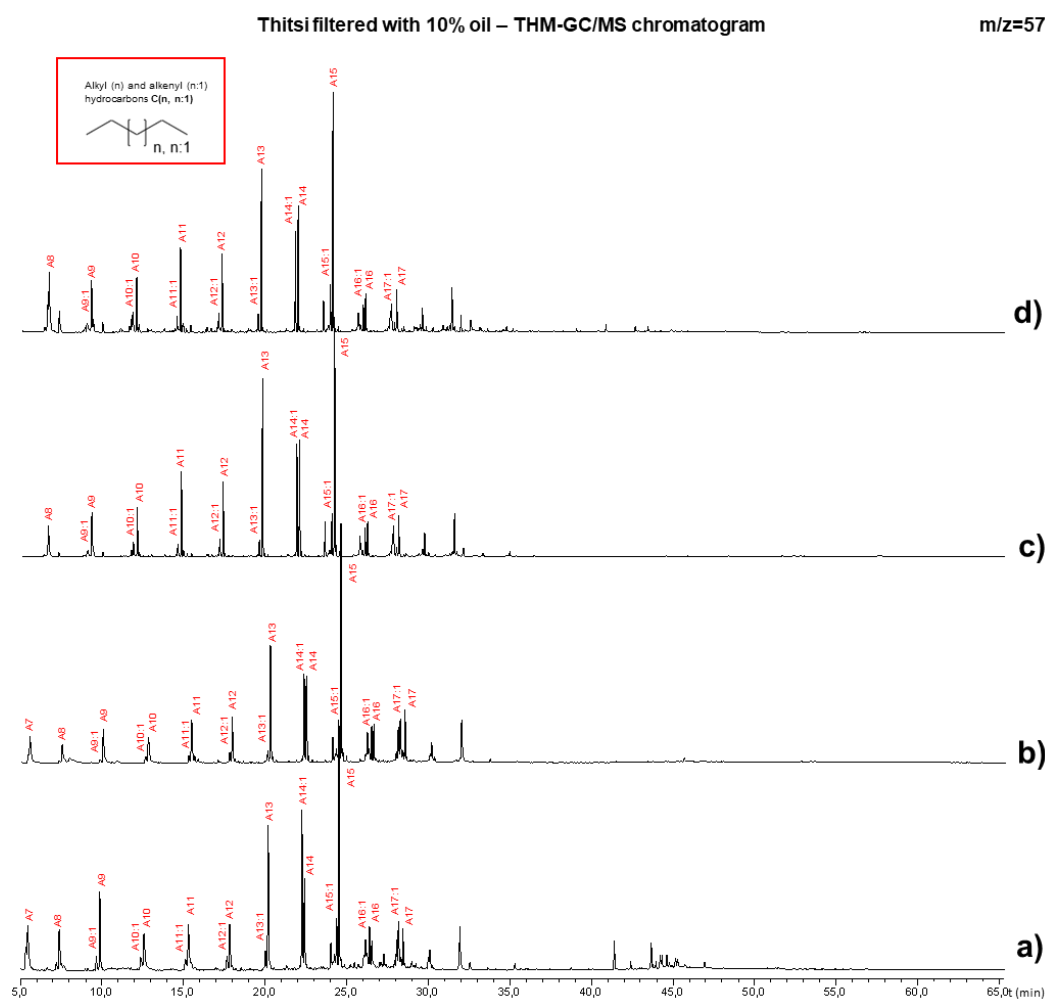


Figure 45. Extracted Ion Chromatograms (EIC) of thitsi filtered with 10% oil acquired by THM-GC/MS and obtained by plotting single ion mass profile at $m/z=57$: **a)** fresh, **b)** dried at the touch (8 weeks), **c)** naturally aged (2 years) and **d)** accelerated artificially daylight aged (28 days, starting from the naturally aged samples set).

Furthermore, the intensity of alkanes is always higher than the alkenes counterpart, except for tetradecene (A14:1) and tetradecane (A14). The tetradecene (A14:1) is higher than tetradecane (A14) in the *fresh* and *dried-at-the-touch* chromatograms, while in *2-year naturally aged* and *28-day accelerated artificially daylight aged* chromatograms tetradecene (A14:1) is lower than tetradecane (A14). The aliphatic hydrocarbon with the maximum chain length is heptadecane (A17), as expected due to the longest side chain of *thitsiol* (seventeen-carbon atoms, Figure 2).

m/z 91- alkyl and alkenyl benzenes

Extracted Ion Chromatograms (EICs) at m/z 91 of thitsi pure, thitsi filtered, and thitsi filtered with 10% oil, are shown in Figure 46, 47 and 48, respectively.

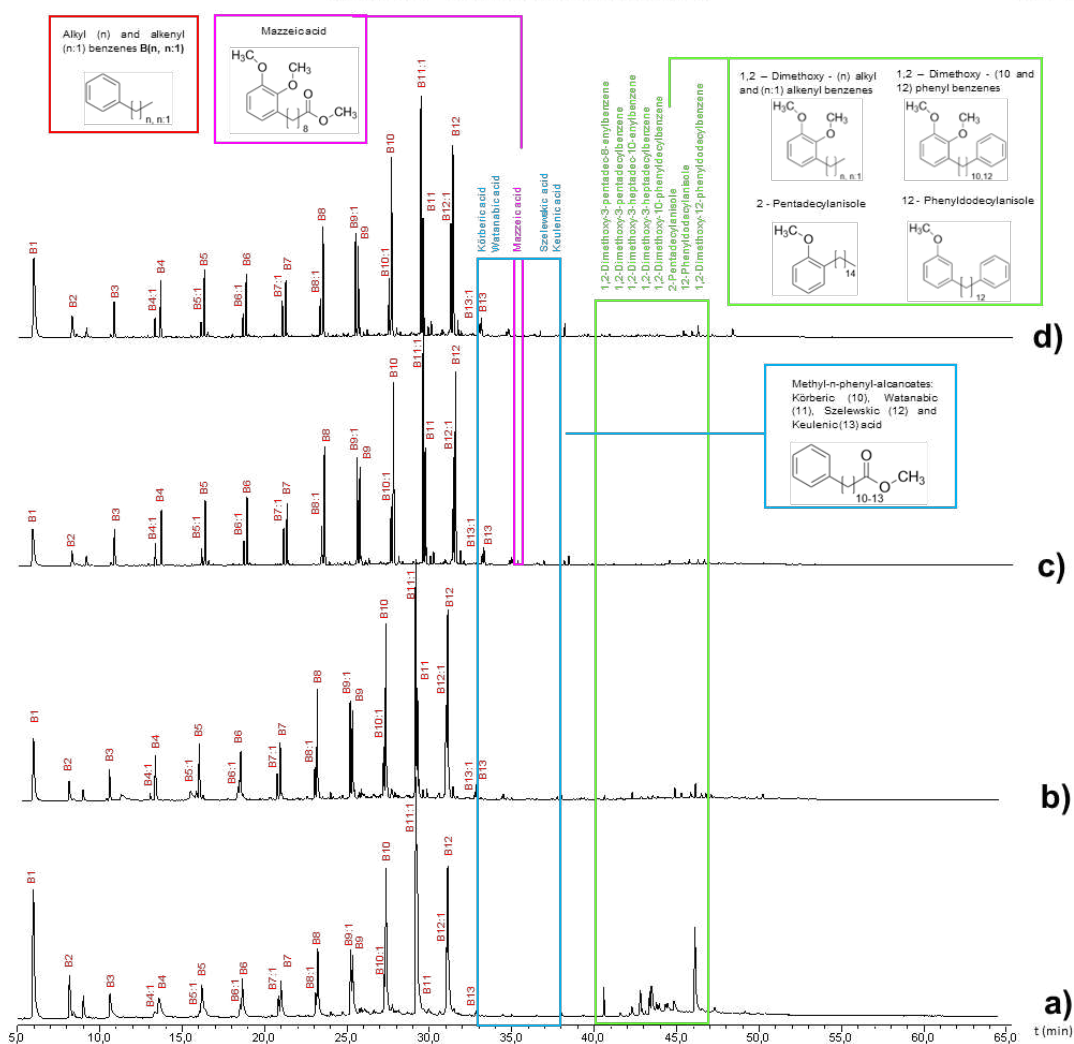


Figure 46. Extracted Ion Chromatograms (EIC) of *thitsi* pure acquired by THM-GC/MS and obtained by plotting single ion mass profile at $m/z=91$: **a)** fresh, **b)** dried at the touch (8 weeks), **c)** naturally aged (2 years) and **d)** accelerated artificially daylight aged (28 days, starting from the naturally aged samples set).

These EICs show alkyl ($m/z=92$ as base peak) and alkenyl ($m/z=91$ as base peak) benzene fragments, which are the pyrolytic products produced by the cleavage at the benzylic position of the 3- and 4-alkylphenylcatechols in *thitsiol* (Figure 2) [56] but also resulting from the dehydration of alkylphenols, intermediate compounds formed from catechols during pyrolysis [19].

EICs at m/z 91 shows a bell-shape in the range of 10-18 RT (peaks B3-B7, with B5 the most abundant of the group) which becomes more evident in the 2-year *naturally aged* chromatogram.

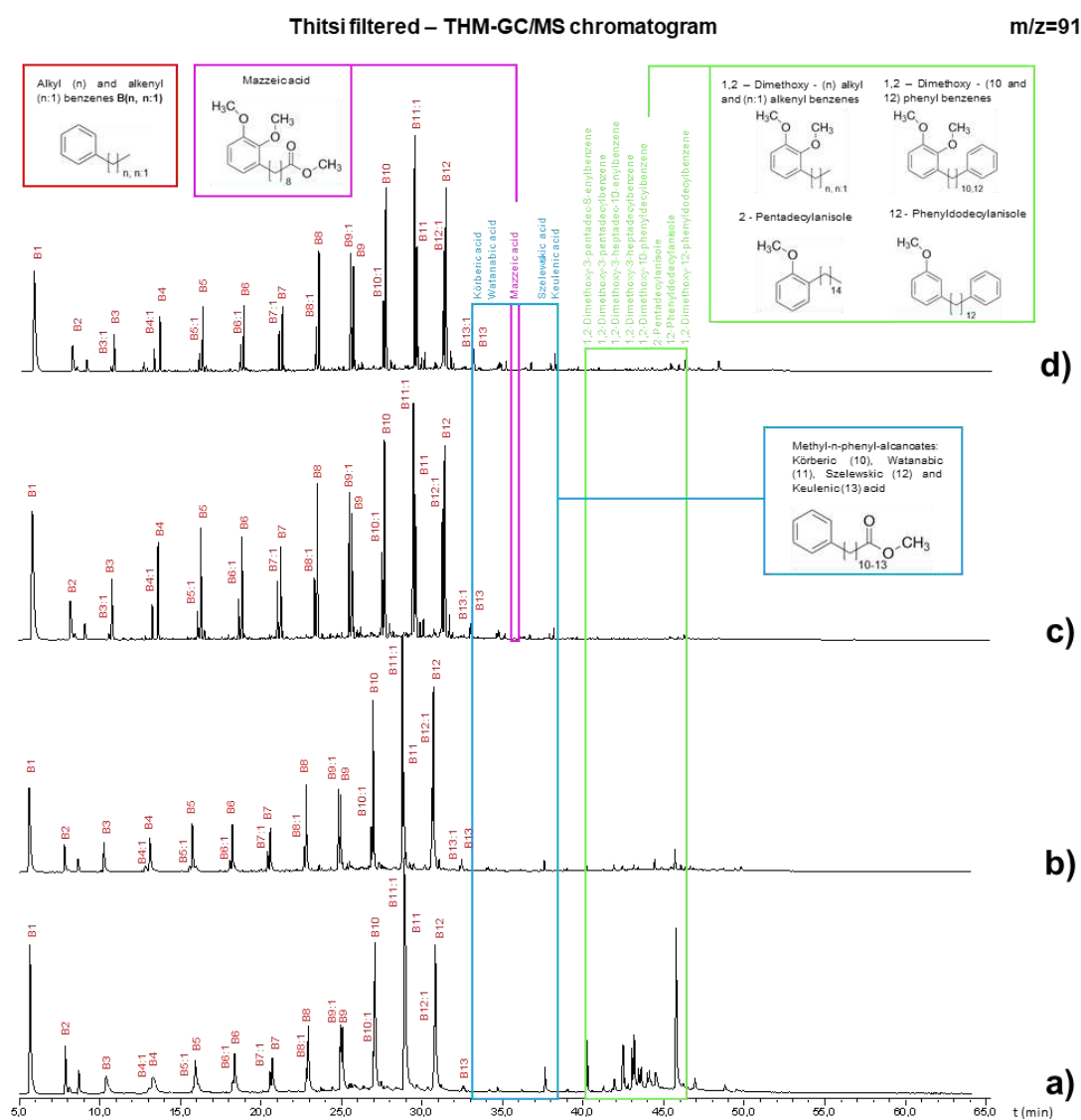


Figure 47. Extracted Ion Chromatograms (EIC) of *thitsi* filtered acquired by THM-GC/MS and obtained by plotting single ion mass profile at $m/z=91$: **a)** fresh, **b)** dried at the touch (8 weeks), **c)** naturally aged (2 years) and **d)** accelerated artificially daylight aged (28 days, starting from the naturally aged samples set).

The *thitsi* EICs m/z 91 show a first intense peak assigned to toluene (B1) followed by a lower ethyl benzene (B2) and around 29 RT the undecenyl benzene (B11:1), the most intense peak of the series, in accordance with the literature [19, 57]. B11:1 is formed during the cleavage at the benzylic position of 3- and 4-(12-phenyldodecyl) cathecols in the *thitsiol* polymeir network [56, 57]. The abundance of alkenyl benzenes was found lower than the one of alkyl benzenes, except for B11:1. The maximum detected alkyl benzenes length is B13 (tridecyl benzene), even though the longest alkyl phenyl side chain has twelve carbon atoms. Le Hô also detected tridecyl benzene in *thitsi* EIC at $m/z=91$ but no explanation has been given [19]. The

abundance of this series of peaks decreases with time, in particular during the 2-week drying process.

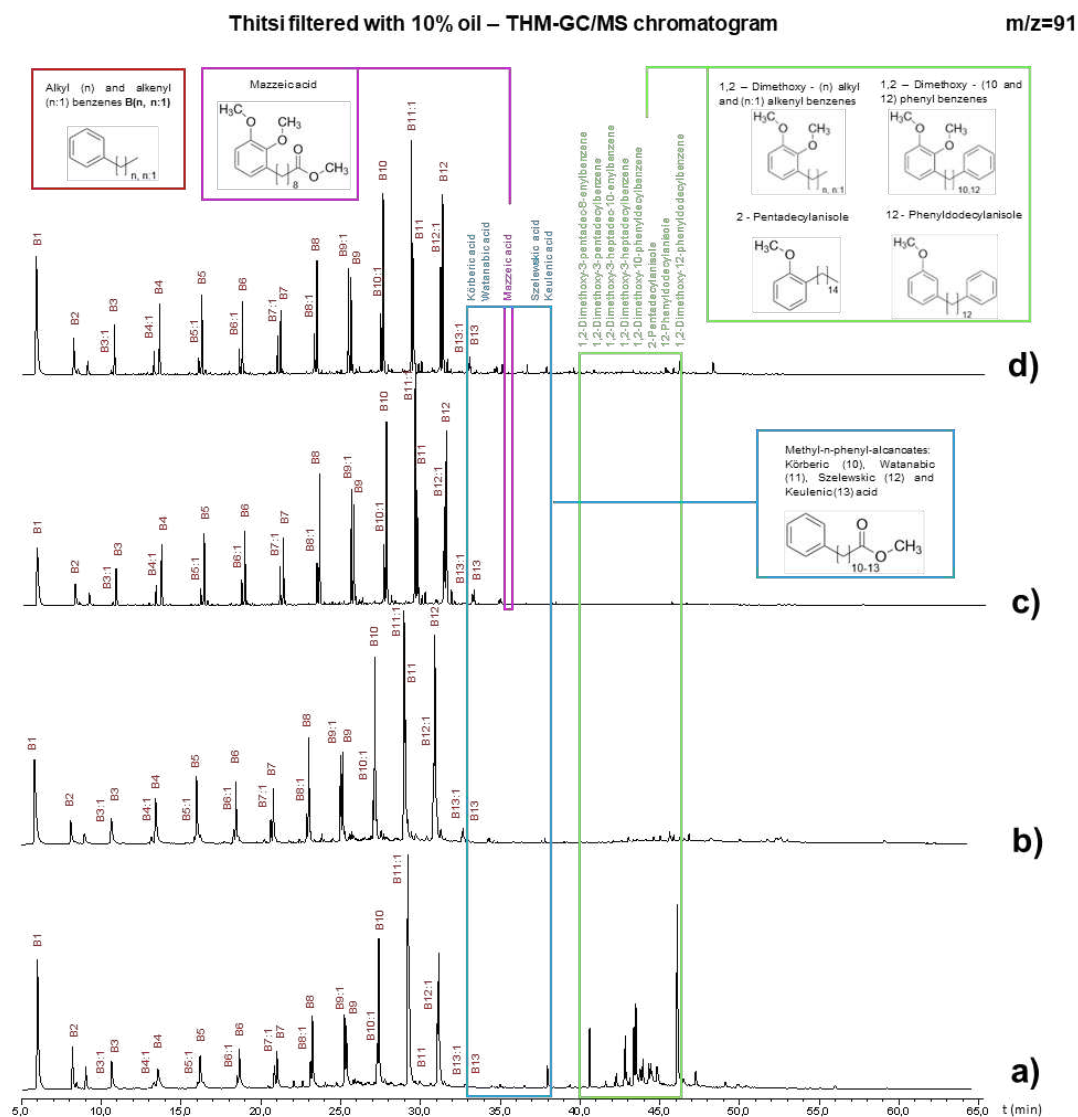


Figure 48. Extracted Ion Chromatograms (EIC) of thitsi filtered with 10% oil acquired by THM-GC/MS and obtained by plotting single ion mass profile at $m/z=91$: **a)** fresh, **b)** dried at the touch (8 weeks), **c)** naturally aged (2 years) and **d)** accelerated artificially daylight aged (28 days, starting from the naturally aged samples set).

In this series of EICs between RT 40 and 48 minutes, alkyl/alkenyl (1,2-dimethoxy-3-pentadec-8-enylbenzene, base peak at $m/z=346$; 1,2-dimethoxy-3-pentadecylbenzene, base peak at $m/z=348$; 1,2-dimethoxy-3-heptadec-10-enylbenzene, base peak at $m/z=374$; 1,2-dimethoxy-3-heptadecylbenzene, base peak at $m/z=376$, highlighted in green) and phenyl benzenes (1,2-dimethoxy-10-phenyldecylbenzene, base peak at $m/z=354$; 1,2-dimethoxy-12-phenyldodecylbenzene, base peak at $m/z=382$, highlighted in green) and alkyl and

phenyl anisoles (2-pentadecylanisole, base peak at $m/z=122$; 12-phenyldodecylanisole, base peak at $m/z=122$, highlighted in green) were detected as well in their methylated form. As explained before (paragraph 4.3), the use of TMAH as derivatizing reagent leads to the methylation of catechols and phenols which are registered at higher m/z values than those reported in the literature (m/z 108 and m/z 123, respectively) [24]. The addition of one and two methyl groups increases the m/z values of 14 to the phenols and 28 to the catechols, respectively. The result is a common base peak at m/z 122 for methylated phenols as anisoles and at m/z 151 for methylated catechols as dimethoxy benzenes. This series of fragments, as already said for the TIC, decreases after 8 weeks of drying in climate chamber. This could be due to the nucleus-nucleus coupling occurring during laccase polymerization, which involves catechol hydroxyl groups in the formation of polymerized network. As a consequence, less hydroxyl groups are available for the methylation with the passage of time.

Finally, one of the main advantages of using a derivatizing reagent such as TMAH for the investigation of Asian lacquers is shown by the detection of some methylated oxidation products between 33 and 38 minutes of RT. These are the catechol acids as methyl 8-(2,3-dimethoxyphenyl) octanoate also known Mazzeic acid (base peak at $m/z=136$, highlighted in blue) and the phenylalkanoic acids group as methyl phenyl alcanoates (base peak at $m/z=91$, highlighted in pink). The methyl phenyl alcanoates group includes methyl 10-phenyl-decanoate (körberic acid, MW= 262), methyl 11-phenyl-undecanoate (watanabic acid, MW=276), methyl 12-phenyl-dodecanoate (szelewskic acid, MW= 290), and methyl 13-phenyl-tridecanoate (keulenenic acid, MW=304).

As shown in the EICs at $m/z=91$, the methyl phenyl alcanoates group was already detected in the *fresh* thitsi, while the presence of Mazzeic acid was evinced not before the 2-years of natural aging. This suggests the relative quick formation of phenylalkanoic acids in the thitsi lacquer in contrast to the catechol acids, which require slower mechanisms of reaction.

According to Tamburini [7] the phenylalkanoic acid as oxidation products are formed through a two-step mechanism in which phenyl catechol is subjected to the opening of catechol ring and finally oxidized to phenylalkanoic acid. The final step of the reaction mechanism shows in Figure 49 (Reaction mechanism 1) is the methylation with TMAH derivatizing reagent. One more oxidation step in Reaction mechanism 1

with the formation of *n*-oxo-phenylalcanoic acid has been proposed by Tamburini. However, nor this oxidation product nor its methylated counterpart has been detected.

The reaction mechanism for the formation of Mazzeic acid has never been proposed. However, it could be formed by the same radical oxidation described in Figure 53 (Reaction mechanism 2) applied to aliphatic catechols.

Reaction mechanism 1

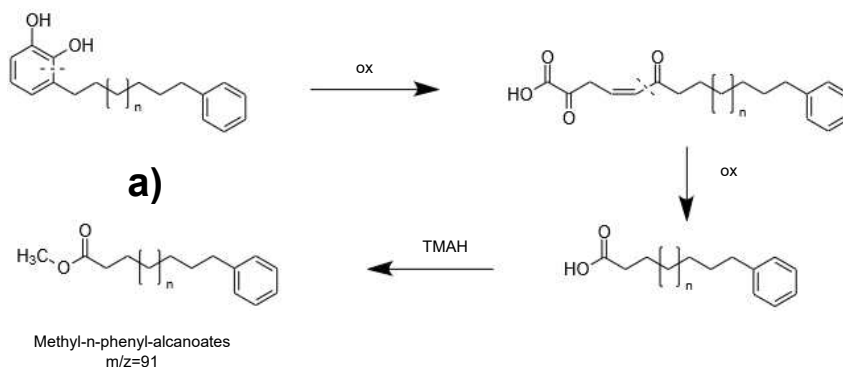


Figure 49. Reaction mechanism proposed by Tamburini for the formation of *n*-phenylalcanoic acids and their subsequently methylation with TMAH in methyl-*n*-phenylalcanoates (a), shown in EICs at $m/z=91$.

$m/z=120$ - alkylphenyl ketones

Extracted Ion Chromatograms (EIC) at $m/z=120$ of thitsi pure, thitsi filtered, and thitsi filtered with 10% oil, are shown in Figure 50, 51 and 52, respectively.

The spectra c) and d) of Figure 50, 51, 52 shows the alkylphenyl ketone. The pyrolytic profile of this serie of products starts with acetophenone (C2, base peak at $m/z=105$) at 14 minutes of RT and proceeds with phenylbutanone (C4, base peak at $m/z=105$), phenylpentanone (C5, base peak at $m/z=105$), phenylhexanone (C6, base peak at $m/z=105$) as the most abundant one, phenylheptanone (C7, base peak at $m/z=105$), phenyloctanone (C8, base peak at $m/z=105$), phenyldecanone (C10, base peak at $m/z=120$), and phenyldodecanone (C12, base peak at $m/z=120$).

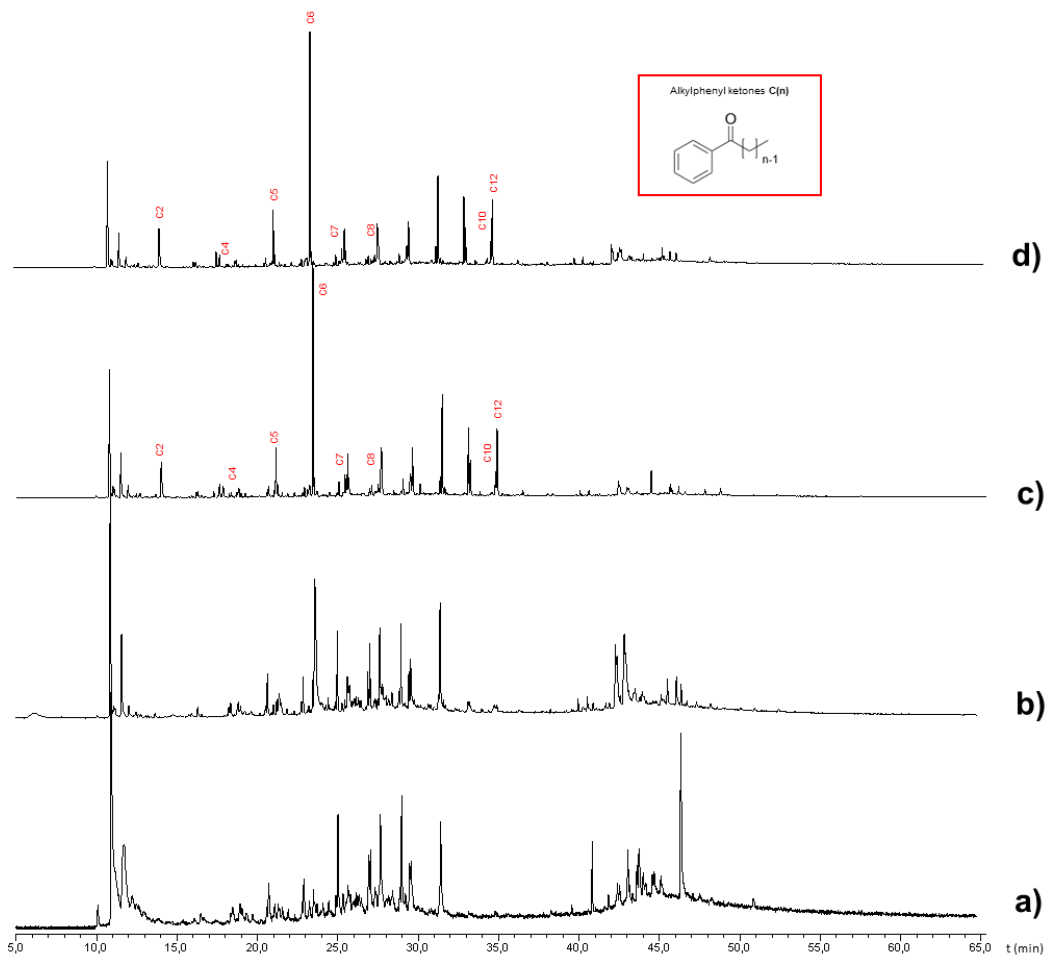


Figure 50. Extracted Ion Chromatograms (EIC) of thitsi pure acquired by THM-GC/MS and obtained by plotting single ion mass profile at $m/z=120$: **a)** fresh, **b)** dried at the touch (8 weeks), **c)** naturally aged (2 years) and **d)** accelerated artificially daylight aged (28 days, starting from the naturally aged samples set).

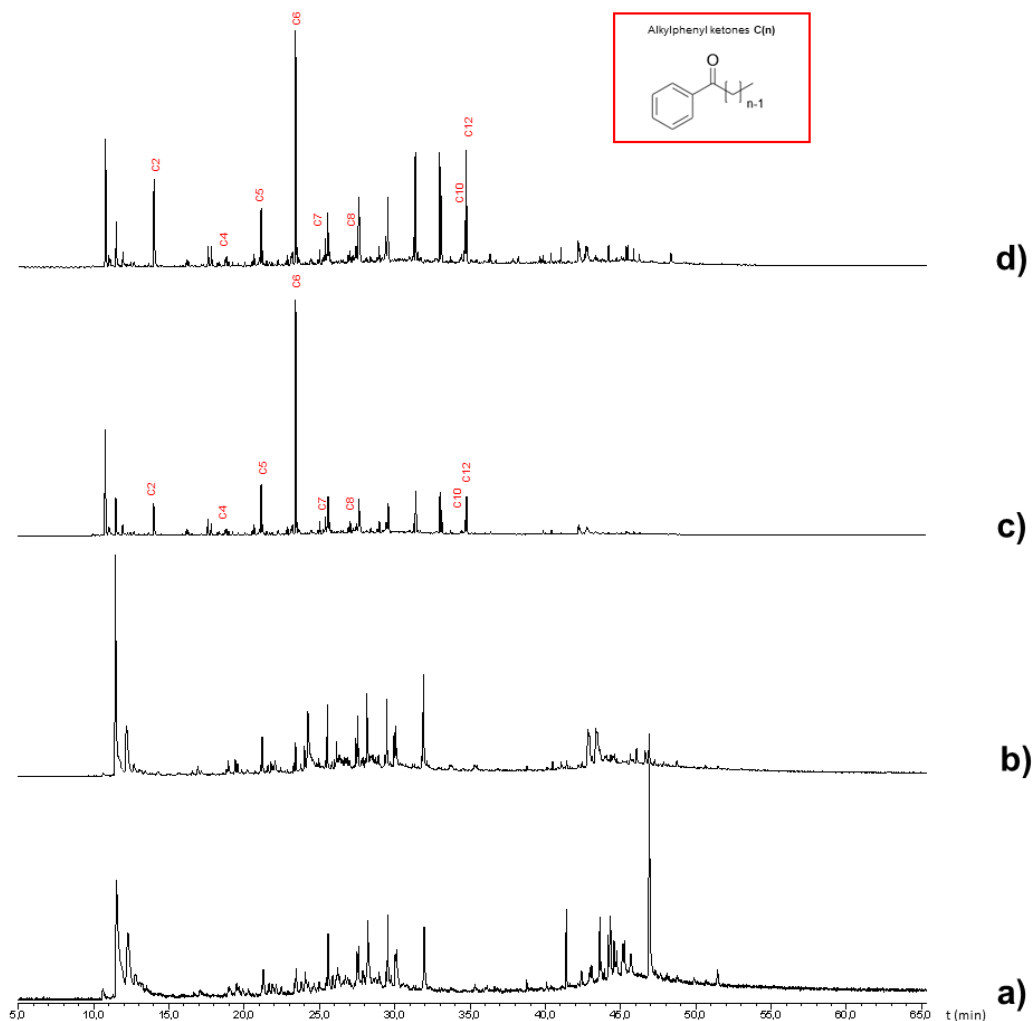


Figure 51. Extracted Ion Chromatograms (EIC) of thitsi filtered acquired by THM-GC/MS and obtained by plotting single ion mass profile at $m/z=120$: **a)** fresh, **b)** dried at the touch (8 weeks), **c)** naturally aged (2 years) and **d)** accelerated artificial daylight aged (28 days, starting from the naturally aged samples set).

According to Tamburini, alkylphenyl ketones are the pyrolysis products of *n*-oxo-alkylphenyl catechols, as shown in Figure 49 (Reaction mechanism 1).

The appearance of this series of fragments in the EIC of the the *2-year naturally aged* lacquer is complemented by the formation of Mazzeic acid, as mentioned before in the paragraph for the m/z 91. The formation of the two groups of oxidation products implies their production during the 2-year long period between the *dried-at-the-touch* state of the material and the *naturally aged* one. Furthermore, in the alkyphenyl ketones series, the abundance of C2, C10 and C12 fragments increases during the accelerated artificial daylight aging.

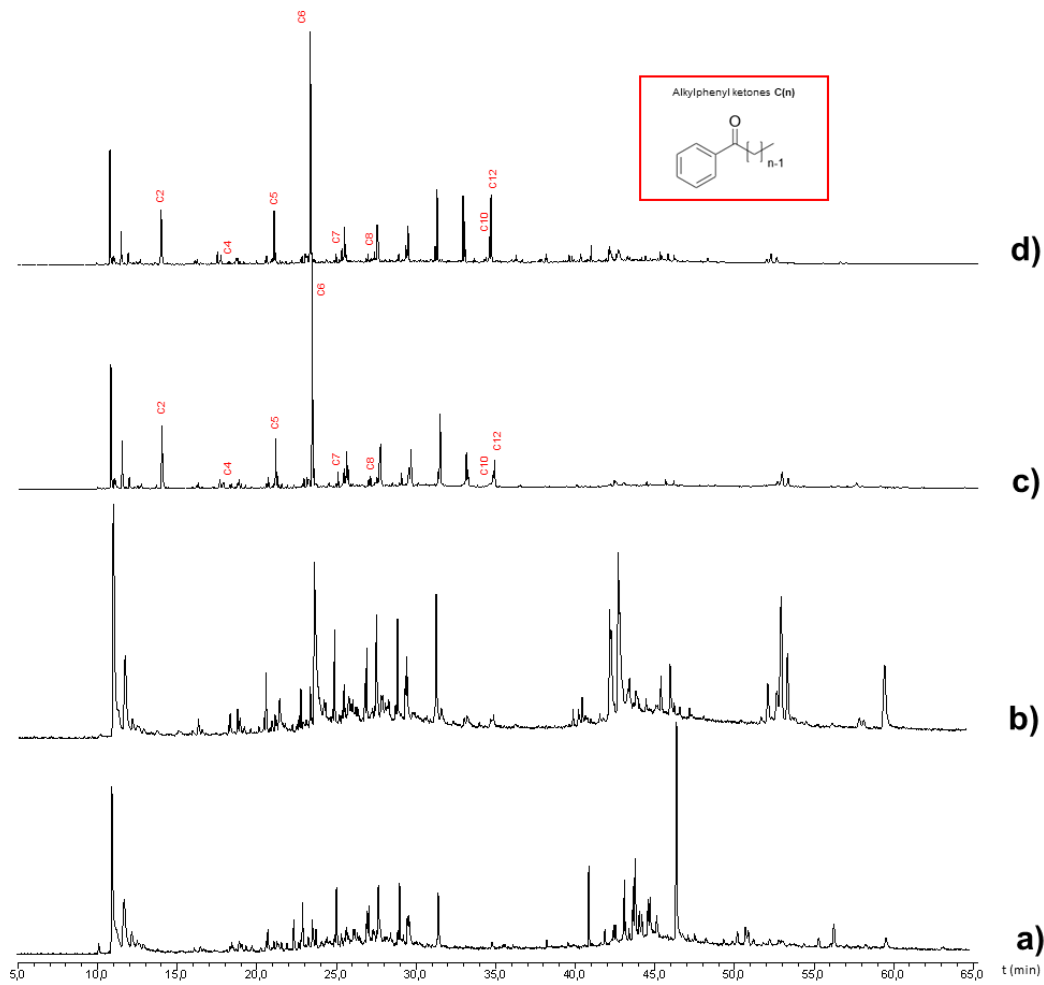


Figure 52. Extracted Ion Chromatograms (EIC) of thitsi filtered with 10% oil acquired by THM-GC/MS and obtained by plotting single ion mass profile at $m/z=120$: **a)** fresh, **b)** dried at the touch (8 weeks), **c)** naturally aged (2 years) and **d)** accelerated artificially daylight aged (28 days, starting from the naturally aged samples set).

Reaction mechanism 2

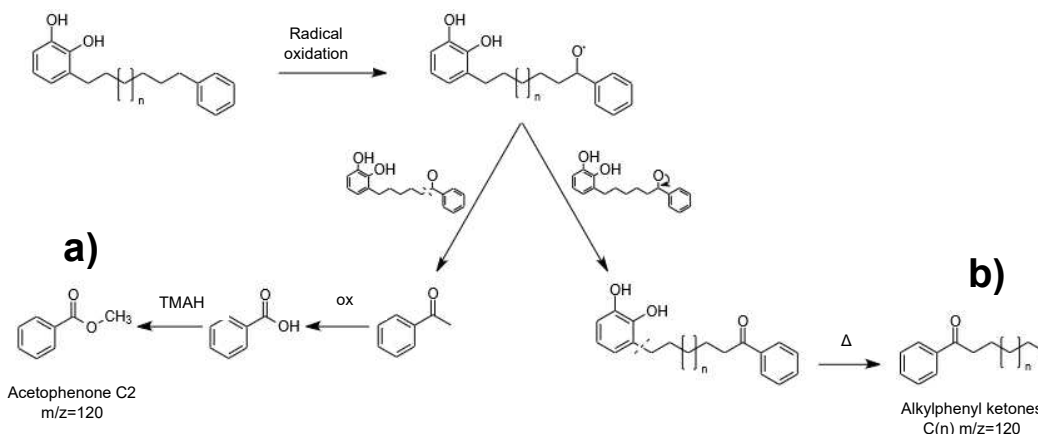


Figure 53. Reaction mechanism proposed by Tamburini for the formation of benzoic acid with its subsequently methylation with TMAH in acetophenone (a), and the alkylphenyl ketones (b). Both these fragments are shown in EICs at $m/z=91$.

5.2 Urushiol

5.2.1 Digital Microscopy

The images obtained with Keyence Digital Microscopy in three different magnifications (100x, 500x, 1000x) of urushi are shown in Figure 54.

Digital Microscopy investigation on urushi, as for thitsi, lacquer gave interesting results about the resistance of the material and the physical changes in its surface when subjected to accelerated artificial daylight aging. During the 28 days of accelerated artificial daylight aging urushi-based samples does not show any cracks in its surface, differently from thitsi-based lacquer. This could be means that the oxidation process, which leads to the decomposition of the polymerized lacquer network [1], in urushi-based lacquer proceeds slower than in thitsi-based lacquers. This could be also explained why thitsi lacquer is considered less durable and stable to light damage than urushi.

However, in the urushi surface, as for thitsi, the appearance of circular spots, even if in a lower density, has been detected after 28 days of accelerated artificial daylight aging. They could be interpreted as the of the dispersed polysaccharide particles in the surface layer, due to the damage of the core–shell structure of polysaccharides and glycoproteins after UV exposure [1], as explained in paragraph 2.2.2.

The small and circular spots in the background are the marks of waterdrops in the lacquer sap [58]. No significant qualitative changes during the 28 days of accelerated artificial daylight aging have been detected.

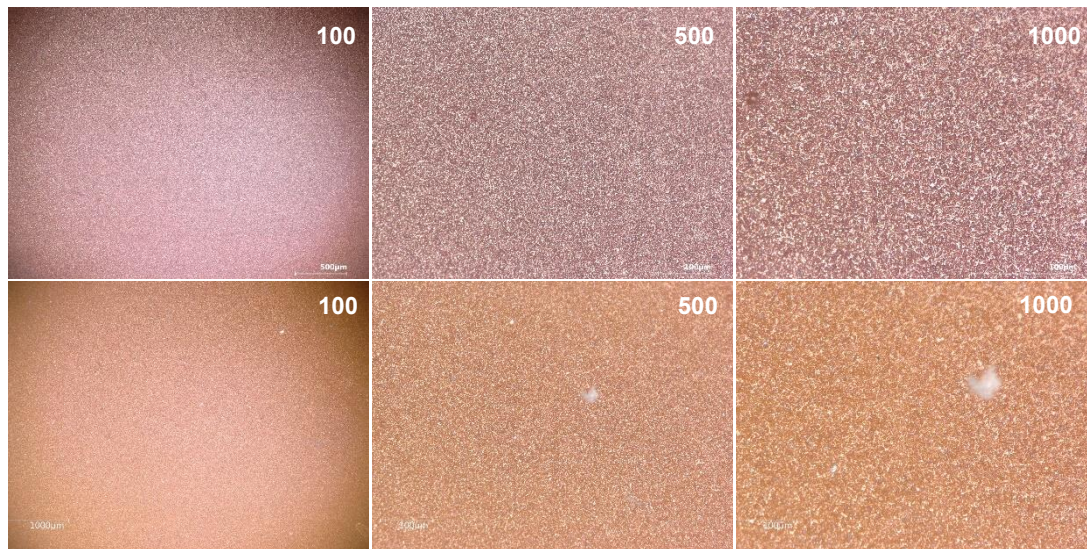


Figure 54. Pre (up) and post (down) accelerated artificial daylight aging images of urushi acquired by digital microscopy in three different magnifications: 100x (left), 500x (middle), 1000x (right).

5.2.2 Colorimetry

Colorimetry investigation on urushi lacquer gave several information useful for the understanding of the material colour and reflectance behaviour during the accelerated artificial daylight aging as already seen for thitsi-based samples.

The reflectance spectra urushi are shown in Figure 55. In urushi-base sample, as for thitsi, a shift to higher reflectance number from the pre aging (blue) to the post aging (orange) has been detected. This means that urushi lacquer type tends to increase its reflecting power after an aging process too.

The $L^*a^*b^*$ space graphic representation of urushi is shown in Figure 56, while the measured values are shown in Table 8 together with their standard deviations. The high heterogeneity of the sample layer on the mock-ups and the low number of measurements performed on each sample determined a very high standard deviation for L^* , a^* and b^* values. The a^* against b^* graph (left) demonstrates a shift to a^*+ coordinate (red in the red/green axis) and b^*+ coordinate (yellow in the yellow/blue

axis) of urushi-based sample. This means that the colour of this material has changed to more red and more yellow hues during the accelerated artificial daylight aging.

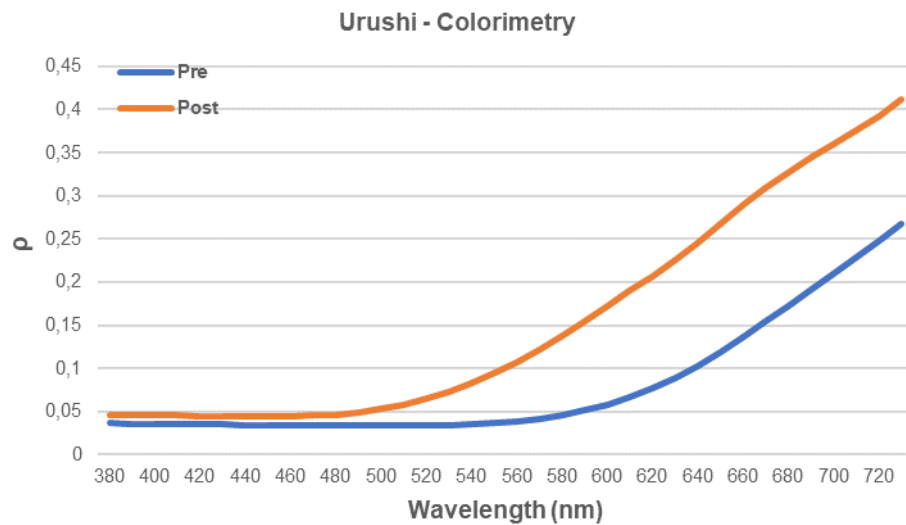


Figure 55. Reflectance spectrum of urushi pre (blue) and post (orange) accelerated artificial daylight aging.

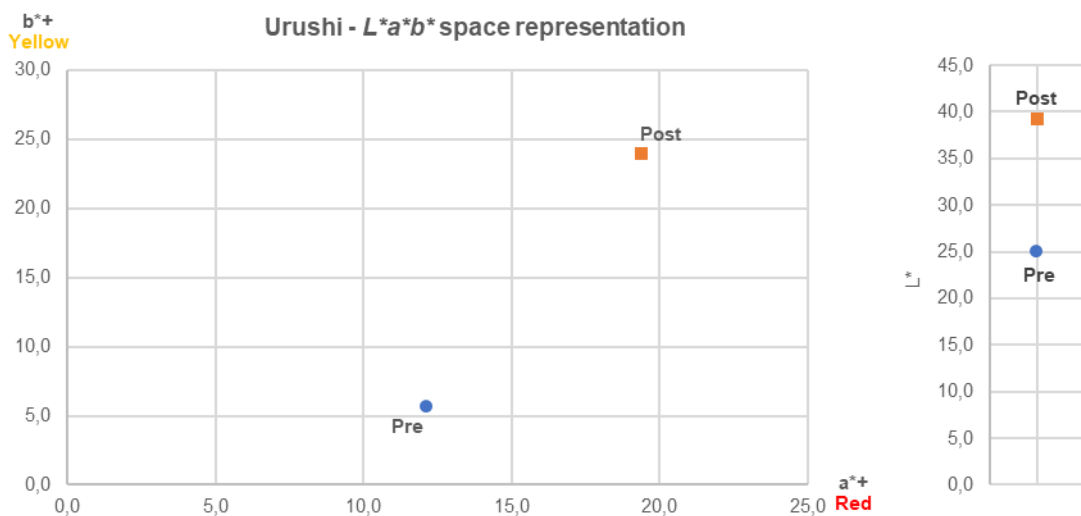


Figure 56. $L^*a^*b^*$ space representation of urushi pre (blue) and post (orange) accelerated artificial daylight aging: a^*b^* graph (left) and L^* graph (right).

More important is the variation of the L^* coordinate. Urushi-based samples, as the thitsi ones, shows an increase of L^* values which means a tendency to shift to brighter colour. As already explain, since the white and black components are correlated to a higher and lower reflectance, respectively, (if light is fully absorbed, the object looks black; if it is fully reflected, the object is white) it is possible to deduce that this material

tends to increase its reflecting power, in agreement with registered reflectance spectra.

The calculated ΔE^* value is shown in TableX: the higher the increase of this number, the higher the total colour change of the material. Comparing with thitsi-based samples, urushi shows the higher increase of ΔE^* number, due to a general increase of the three parameters L^* , a^* and b^* . A $\Delta E^*=24,3$, according with TableX, means that “colours are more similar then opposite”.

	L^*	$s_x(L^*)$	a^*	$s_x(a^*)$	b^*	$s_x(b^*)$	ΔE^*
Urushi Pre	25,0	3,0	12,1	4,5	5,7	5,0	
Urushi Post	39,2	4,1	19,4	0,6	23,9	6,4	24,3

Table 8. L^* , a^* and b^* values and their standard deviations measured for urushi-based sample before (pre) and after (post) 28 days of accelerated artificial daylight aging and the calculated ΔE^* .

5.2.3 FTIR

In the following section Transmission mode FTIR spectra and Attenuated Total Reflection mode (ATR) FTIR spectra of urushi are shown. As described in the timeline scheme (Figure 23), Transmission spectra have been registered since the mock-ups preparation when the material was still in a liquid state (*fresh*) and then in every step of their physical state change: after the drying in climate chamber (*dried at the touch*), after 2 years of natural aging (*naturally aged*), and after 28 days of accelerated artificial daylight aging (*accelerated artificially daylight aged*). ATR spectra have been registered only for *naturally aged* and *accelerated artificial daylight aged* urushi, due to liquid and semiliquid state of the material in the first two steps.

Transmission mode

The Transmission Spectra of urushi are shown in Figure 57.

The complete peaks assignment is shown in Table 9.

The spectra show the changes of functional groups in urushi during the drying, natural aging and accelerated artificial daylight aging process. The absorption at 3011 cm^{-1} , assigned to the stretching of cis double bonds in the side chain of urushiol, decreases between the *fresh* and the *dried at the touch* state of the material and almost disappears after two years of natural aging. Differently from thitsi, in the region between 3100 and 3000 cm^{-1} , only the absorption at 3011 cm^{-1} was detected,

according with the prevalence of 3-alkylcatechols in urushiol (Figure 7). The decrease of the peak at 3011 cm^{-1} could be due to the side chain- nucleus coupling of urushiol polymerization, which involves double bonds in the side chains (Figure 7).

The peaks at 2924 and 2853 cm^{-1} have been assigned to asymmetric and symmetric C-H in the side chain, respectively, and no changes in the ratio of their absorbance values has been noted, in agreement with the literature [1].

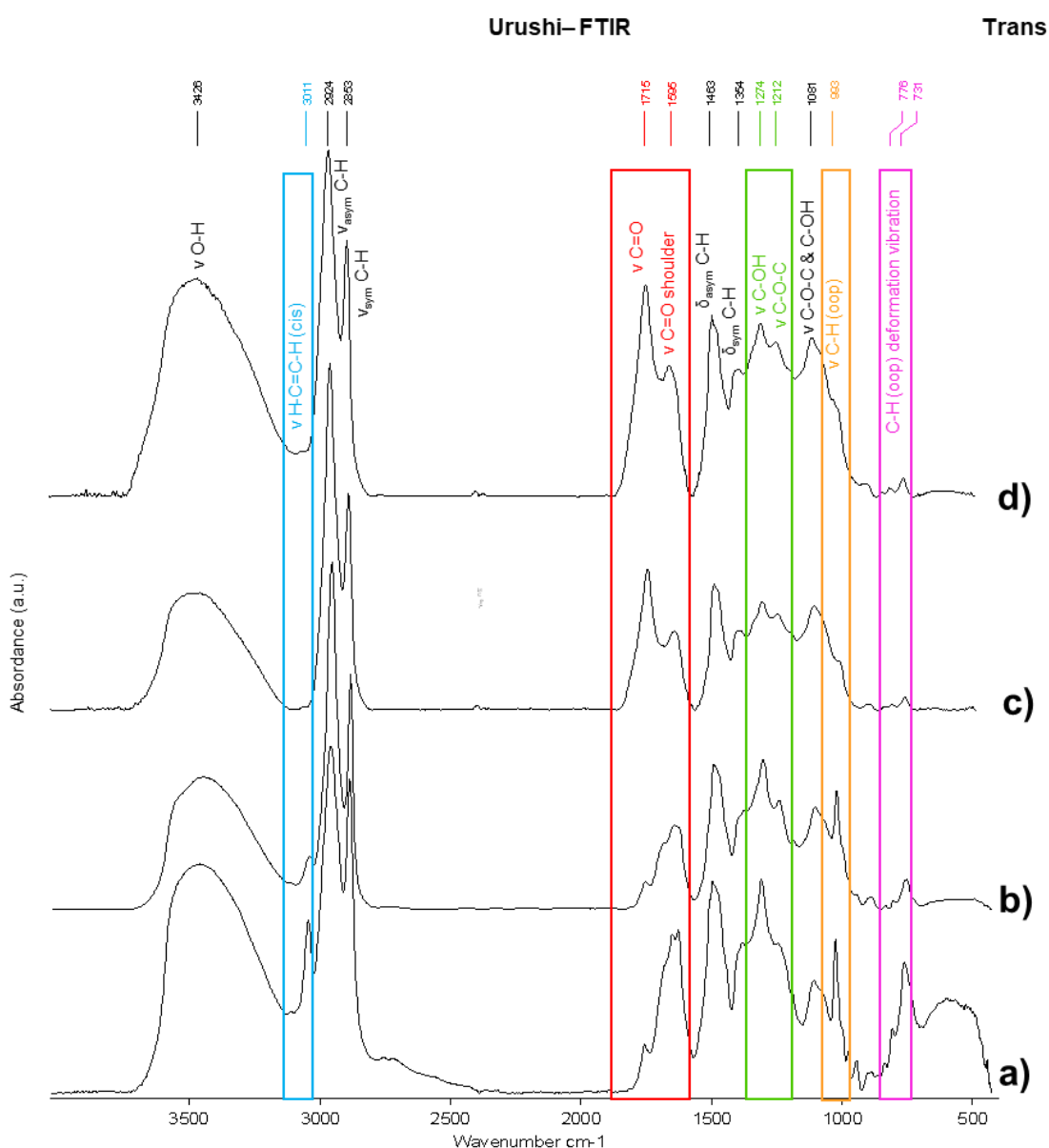


Figure 57. Transmission FTIR spectra of urushi: **a)** fresh, **b)** dried at the touch (8 weeks), **c)** naturally aged (2 years) and **d)** accelerated artificially daylight aged (28 days, starting from the naturally aged samples set).

The most significant variation in terms of intensities ratio, as already mentioned for thitsi, has been detected for the peaks at 1715 and 1595 cm^{-1} , assigned to carbonyl and C=C stretching of the aromatic ring skeletal vibrations of the polymerized catechol derivatives, respectively. In the spectrum registered on fresh urushi, the absorption at 1595 cm^{-1} is more intense in comparison with the one at 1725 cm^{-1} . The drying and both natural and artificial ageing promote the same variations described in thitsi system, as consequence of photooxidative processes [17]. Transmission mode spectra of urushi-based sample shows different similarities with thitsi-based samples. The absorption at 1274 cm^{-1} , assigned to C-OH stretching in catechols and phenols, progressively decreases, due to the photo-oxidation of lacquer which leads to a loss of hydroxyl functions on the catechol ring [1] and that the catechol in the monomer decreased as the laccase polymerization advanced, as described for thitsi-based samples.

Wavenumber (cm^{-1})	Peaks Assignment
3426	O-H stretching of catechol ring or polysaccharides [1, 9, 20, 27, 41, 61, 63, 64, 65]
3011	H-C=C-H (cis) stretching of side chain double bond [1, 20, 27, 63]
2924	C-H stretching asymmetric of CH_2 and CH_3 of the side chain [9, 17, 41, 63, 64, 65]
2853	C-H stretching symmetric of CH_2 and CH_3 of the side chain [1, 9, 27, 41, 64, 65]
1715	C=O stretching [1, 9, 17, 41, 61, 63, 64]
1595	C=C stretching (C=O shoulder) of the aromatic ring skeletal vibrations of the polymerized catechol derivatives [41, 64]
1453	C-H bending (asymmetric) of side chain [17, 63, 64, 65]
1354	CH_3 bending (symmetric) [9, 63]
1274	C-OH stretching of phenol [41, 64, 66]
1212	C-O-C [1]
1081	C-O-C of sugar units [61] or C-OH stretching of polysaccharides [1, 41, 64]
993	C-H out of plane stretching of conjugated trienes in the side chain [1, 9, 20, 58, 67]
945	H-C=C-H (trans) bending out-of-plane [63]
775 - 719	C-H deformation vibration out-of-plane [62]

Table 9. Transmission FTIR peaks and their assignments for urushi.

The absorption at 993 cm^{-1} , assigned to C-H out of plane stretching of conjugated trienes in the side chain, has been detected. Its decrease has been interpreted, as seen for thitsi, as a decrease in the number of unsaturated side chains, as the polymerization occurs [1]. In the region between $800\text{-}700\text{ cm}^{-1}$, assigned to C-H deformation vibrations out-of-plane, one peak less than thitsi has been detected.

ATR mode

The ATR Spectra of urushi are shown in Figure 58.

The complete peaks assignment is shown in Table 10.

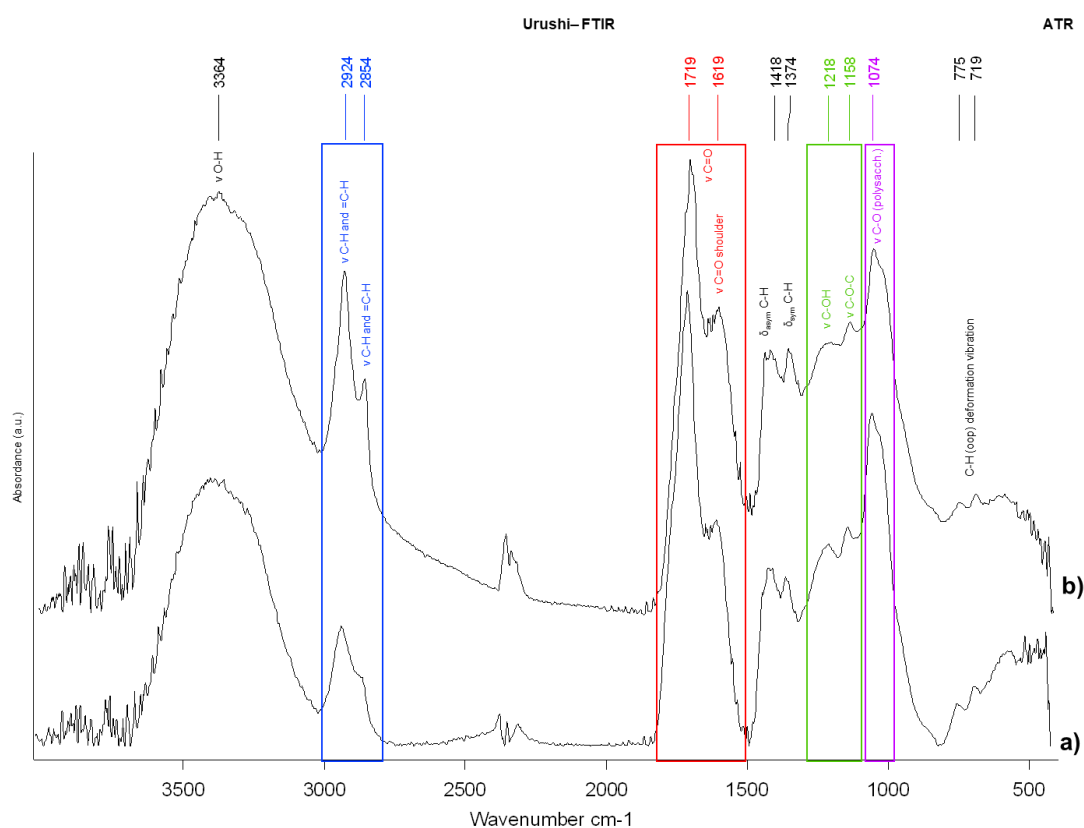


Figure 58. ATR FTIR spectra of urushi: **a)** naturally aged (2 years) and **b)** accelerated artificially daylight aged (28 days, starting from the naturally aged samples set).

The spectra show the changes of functional groups in urushi's surface after the natural aging and accelerated artificial daylight aging processes. As already noticed for thitsi-based samples, in ATR mode spectra the characteristic peak at 3011 cm^{-1} detected in Transmission spectra is not present in the ATR one.

The absorption at 2924 and 2854 cm^{-1} , assigned to C-H in the side chain, increase due to the disintegration of polymerized network after 28 days of accelerated artificial

daylight aging. As detected for thitsi, carbonyl (C=O) and C=C stretching (C=O shoulder) of the aromatic ring does not show a significant change.

In the region between 1300-1100 cm^{-1} two different peaks have been detected: the first at 1218 cm^{-1} has been assigned to C-OH stretching in the catechols and phenol groups and the second at 1158 cm^{-1} , assigned to C-O-C stretching in phenol groups. In thitsi ATR spectra the former has not been detected while the latter shows a consistent broadening. This evidence is representative of the different paths during the polymerization process: thitsi preferentially follows a nucleus-nucleus coupling which leads to the formation of dibenzofurans (C-O-C) while urushi follows both nucleus-nucleus and nucleus-side chain couplings.

The peak at 1074 cm^{-1} , assigned to the polysaccharide component, is more intense in urushi ATR spectra than in thitsi one. The higher intensity is related to the majority of polysaccharide component in urushi respect to thitsi. Contrary to the thitsi, the polysaccharide marker does not change in intensity during the accelerated ageing. The persistence of the absorption could indicate that the photooxidative process is on its initial step, not detectable by ATR. Macroscopically the absence of crack on aged urushi sample can support this hypothesis.

Wavenumber (cm^{-1})	Peaks Assignment
3364	O-H stretching of catechol ring or polysaccharides [9, 20, 27, 41]
2924	C-H and H-C=C-H stretching [62]
2854	C-H and H-C=C-H stretching [62]
1719	C=O stretching [62]
1619	C=C stretching (C=O shoulder) of the aromatic ring skeletal vibrations of the polymerized catechol derivatives [62]
1418	C-H bending (asymmetric) of side chain [17, 63, 64, 65]
1374	CH ₃ bending (symmetric) [9, 63]
1218	C-OH stretching in phenol groups [62]
1158	C-O-C stretching [62]
1074	C-O stretching in polysaccharides [1, 41]
775 - 719	C-H deformation vibration out-of-plane [62]

Table 10. ATR FTIR peaks and their assignments for urushi.

5.2.4 THM-Py-GC/MS

In the following section Total Ion Current (TIC) and the most significant Extracted Ion (EIC) Chromatograms of urushi are shown. As described in the timeline scheme (Figure 23), these chromatograms were registered at different timing, starting when the lacquers were freshly applied on the glass-slides and in a liquid state (*fresh*), followed by different and consequent periods of time corresponding to their chemical-physical change: after the drying in climate chamber (*dried at the touch*), after 2 years of natural aging (*naturally aged*), and finally after 28 days of accelerated artificial daylight aging (*accelerated artificially daylight aged*).

TIC

Total Ion Chromatograms (TIC) of urushi are shown in Figure 59.

The TIC profile of urushi-based Asian lacquer model, as seen for thitsi TIC profile, shows two main groups of peaks: the first, between 5-33 minutes of retention time (RT) and the second, between 40-48 minutes of retention time, due to dimethoxy alkyl and phenyl benzenes, due to the methylation of catechols with the TMAH reagent. Urushi-based sample presents a different TIC profile from thitsi-based samples in the region between 5-33 RT, due to a lower abundance and a different profile of alkylbenzene fragments (EICs at $m/z=91$). This fact depends on the absence of alkyl phenyl side chains in *urushiol*. However, as observed for thitsi, urushi TIC becomes thicker with time.

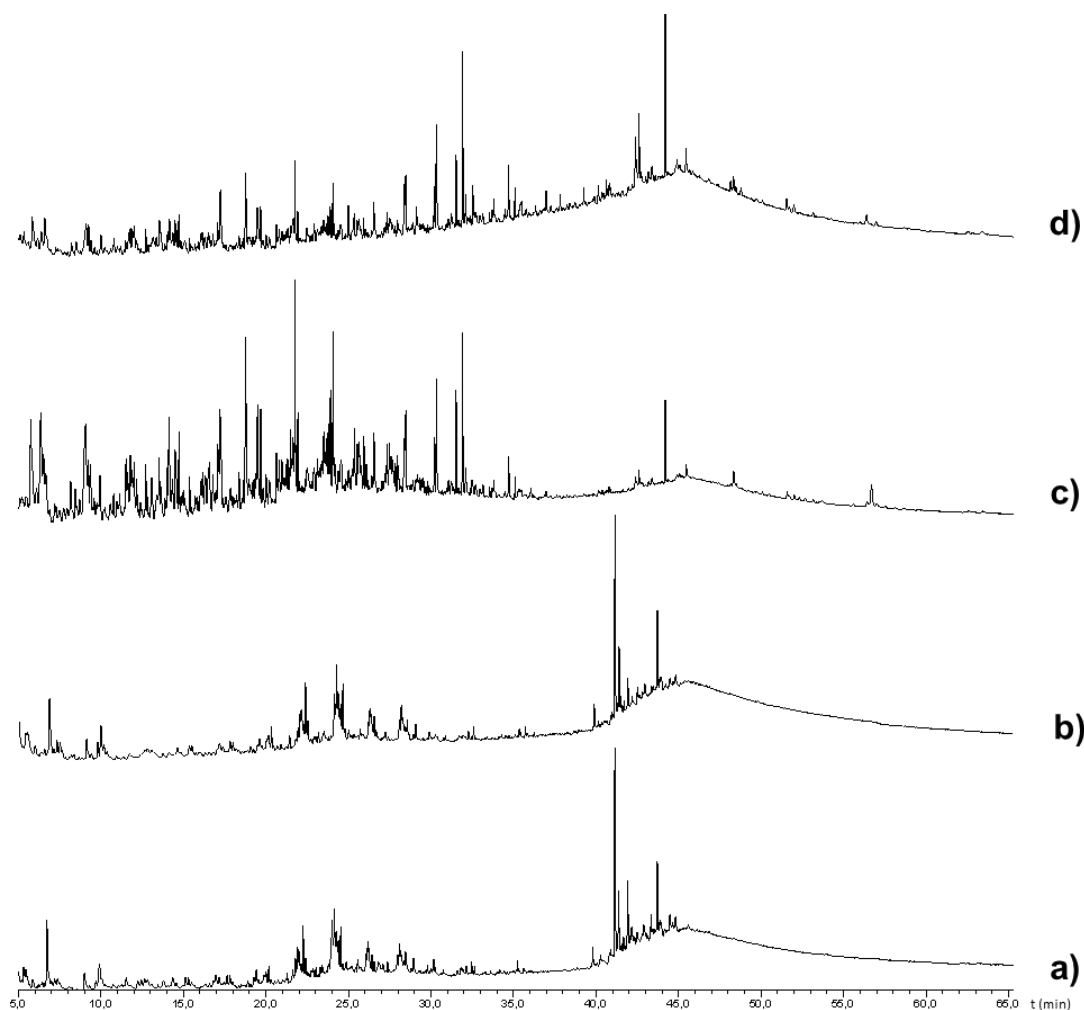


Figure 59. Total Ion Chromatograms (TIC) of urushi acquired by THM-GC/MS: **a)** fresh, **b)** dried at the touch (2 weeks), **c)** naturally aged (2 years) and **d)** accelerated artificially daylight aged (28 days, starting from the naturally aged samples set).

$m/z=57$ – alkanes and alkenes

Extracted Ion Chromatograms (EIC) at $m/z=57$ of urushi are shown in Figure 60.

These EICs show alkyl ($m/z=57$ as base peak) and alkenyl ($m/z=55$ as base peak) hydrocarbons fragments which are the pyrolytic products produced by the cleavage of the linear saturated and unsaturated side chain hydrocarbon on the aromatic ring of catechol, such as on 3-alkylcatechols in *urushiol* (Figure 7) [19].

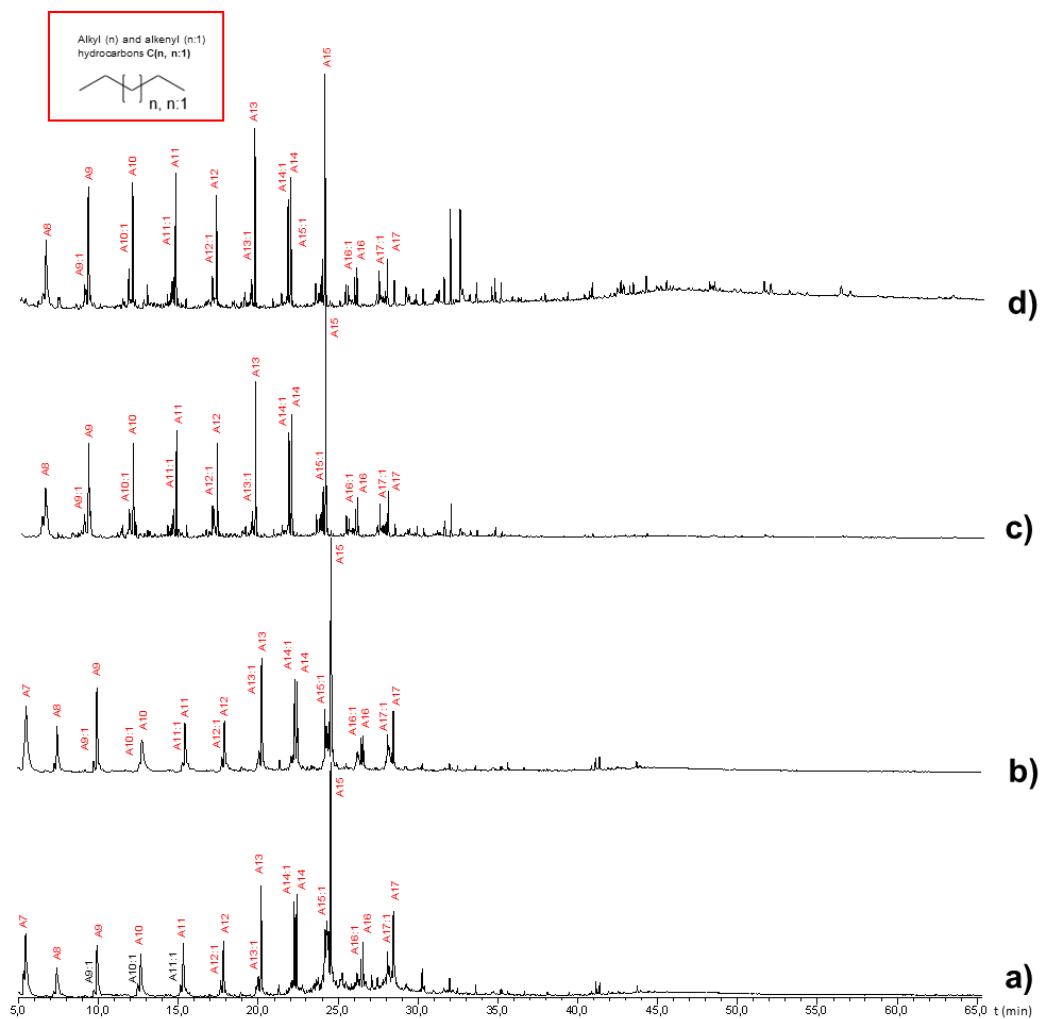


Figure 60. Extracted Ion Chromatograms (EIC) of urushi acquired by THM-GC/MS and obtained by plotting single ion mass profile at $m/z=57$: **a)** fresh, **b)** dried at the touch (2 weeks), **c)** naturally aged (2 years) and **d)** accelerated artificially daylight aged (28 days, starting from the naturally aged samples set).

By looking at the pyrolytic profiles of the EICs at $m/z=57$ registered for *2-year naturally aged* (c) and *accelerated artificially daylight aged* (d) urushi it is possible to notice a bell-shape between RT 10 and 18 minutes (A9-A12) with A11 the most intense peak. In *fresh* (a) and *dried-at-the-touch* (b) urushi no particular shape profiles have been noted. This could be due to the shift of double bonds in *urushiol* side chain, due to the several nucleus-side chain and/or side chain-side chain couplings that occurs with polymerization. The pyrolytic fragmentation could, in this way, change its preferential positions along the side chain. The artificial accelerated daylight ageing did not influence any change in this chromatographic range.

For EIC at $m/z=57$ of urushi-based model sample, the series of alkyl and alkenyl hydrocarbons starts with heptane (A7) and ends with heptadecane (A17). This means that the longest detected alkane (seventeen carbon atoms) is longer than the maximum *urushiol* side aliphatic side chain (fifteen carbon atoms). The same experimental evidence has been reported in literature [19]. A speculation for this experimental evidence could involve the fragmentation of side chain-side chain coupled catechols in the polymerized network, as shown in Figure 61.

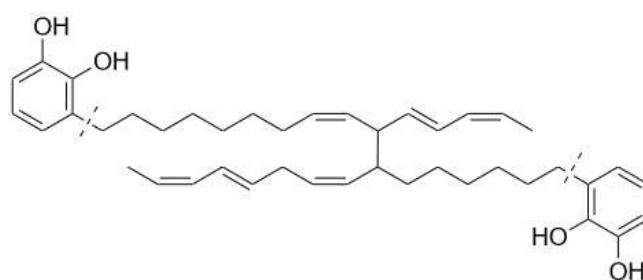


Figure 61. Speculated fragmentation of a nucleus-nucleus coupled dimer of urushiol in polymerized.

The most abundant aliphatic hydrocarbon in all the EICs at $m/z=57$ of urushi-based sample is the pentadecane (A15), followed by tridecane in accordance with literature data [7, 19, 56, 60]. The most abundant alkene has been assigned to tetradecene (A14:1). In the literature a similar EIC at $m/z=57$ for thitsi acquired by THM-GC/MS has been obtained by Le Hô: the most abundant alkanes have been assigned to pentadecane and tridecane, however, the most abundant alkene has been assigned to heptane. [19].

Furthermore, the intensity of alkanes is always higher than the alkenes counterpart, except for tetradecene (A14:1) and tetradecane (A14) in the *dried-at-the-touch* urushi (chromatogram b).

$m/z=91$

Extracted Ion Chromatograms (EIC) at $m/z=91$ of urushi are shown in Figure 62.

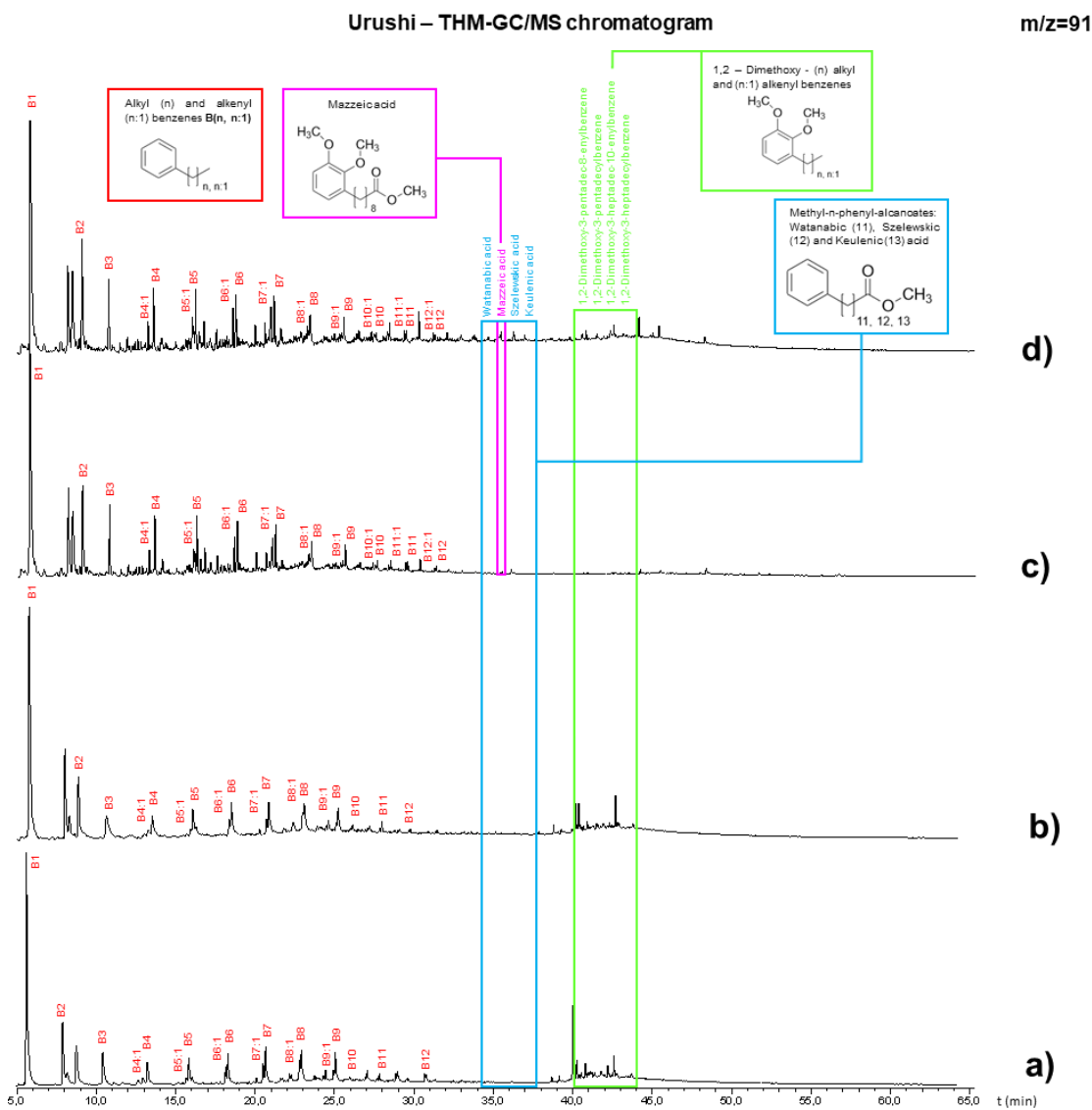


Figure 62. Extracted Ion Chromatograms (EIC) of urushi acquired by THM-GC/MS and obtained by plotting single ion mass profile at $m/z=91$: **a)** fresh, **b)** dried at the touch (2 weeks), **c)** naturally aged (2 years) and **d)** accelerated artificially daylight aged (28 days, starting from the naturally aged samples set).

These EICs show alkyl ($m/z=92$ as base peak) and alkenyl ($m/z=91$ as base peak) benzene fragments which are the pyrolytic products resulting from the dehydration of alkylphenols, intermediate compounds formed from catechols during pyrolysis [19].

The *fresh* and *dried-at-the-touch* EICs at $m/z=91$ of urushi-based model sample shows a bell-shape in the range of 13-28 RT (peaks B4-B9, with B7 the most abundant of the group). After 2 years of natural aging the EICs profile changes: peaks

between B3-B7 significantly increase, as observed for thitsi EICs at $m/z=91$. B2 increases too.

The urushi EIC $m/z=91$ shows a first intense peak assigned to toluene (B1), the most intense peak of the series, according with the literature [19], and ends with the dodecyl benzene (B12), the longest detected peak. This is in agreement with the fact that the maximum side chain in *urushiol* has twelve carbon atoms. The urushi EICs at $m/z=91$ are completely different from the thitsi EICs at $m/z=91$, in every step of drying and aging processes. As expected, the general abundance of the peaks in urushi EICs at $m/z=91$ is lower than thitsi EICs at $m/z=91$, due to the missing contribute of alkylphenyl side chains.

In this series of EIC, between minute 40 and minute 44, the methylated alky/alkenyl benzenes (1,2-dimethoxy-3-pentadec-8-enylbenzene, base peak at $m/z=346$; 1,2-dimethoxy-3-pentadecylbenzene, base peak at $m/z=348$; 1,2-dimethoxy-3-heptadec-10-enylbenzene, base peak at $m/z=374$; 1,2-dimethoxy-3-heptadecylbenzene, base peak at $m/z=376$, highlighted in green) have been found too. Methylated phenyl benzenes and alkyl and phenyl anisoles detected in thitsi-based samples have not been found in urushi sample, according with the fact that *urushiol* has not alkylphenyl side chains in its chemical composition. They are the results of the methylation reaction of catechols with TMAH reagents, as already explained in paragraph 5.1.4. Contrary from thitsi EICs at $m/z=91$, EICs at $m/z=91$ of urushi shows an increase of the abundance of methylated alky/alkenyl benzenes, in particular for the 1,2-dimethoxy-3-heptadec-10-enylbenzene (base peak at $m/z=374$), after 2 weeks of drying in climate chamber.

Finally, one of the main advantages of using a derivatizing reagent such as TMAH for the investigation of Asian lacquers is shown by the detection of some methylated oxidation products between 34 and 38 minutes of RT. These are the catechol acids as methyl 8-(2,3-dimethoxyphenyl) octanoate also known Mazzeic acid (base peak at $m/z=136$, highlighted in blue) and the phenylalkanoic acids group as methyl phenyl alcanoates (base peak at $m/z=91$, highlighted in pink). The methyl phenyl alcanoates group includes methyl 11-phenyl-undecanoate (watanabic acid, MW=276), methyl 12-phenyl-dodecanoate (szelewskic acid, MW= 290), and methyl 13-phenyl-tridecanoate (keulenic acid, MW=304).

As shown in the EICs at $m/z=91$, the methyl phenyl alcanoates group was already detected in the *fresh* urushi, while the presence of Mazzeic acid was evinced not before the 2 years of natural aging. This suggests the relative quick formation of

phenylalkanoic acids in the thitsi lacquer in contrast to the catechol acids, which require slower mechanisms of reaction.

The reaction mechanisms proposed by Tamburini (Figure 49, Reaction mechanism 1) to explain the presence of methyl phenyl alcanoates is not valid for urushi which has not phenyl side chains. However, it is possible that, after the dehydration of alkylcatechol and alkylphenols [19], a similar reaction mechanism could occur.

The reaction mechanism for the formation of Mazzeic acid has never been proposed. However, it could be formed by the same radical oxidation described in Figure 53 (Reaction mechanism 2) of aliphatic catechols.

m/z=120

Extracted Ion Chromatograms (EIC) at *m/z*=120 of urushi are shown in Figure 63.

In urushi EIC at *m/z*=120 only acetophenone (C2, base peak at *m/z*=105) at 14 minutes of RT has been detected. The abundance of acetophenone does not show any changes during the 28 days of accelerated artificial daylight aging. No alkyl phenyl ketones have been found and this agrees with the fact that *urushiol* has not alkylphenyl substituted catechols, contrary to *thitsiol*.

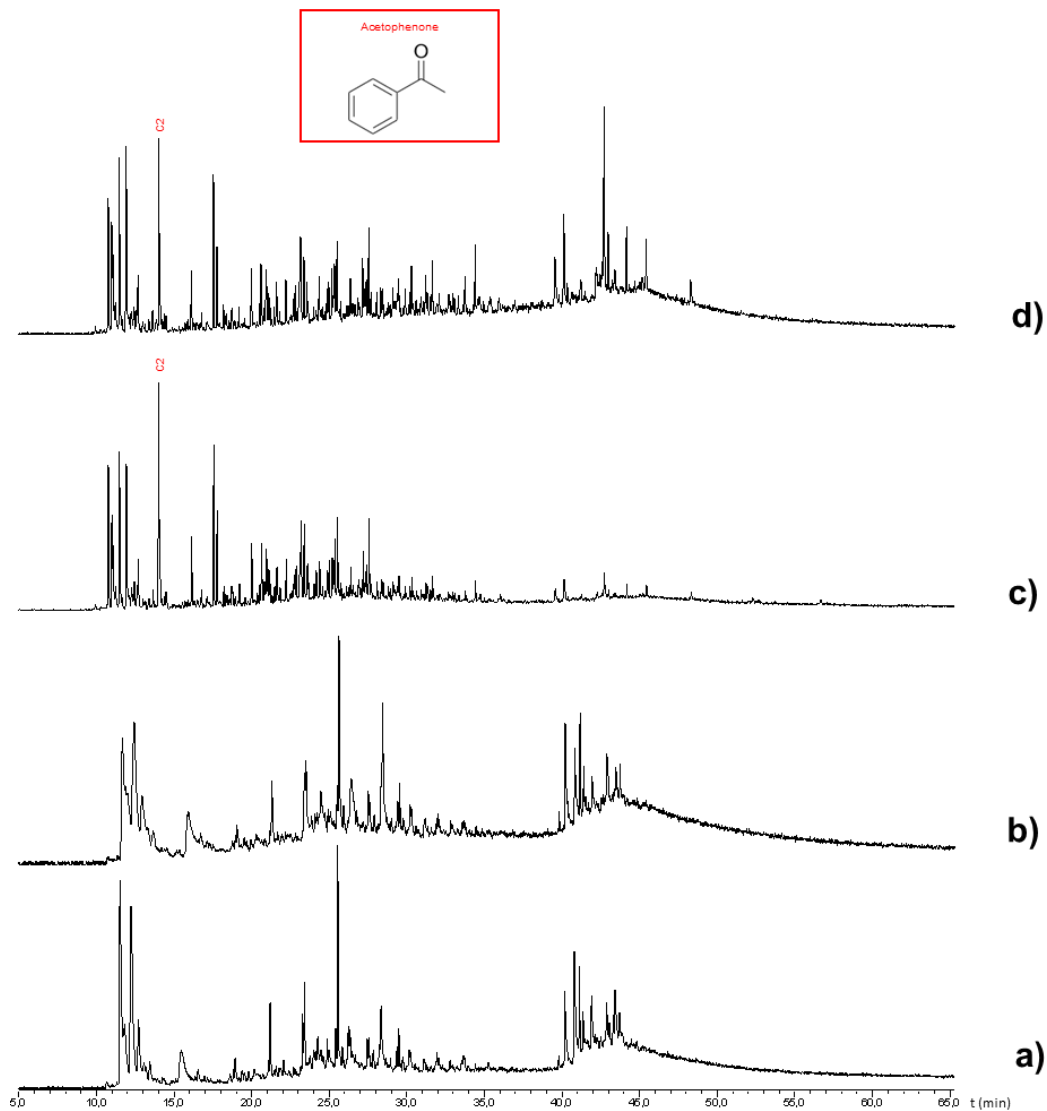


Figure 63. Extracted Ion Chromatograms (EIC) of urushi acquired by THM-GC/MS and obtained by plotting single ion mass profile at $m/z=120$: **a)** fresh, **b)** dried at the touch (2 weeks), **c)** naturally aged (2 years) and **d)** accelerated artificially daylight aged (28 days, starting from the naturally aged samples set).

5.3 Blend of *urushiol* and *thitsiol*

5.3.1 Digital Microscopy

The images obtained with Keyence Digital Microscopy in three different magnifications (100x, 500x, 1000x) of urushi added with thitsi filtered in a 20:80 ratio, urushi added with thitsi filtered in a 1:1 ratio and urushi added with thitsi filtered with 10% oil are shown in Figure 64, 65 and 66, respectively.

Digital Microscopy investigation on thitsi lacquer gave interesting results about the resistance of the material and the physical changes in its surface when subjected to accelerated artificial daylight aging. After 28 days in UV chamber urushi/thitsi blended-based samples showed a geometric network of cracks in the surface. This is less evident and less marked than thitsi network of cracks. No difference between the three blended lacquers has been noted.

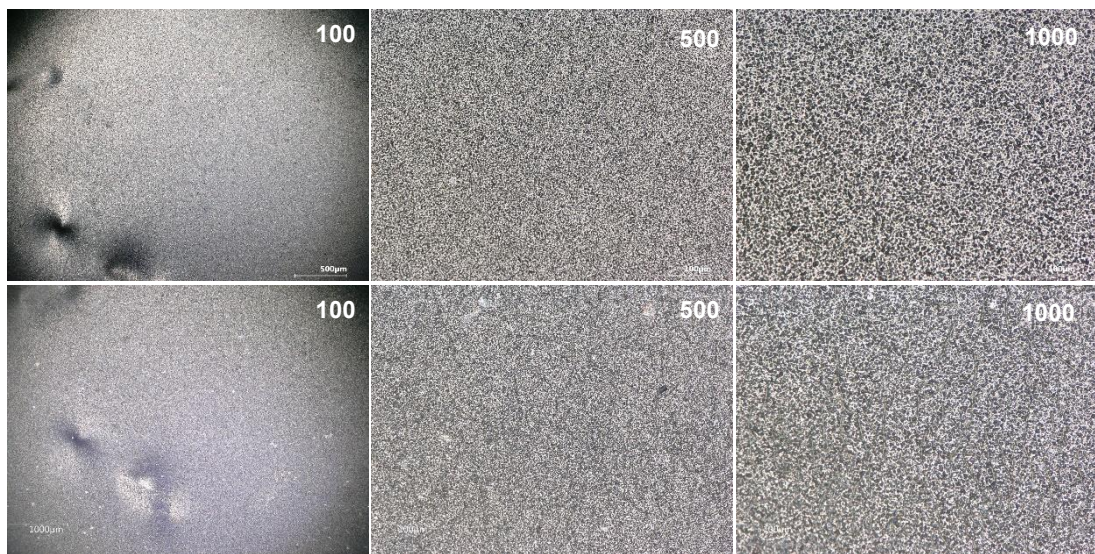


Figure 64. Pre (up) and post (down) accelerated artificial daylight aging images of urushi added with thitsi filtered in a 20:80 ratio acquired by digital microscopy in three different magnifications: 100x (left), 500x (middle), 1000x (right).

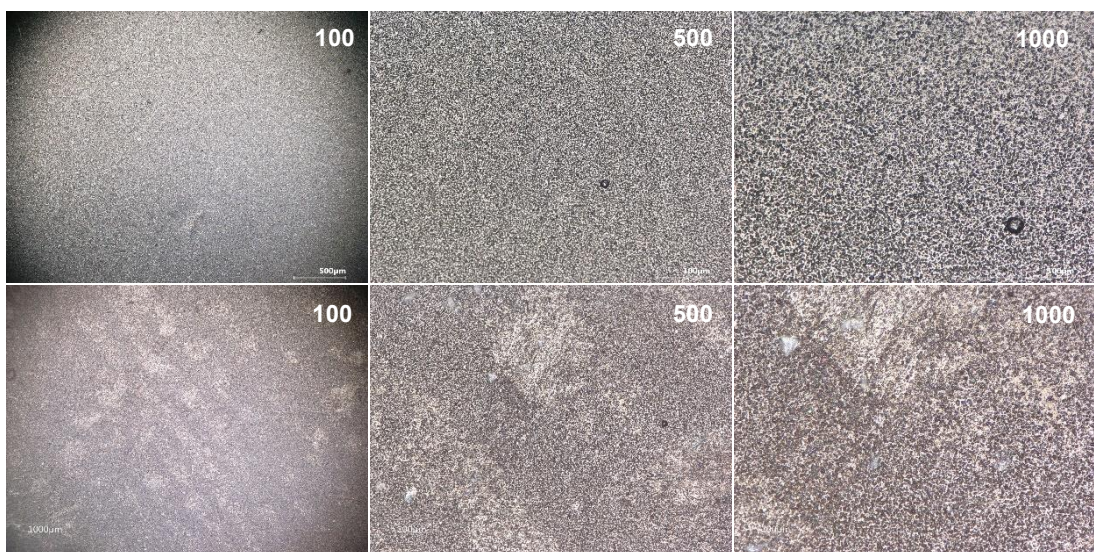


Figure 65. Pre (up) and post (down) accelerated artificial daylight aging images of urushi added with thitsi filtered in a 1:1 ratio acquired by digital microscopy in three different magnifications: 100x (left), 500x (middle), 1000x (right).

This network of cracks is the physical evidence that an oxidation process has happened. According to the literature, this process begins on the surface of the material and with the occurring of the oxidation process the cracks become deeper and deeper [1]. As reported in paragraph 2.1.2 the oxidation process leads to the oxidation of the conjugated side chain of catechol and subsequently to the formation of a series of oxidation products which, in the end, leads to the decomposition of the polymerized lacquer network [1]. In case of blended Asian lacquers, the oxidation process seems to be at an intermediate stage between urushi and thitsi-based lacquers. It could be speculated that the oxidation rate in urushi/thitsi blended samples is faster than urushi-based sample and slower than thitsi-based samples.

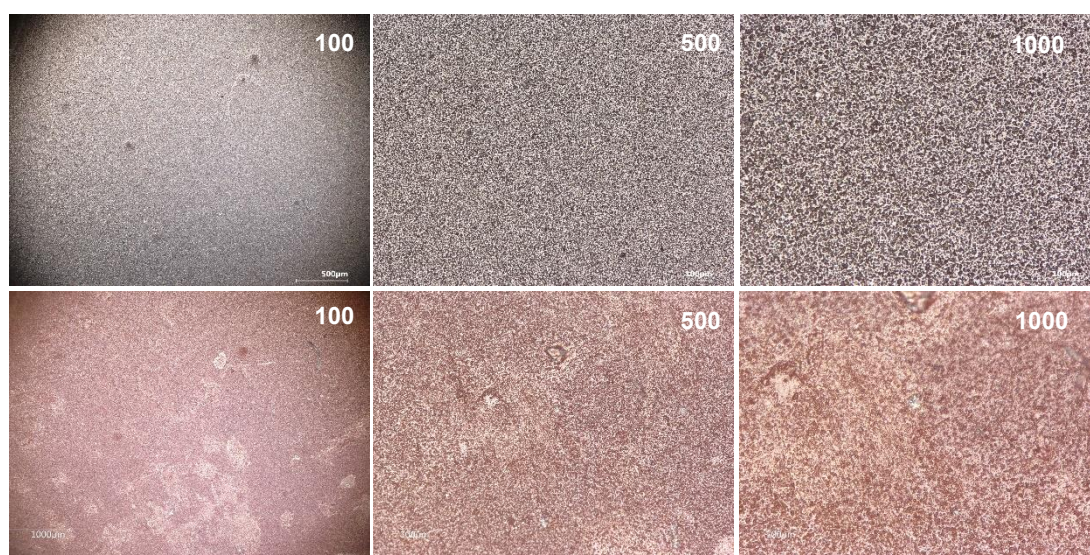


Figure 66. Pre (up) and post (down) accelerated artificial daylight aging images of urushi added with thitsi filtered with 10% oil acquired by digital microscopy in three different magnifications: 100x (left), 500x (middle), 1000x (right).

In urushi/thitsi blended-based samples, as in thitsi-based samples, the presence of circular spots in the surface of the lacquers after 28 days of accelerated artificial daylight aging. They could be interpreted as the of the dispersed polysaccharide particles in the surface layer, due to the UV exposure. In fact, under light exposure, the core–shell structure, composed of a thin shell of polysaccharides and glycoproteins and surrounding the polymerized catechols, is damaged. This fact has been detected in the literature [1] with the appearance of circular spots in the surface of some artificially aged Asian lacquer samples.

The black small and circular spots in the background are the marks of waterdrops in the lacquer sap [58]. No significant qualitative changes during the 28 days of accelerated artificial daylight aging have been detected.

5.3.2 Colorimetry

Colorimetry investigation on urushi added with thitsi filtered in 20:80 ratio, urushi added with thitsi filtered in 1:1 ratio and urushi added with thitsi filtered with 10% oil lacquer gave different information useful for the understanding of the material colour and reflectance behaviour during the 28 days of accelerated artificial daylight aging.

The reflectance spectra of urushi added with thitsi filtered in 20:80 ratio, urushi added with thitsi filtered in 1:1 ratio and urushi added with thitsi filtered with 10% oil are shown in Figure 67, 68 and 69, respectively. In all three spectra it is easily possible to notice a shift to higher reflectance number from the pre aging (blue) to the post aging (orange), as already noted for both thitsi and urushi-based samples. This means that thitsi lacquer type tends to increase its reflecting power after an aging process.

The $L^*a^*b^*$ space graphic representations of urushi added with thitsi filtered in 20:80 ratio, urushi added with thitsi filtered in 1:1 ratio and urushi added with thitsi filtered with 10% oil, are shown in Figure 70, 71 and 72, respectively while the measured values are shown in Table 11 together with their standard deviations.

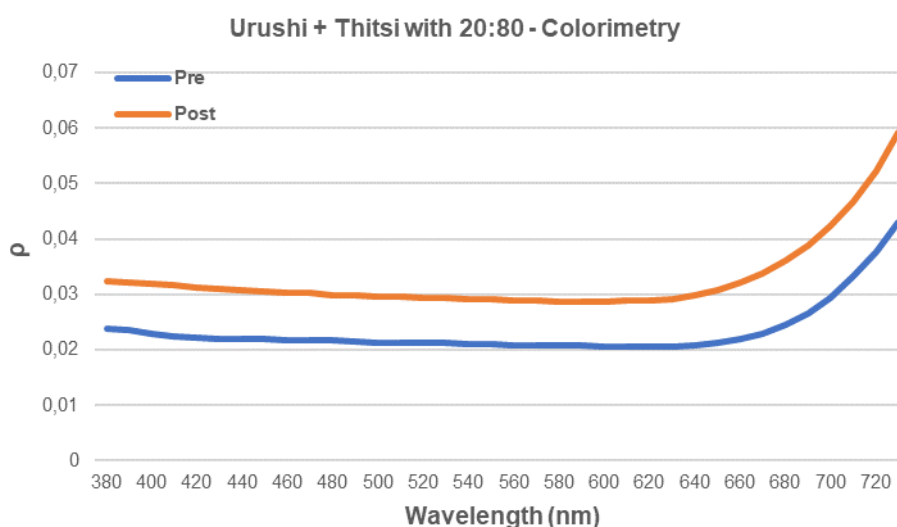


Figure 67. Reflectance spectrum of urushi added with thitsi filtered in 20:80 ratio pre (blue) and post (orange) accelerated artificial daylight aging.

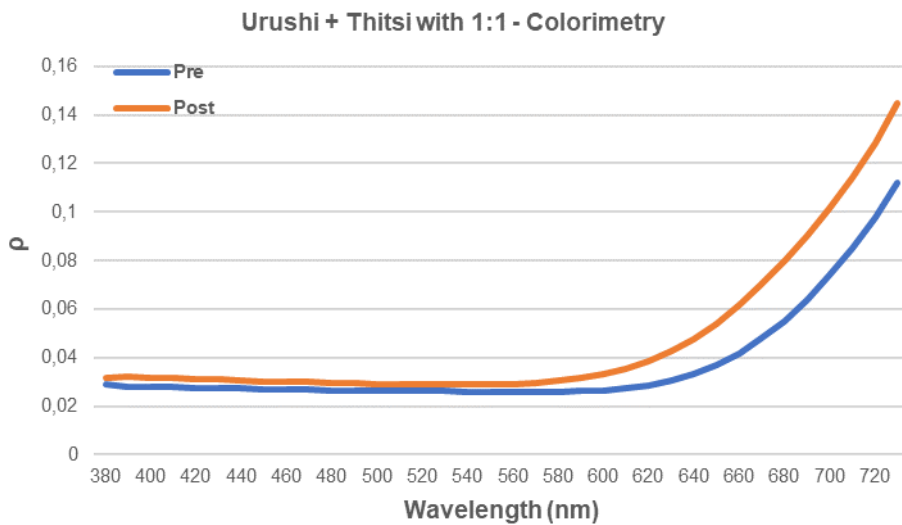


Figure 68. Reflectance spectrum of urushi added with thitsi filtered in 1:1 ratio pre (blue) and post (orange) accelerated artificial daylight aging.

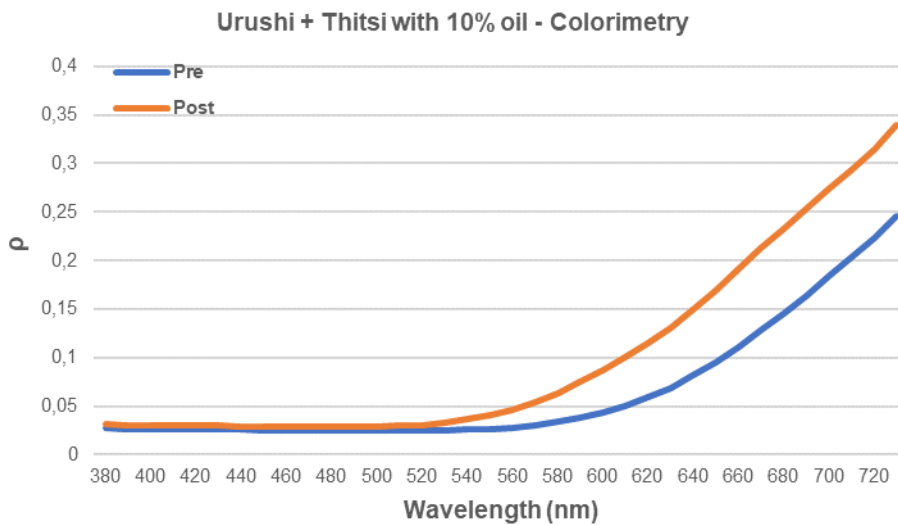


Figure 69. Reflectance spectrum of urushi added with thitsi filtered with 10% oil pre (blue) and post (orange) accelerated artificial daylight aging.

The high heterogeneity of the sample layer on the mock-ups and the low number of measurements performed on each sample determined a very high standard deviation for L^* , a^* and b^* values. In 1:1 urushi/thitsi blend and with 10% oil urushi/thitsi blend the a^* against b^* graphs it is demonstrated that the respective blended lacquers are subjected to a common shift to a^*+ coordinate (red in the red/green axis) and b^*+ coordinate (yellow in the yellow/blue axis), as seen for both thitsi and urushi-based samples. However, in the 20:80 urushi/thitsi blend a^* against b^* graph a different shift

has been shown: the a^* coordinate still shifts to redder coordinate (a^{+*}) but b^* coordinate shifts to bluer coordinate (b^{-*}). As observe in case of thitsi filtered with 10% oil, the urushi/thitsi blend with 10% oil shows the greater ΔE^* due to the greater Δb^* , probably because of the presence of the oil [59].

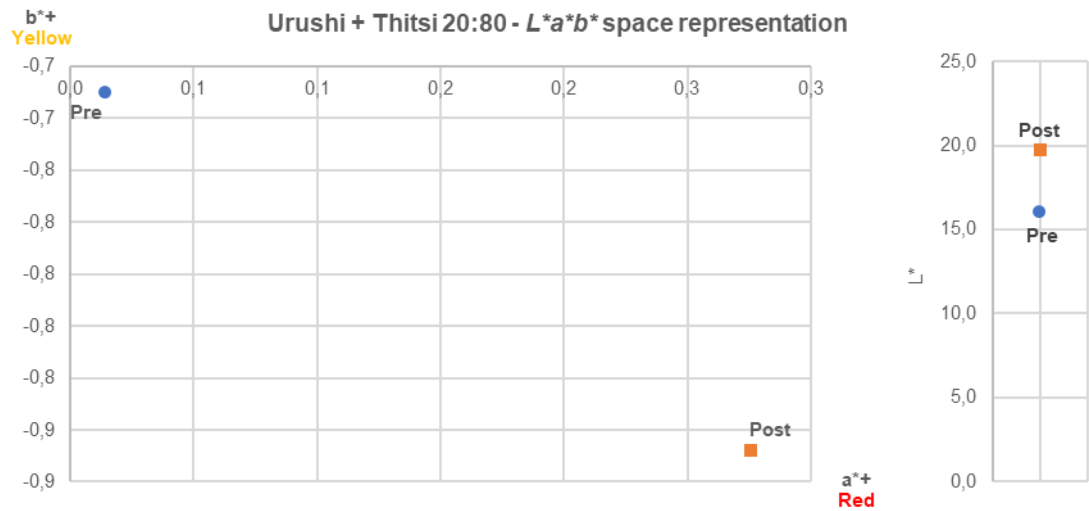


Figure 70. $L^*a^*b^*$ space representation of urushi added with thitsi filtered in 20:80 ratio pre (blue) and post (orange) accelerated artificial daylight aging: a^*b^* graph (left) and L^* graph (right).

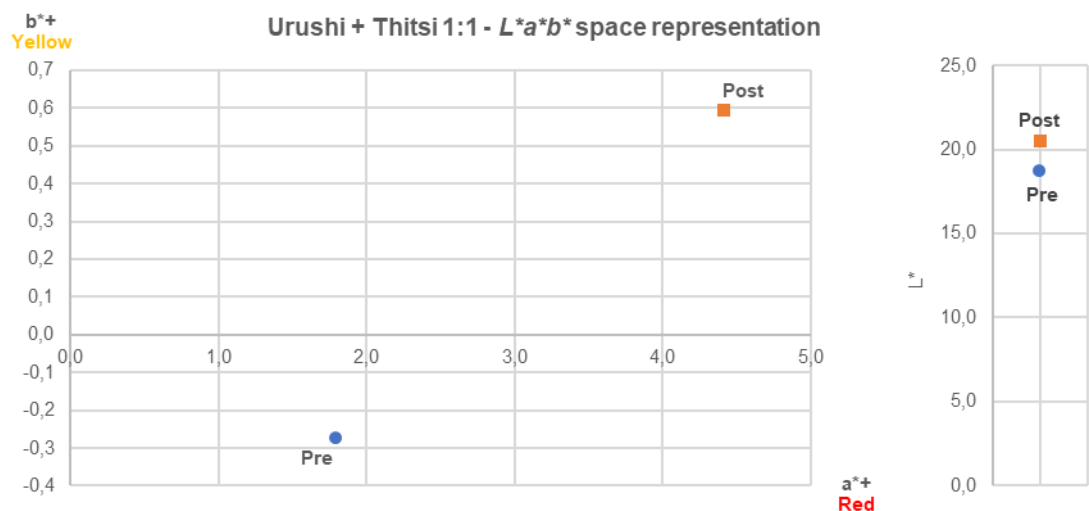


Figure 71. $L^*a^*b^*$ space representation of urushi added with thitsi filtered in 1:1 ratio pre (blue) and post (orange) accelerated artificial daylight aging: a^*b^* graph (left) and L^* graph (right).

More important is the variation of the L^* coordinate. Each blend-based sample shows an increase of L^* values which means a common tendency to shift to brighter colour. As already said for both thitsi and urushi-based samples, it is possible to deduce that

this material tends to increase its reflecting power, in agreement with reflectance spectra.

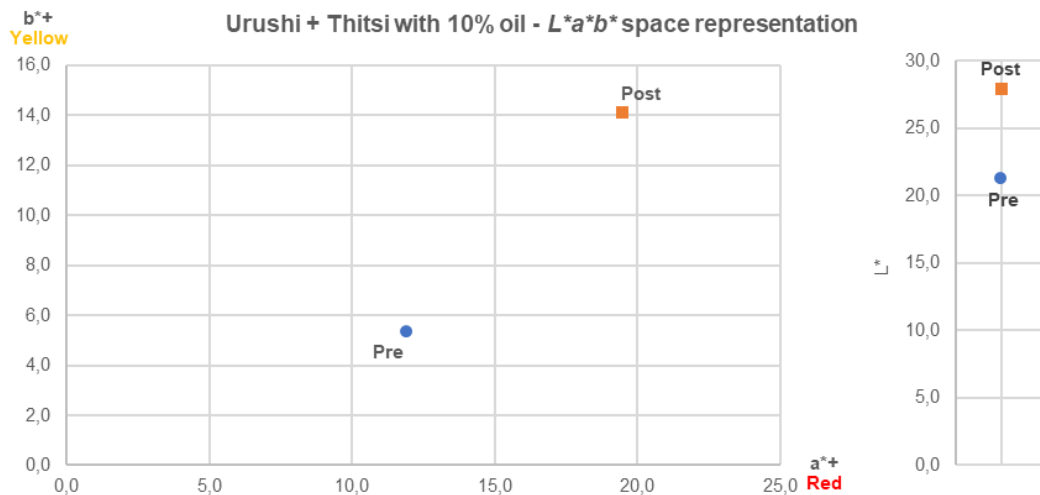


Figure 72. $L^*a^*b^*$ space representation of urushi added with thitsi filtered with 10% oil pre (blue) and post (orange) accelerated artificial daylight aging: a^*b^* graph (left) and L^* graph (right).

The calculated ΔE^* values are shown in Table 11: the higher the increase of this number, the higher the total colour change of the material. According to Table X, 20:80 urushi/thitsi blend and 1:1 urushi/thitsi blend-based samples have a calculated ΔE^* between 2-10 which means that the colour change is “perceptible at a glance” while urushi/thitsi blend with 10% oil has a ΔE^* between 10-49 which means that “colours are more similar than opposite”.

	L^*	$s_x(L^*)$	a^*	$s_x(a^*)$	b^*	$s_x(b^*)$	ΔE^*
Urushi + Thitsi 20:80 Pre	16,0	2,0	0,01	4,4	-0,73	3,7	
Urushi + Thitsi 20:80 Post	19,7	1,6	0,28	2,1	-0,87	3,4	3,7
Urushi + Thitsi 1:1 Pre	18,7	0,2	1,8	1,1	-0,3	0,4	
Urushi + Thitsi 1:1 Post	20,5	0,7	4,4	2,5	0,6	1,2	3,3
Urushi + Thitsi with 10% oil Pre	21,3	0,5	11,9	0,31	5,3	0,06	
Urushi + Thitsi with 10% oil Post	27,9	0,3	19,5	0,6	14,1	0,3	13,4

Table 11. L^* , a^* and b^* values and their standard deviations measured for urushi added with thitsi filtered in 20:80 ratio, urushi added with thitsi in 1:1 ratio and urushi added with thitsi filtered with 10% oil before (pre) and after (post) accelerated artificial daylight aging and the calculated ΔE^* .

5.3.3 FTIR

In the following section both Transmission and ATR of the different urushi and thitsi mixture are presented and discussed. As described in the timeline scheme (Figure 23), Transmission spectra have been registered since the mock-ups preparation when the material was still in a liquid state (*fresh*) and then in every step of their physical state change: after the drying in climate chamber (*dried at the touch*), after 2 years of natural aging (*naturally aged*), and after 28 days of accelerated artificial daylight aging (*accelerated artificial daylight aged*). ATR spectra have been registered only for *naturally aged* and *accelerated artificial daylight aged* urushi/thitsi blends, due to liquid and semiliquid state of the materials in the first two steps.

Transmission mode

The Transmission Spectra urushi added with thitsi filtered in a 20:80 ratio, urushi added with thitsi filtered in a 1:1 ratio and urushi added with thitsi filtered with 10% oil are shown in Figure 73, 74 and 75, respectively.

The complete peaks assignment is shown in Table 12.

The spectra show the changes of functional groups in urushi/thitsi blend-based samples during the drying, natural aging and accelerated artificial daylight aging process. In the region between 3100-3000 cm^{-1} a pattern of three peaks have been detected, as detected for thitsi-based samples. The differences among the three samples derive from the different ratio between thitsi and urushi. The 20:80 urushi/thitsi blend shows an intense absorption at 3024 cm^{-1} , according with the high percentage (80%) of thitsi. On the contrary in the 1:1 and oil added mixture the noticeable absorption is centred at 3010 cm^{-1} , as in pure urushi.

The most significant variation in terms of intensities ratio has been detected in the peaks around 1715 and 1621 cm^{-1} , as already seen for both thitsi and urushi -based samples. These two peaks have been assigned to carbonyl and C=C stretching of the aromatic ring skeletal vibrations of the polymerized catechol derivatives, respectively. Their behaviour is consistent with the one described paragraph 5.1.3 and 5.2.3: a shift to lower wavenumber and an increasing of the intensity ratio of the two peaks (1715/1621) have been detected with the increasing in ageing time. This has been associated to the progressing of oxidation process [17].

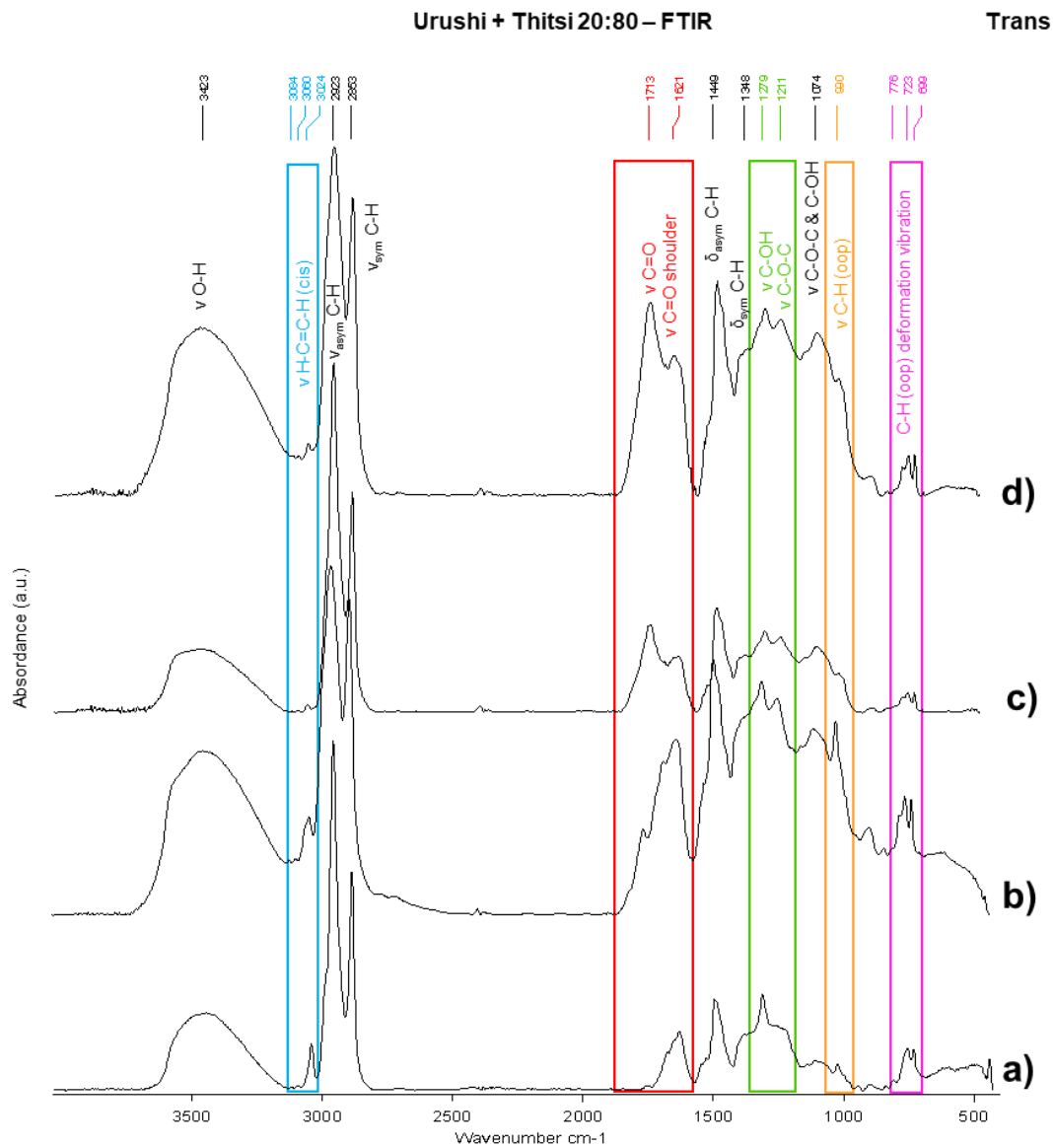


Figure 73. Transmission FTIR spectra of urushi added with thitsi filtered in a 20:80 ratio: **a)** fresh, **b)** dried at the touch (8 weeks), **c)** naturally aged (2 years) and **d)** accelerated artificially daylight aged (28 days, starting from the naturally aged samples set).

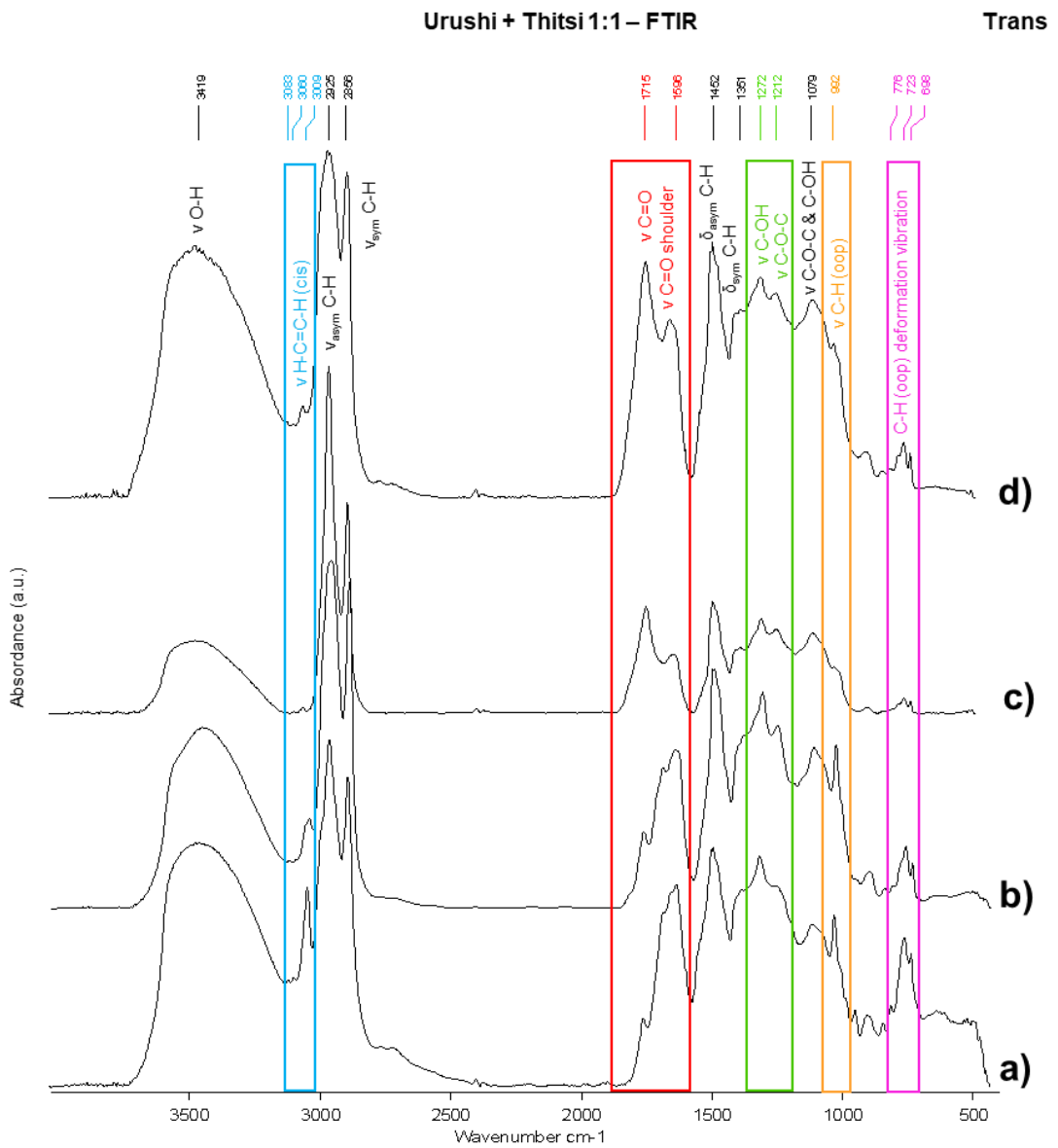


Figure 74. Transmission FTIR spectra of urushi added with thitsi filtered in a 1:1 ratio: **a)** fresh, **b)** dried at the touch (8 weeks), **c)** naturally aged (2 years) and **d)** accelerated artificially daylight aged (28 days, starting from the naturally aged samples set).

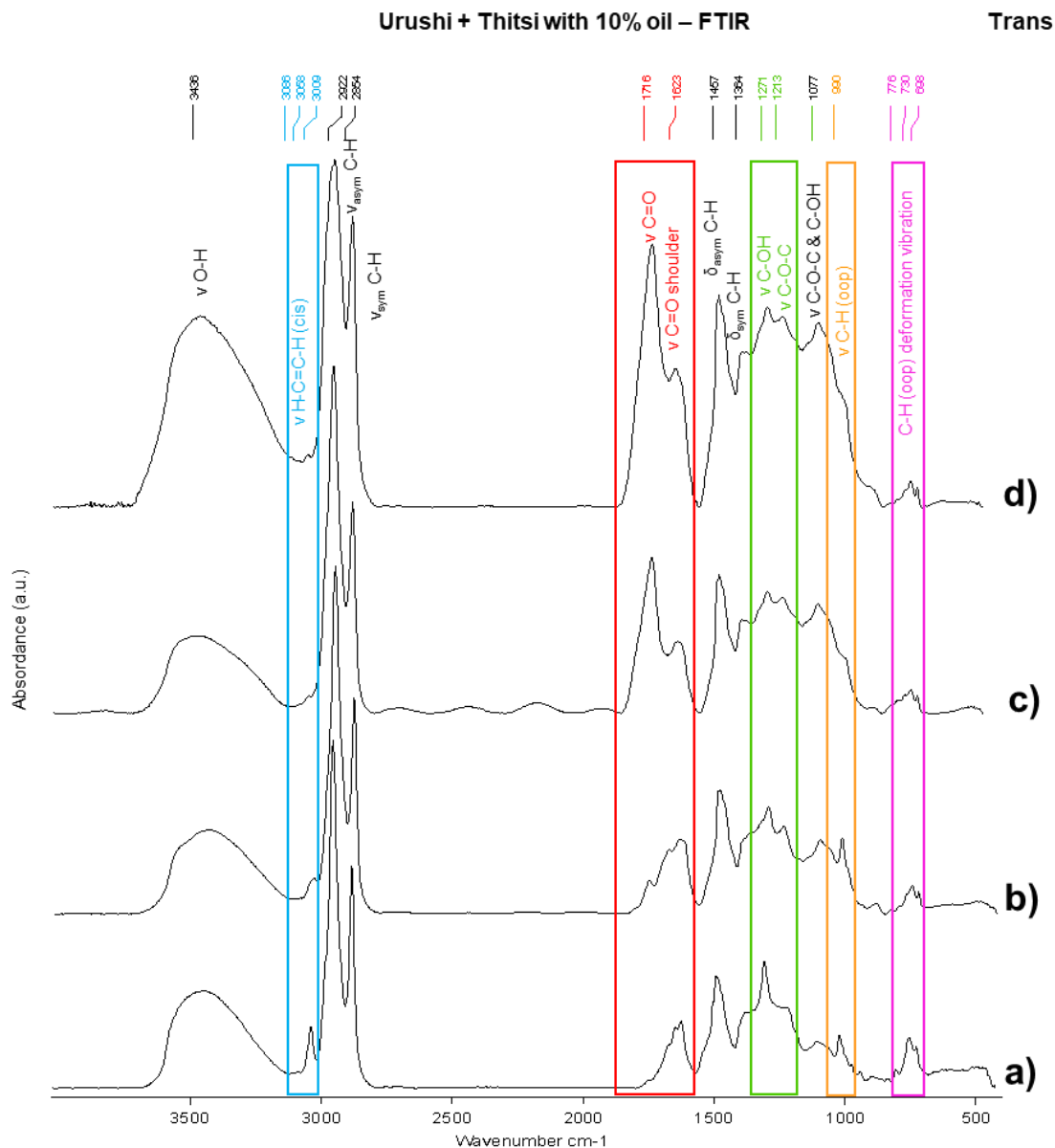


Figure 75. Transmission FTIR spectra of urushi added with thitsi filtered with 10% oil: **a)** fresh, **b)** dried at the touch (8 weeks), **c)** naturally aged (2 years) and **d)** accelerated artificially daylight aged (28 days, starting from the naturally aged samples set).

As detected in both thitsi and urushi, peak around 1272 cm^{-1} , assigned to C-OH stretching in catechols and phenols, decreases in blended lacquers too, due to the progressing of photo-oxidation, as already explained in paragraph 5.3.1.

The peak at 1081 cm^{-1} , assigned to C-OH stretching of polysaccharides, does not show significant changes.

The absorption at 993 cm^{-1} , assigned to C-H out of plane stretching of conjugated trienes in the side chain, does not show any differences from thitsi and urushi. Its

decrease has been interpreted as a decrease in the number of unsaturated side chains, as the polymerization occurs [1].

Ur/Th 20:80 (cm ⁻¹)	Ur/Th 1:1 (cm ⁻¹)	Ur/Th + 10% oil (cm ⁻¹)	Peaks Assignment
3423	3419	3436	O-H stretching of catechol ring or polysaccharides [9, 20, 27, 41]
3084 – 3060 - 3024	3083 – 3060 - 3009	3086 – 3058 - 3009	H-C=C-H stretching of the different substituted catechols, phenols and aromatic side chains in <i>thitsiol</i> [60]
2923	2925	2922	C-H stretching asymmetric of CH ₂ and CH ₃ of the side chain [9, 17, 41]
2853	2856	2854	C-H stretching symmetric of CH ₂ and CH ₃ of the side chain [9, 27, 41]
1713	1715	1716	C=O stretching [9, 17, 41]
1621	1598	1623	C=C stretching (C=O shoulder) of the aromatic ring skeletal vibrations of the polymerized catechol derivatives [41]
1449	1452	1457	C-H bending (asymmetric) of side chain [17, 41]
1348	1361	1364	CH ₃ bending (symmetric) [9]
1279	1272	1272	C-OH stretching of phenol [41]
1211	1212	1210	C-O-C glycosidic group [1, 41]
1074	1079	1077	C-O-C of sugar units [9] or C-OH stretching of polysaccharides [41]
990	992	990	C-H out of plane stretching of conjugated trienes in the side chain [9, 20]
776	776	776	C-H deformation vibration out-of-plane [41]
723	723	730	C-H deformation vibration out-of-plane [41] due to catechol in the monomer [20]
699	698	698	C-H deformation vibration out-of-plane [41] due to catechol in the monomer [20]

Table 12. Transmission FTIR peaks and their assignments for urushi added with thitsi filtered in a 20:80 ratio, urushi added with thitsi filtered in a 1:1 ratio and urushi added with thitsi filtered with 10% oil.

ATR mode

The ATR Spectra of urushi added with thitsi filtered in a 20:80 ratio, urushi added with thitsi filtered in a 1:1 ratio and urushi added with thitsi filtered with 10% oil are shown in Figure 76, 77 and 78, respectively.

The complete peaks assignment is shown in Table 13.

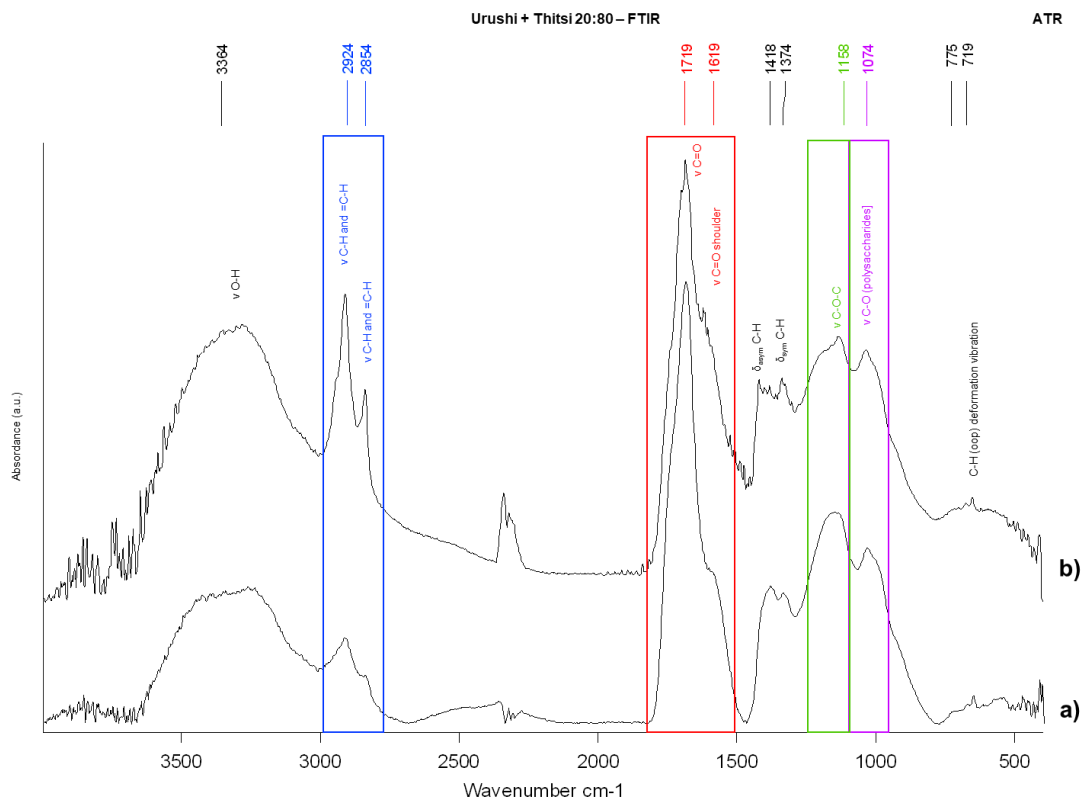


Figure 76. Attenuated Total Reflection FTIR spectra of urushi added with thitsi filtered in a 20:80 ratio: **a)** fresh, **b)** dried at the touch (8 weeks), **c)** naturally aged (2 years) and **d)** accelerated artificially daylight aged (28 days, starting from the naturally aged samples set).

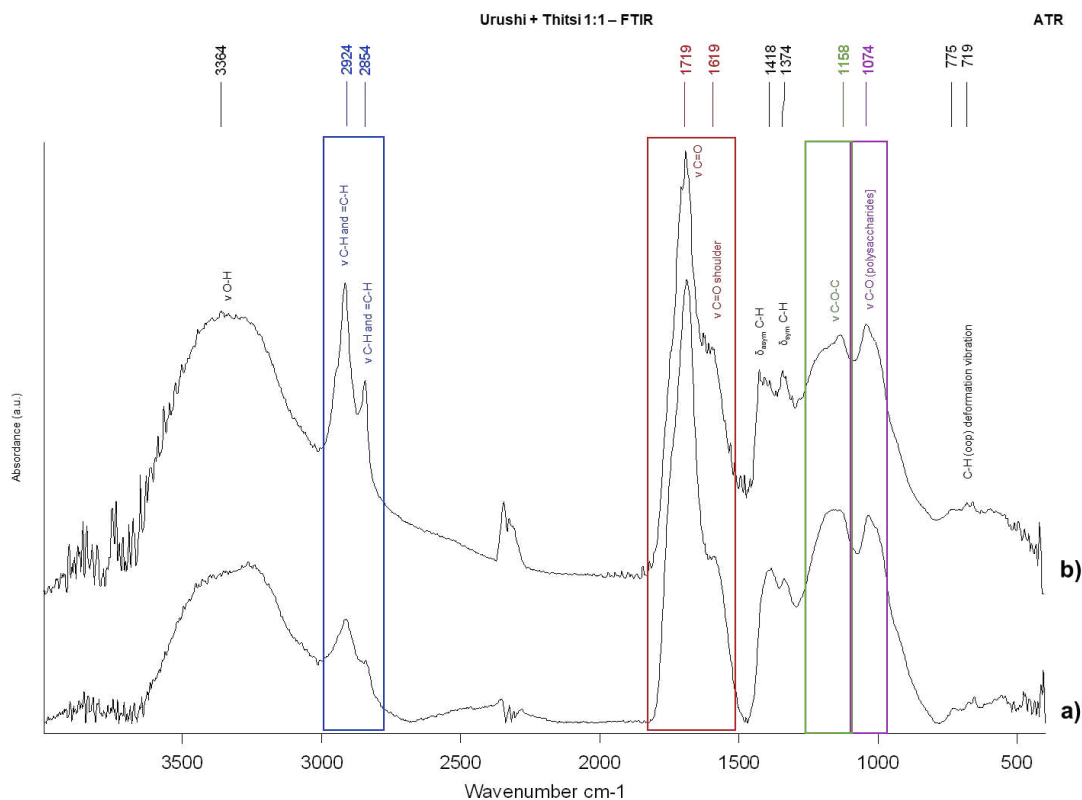


Figure 77. Attenuated Total Reflection FTIR spectra of urushi added with thitsi filtered in a 1:1 ratio: **a)** fresh, **b)** dried at the touch (8 weeks), **c)** naturally aged (2 years) and **d)** accelerated artificially daylight aged (28 days, starting from the naturally aged samples set).

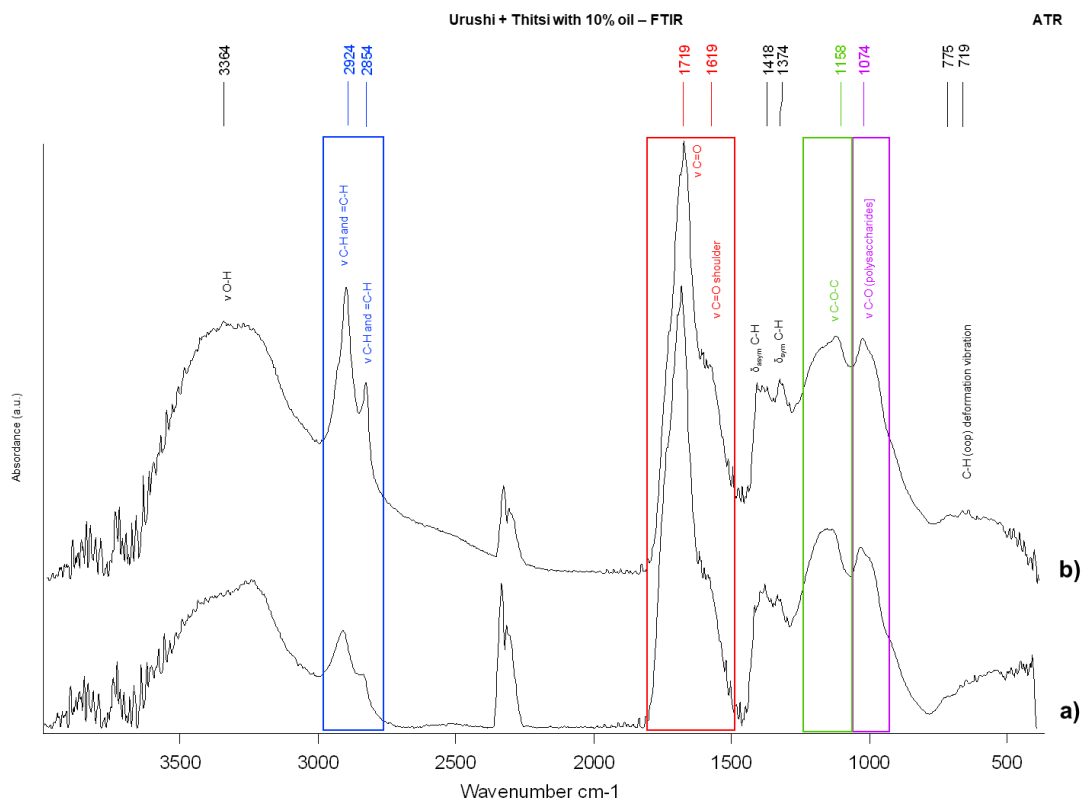


Figure 78. Attenuated Total Reflection FTIR spectra of urushi added with thitsi filtered with 10% oil: **a)** fresh, **b)** dried at the touch (8 weeks), **c)** naturally aged (2 years) and **d)** accelerated artificially daylight aged (28 days, starting from the naturally aged samples set).

The spectra show the changes of functional groups in *urushi/thitsi* blend-based samples' surface after the natural aging and accelerated artificial daylight aging processes.

ATR spectra of blended lacquers do not show any significant differences from thitsi and urushi ones. In the region between 1100-1330 cm^{-1} a broad peak at 1158 cm^{-1} assigned to C-O-C stretching in the phenol groups, has been detected, as detected in thitsi-based samples. Differently from urushi, no peak around 1218 cm^{-1} has been detected.

The peak at 1074 cm^{-1} shows a blandly increase in all the three blended lacquers, as detected in thitsi-based samples. As already reported in the evaluation of both thitsi and urushi ATR spectra, this could be due to the break of the core-shell structure of polysaccharide and glycoproteins after UV exposure [1]. This agrees with the digital microscopy evidence which show microcrack on the urushi/thitsi blend-based samples' surface, independently from the type of blended lacquer.

Wavenumber (cm ⁻¹)	Peaks Assignment
3364	O-H stretching of catechol ring or polysaccharides [9, 20, 27, 41]
2924	C-H and H-C=C-H stretching [62]
2854	C-H and H-C=C-H stretching [62]
1719	C=O stretching [62]
1619	C=C stretching (C=O shoulder) of the aromatic ring skeletal vibrations of the polymerized catechol derivatives [62]
1418	C-H bending (asymmetric) of side chain [17, 41]
1374	CH ₃ bending (symmetric) [9]
1158	C-O-C stretching in phenol groups [62]
1074	C-O stretching in polysaccharides [1, 41]
775 - 719	C-H deformation vibration out-of-plane [62]

Table 13. ATR FTIR peaks and their assignments for urushi added with thitsi filtered in a 20:80 ratio, urushi added with thitsi filtered in a 1:1 ratio and urushi added with thitsi filtered with 10% oil.

5.3.4 THM-Py-GC/MS

In the following section Total Ion Current (TIC) and the most significant Extracted Ion (EIC) Chromatograms of urushi added with thitsi filtered in a 20:80 ratio, urushi added with thitsi filtered in a 1:1 ratio and urushi added with thitsi filtered with 10% oil are shown. As described in the timeline scheme (Figure 23), these chromatograms were registered at different timing, starting when the lacquers were freshly applied on the glass-slides and in a liquid state (*fresh*), followed by different and consequent periods of time corresponding to their chemical-physical change: after the drying in climate chamber (*dried at the touch*), after 2 years of natural aging (*naturally aged*), and finally after 28 days of accelerated artificial daylight aging (*accelerated artificially daylight aged*).

TIC

Total Ion Chromatograms (TIC) of urushi added with thitsi filtered in a 20:80 ratio, urushi added with thitsi filtered in a 1:1 ratio and urushi added with thitsi filtered with 10% oil are shown in Figure 79, 80 and 81, respectively.

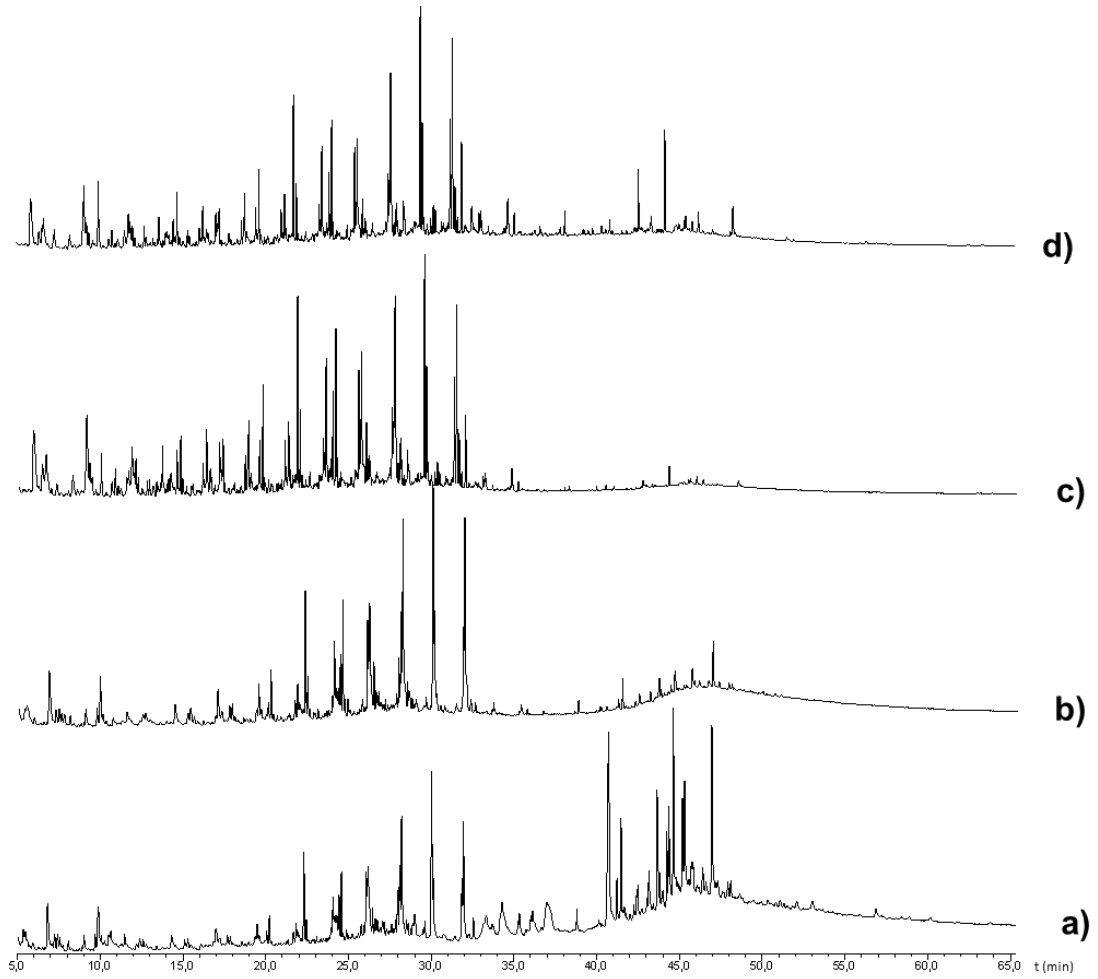


Figure 79. Total Ion Chromatograms (TIC) of urushi added with thitsi filtered in a 20:80 ratio acquired by THM-GC/MS: **a)** fresh, **b)** dried at the touch (8 weeks), **c)** naturally aged (2 years), and **d)** accelerated artificially daylight aged (28 days, starting from the naturally aged samples set).

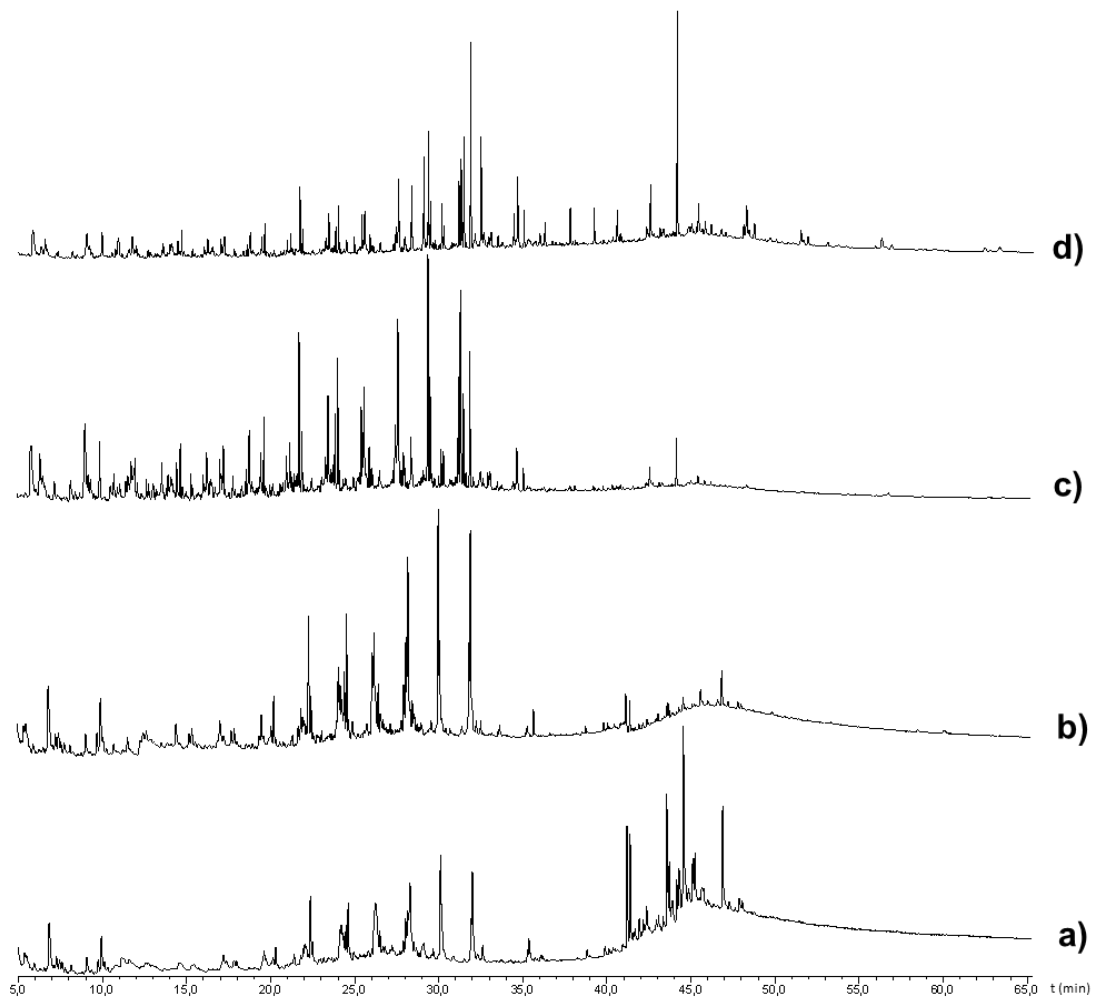


Figure 80. Total Ion Chromatograms (TIC) of urushi added with thitsi filtered in a 1:1 ratio acquired by THM-GC/MS: **a)** fresh, **b)** dried at the touch (8 weeks), **c)** naturally aged (2 years), and **d)** accelerated artificially daylight aged (28 days, starting from the naturally aged samples set).

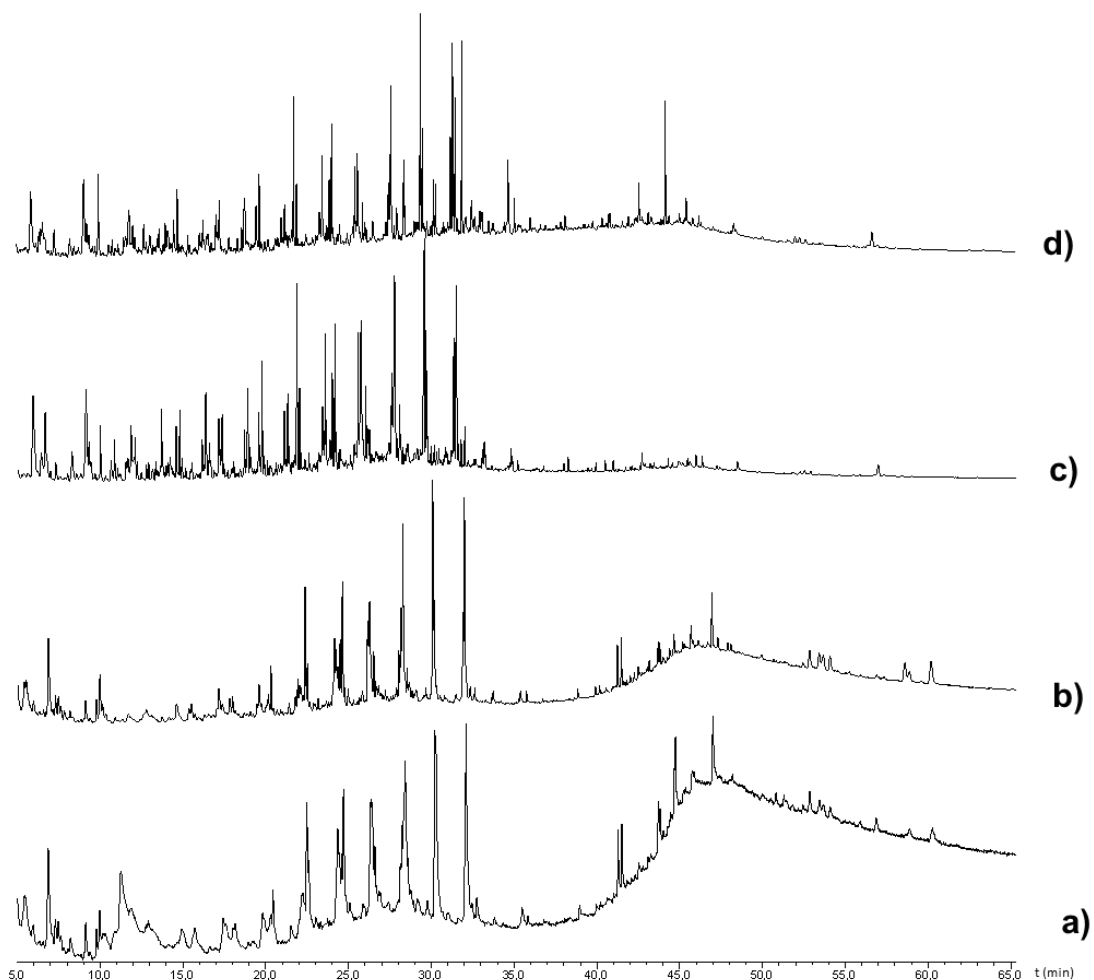


Figure 81. Total Ion Chromatograms (TIC) of urushi added with thitsi filtered with 10% oil acquired by THM-GC/MS: **a)** fresh, **b)** dried at the touch (8 weeks), **c)** naturally aged (2 years), and **d)** accelerated artificial daylight aged (28 days, starting from the naturally aged samples set).

In general, the urushi/thitsi blend TICs show two main groups of peaks, exactly as thitsi and urushi and independently from the ratio of the two lacquer components: the first, between 5-33 minutes of retention time (RT), with the most intense peak at 30 RT. and the second, between 40-48 minutes of retention time, assigned to dimethoxy alkyl and phenyl benzenes, due to the methylation of catechols with the TMAH reagent. They all have an irregular shape and become thicker after 2 years of natural aging. Furthermore, the alkyl and phenyl benzenes series show a decrease after the 8 weeks of drying in climate chamber. As already said for thitsi, it could be due to the nucleus-nucleus coupling occurring during laccase polymerization for both thitsi and urushi lacquers. This type of coupling involves catechol hydroxyl groups in the formation of polymerized network and, as a consequence, less hydroxyl groups are available for the methylation with the time.

$m/z=57$ – alkanes and alkenes

Extracted Ion Chromatograms (EIC) at $m/z=57$ of urushi added with thitsi filtered in a 20:80 ratio, urushi added with thitsi filtered in a 1:1 ratio and urushi added with thitsi filtered with 10% oil, are shown in Figure 82, 83 and 84, respectively.

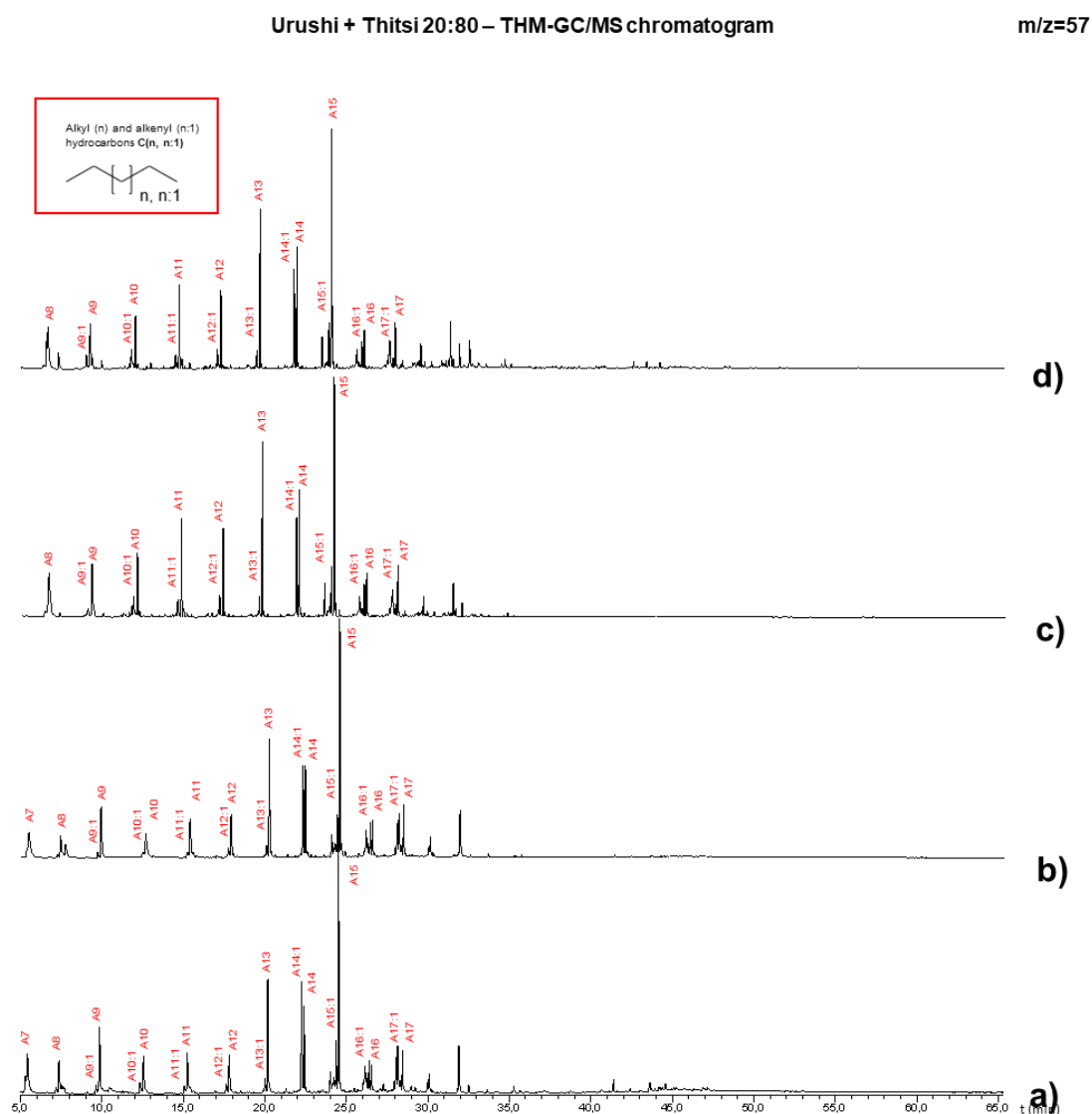


Figure 82. Extracted Ion Chromatograms (EIC) of urushi added with thitsi filtered in a 20:80 ratio acquired by THM-GC/MS and obtained by plotting single ion mass profile at $m/z=57$: **a)** fresh, **b)** dried at the touch (8 weeks), **c)** naturally aged (2 years) and **d)** accelerated artificially daylight aged (28 days, starting from the naturally aged samples set).

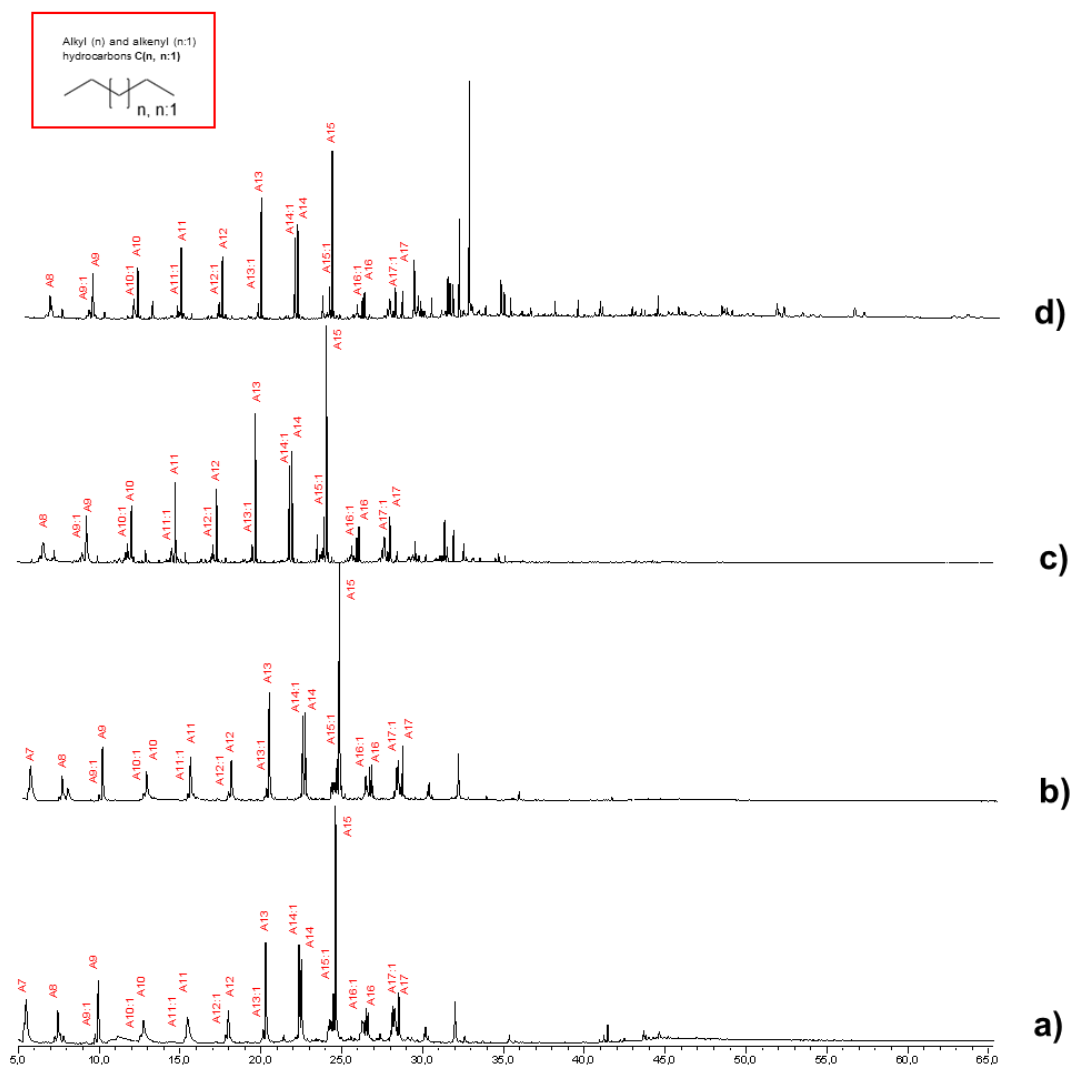


Figure 83. Extracted Ion Chromatograms (EIC) of urushi added with thitsi filtered in a 1:1 ratio acquired by THM-GC/MS and obtained by plotting single ion mass profile at m/z=57: a) fresh, b) dried at the touch (8 weeks), c) naturally aged (2 years) and d) accelerated artificially daylight aged (28 days, starting from the naturally aged samples set).

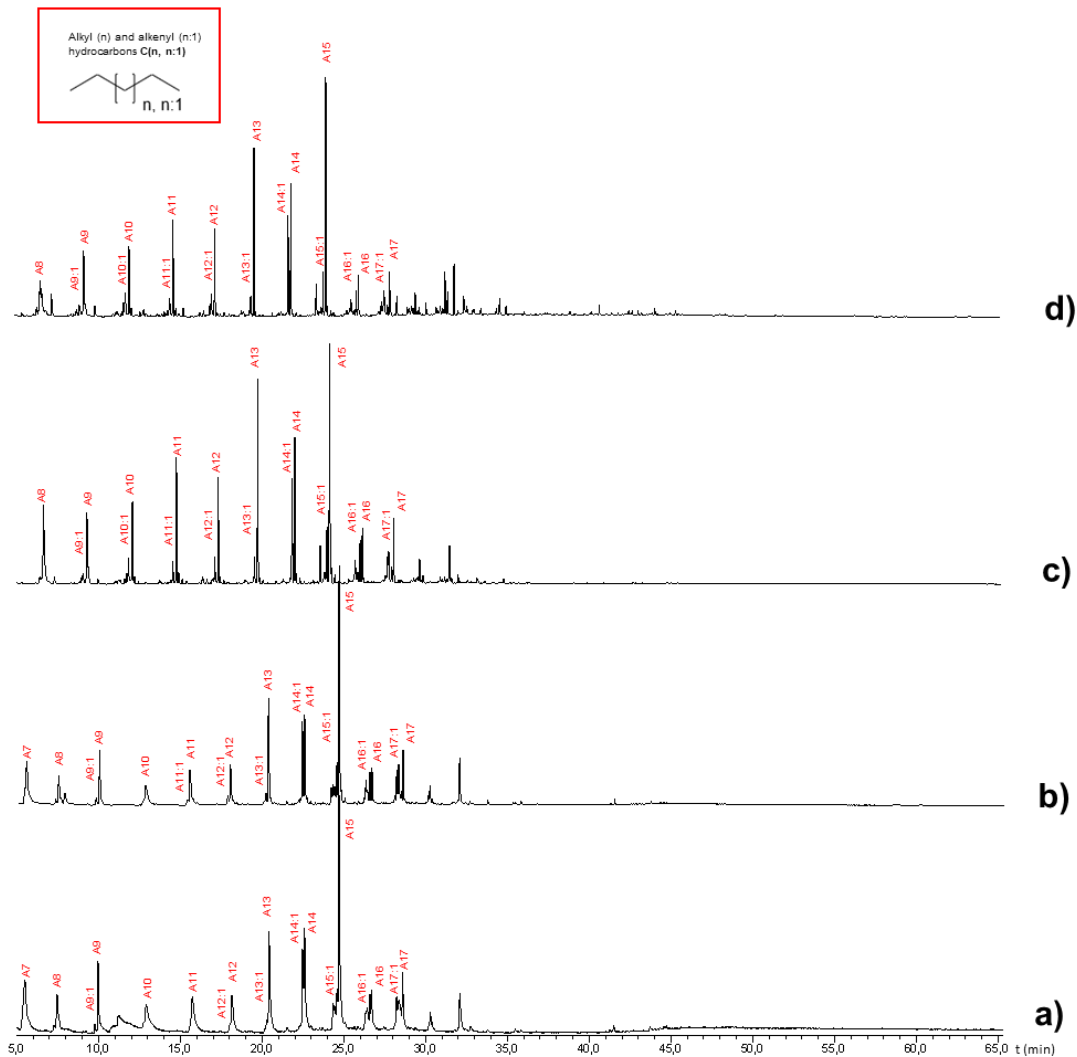


Figure 84. Extracted Ion Chromatograms (EIC) of urushi added with thitsi filtered with 10% oil acquired by THM-GC/MS and obtained by plotting single ion mass profile at $m/z=57$: **a)** fresh, **b)** dried at the touch (8 weeks), **c)** naturally aged (2 years) and **d)** accelerated artificially daylight aged (28 days, starting from the naturally aged samples set).

These EICs show alkyl ($m/z=57$ as base peak) and alkenyl ($m/z=55$ as base peak) hydrocarbons fragments which are the pyrolytic products produced by the cleavage of the linear saturated and unsaturated side chain hydrocarbon on the aromatic ring of catechol such as on the 3- and 4-alkylcatechols in *thitsiol* (Figure 2) and 3-alkylcatechols in *urushiol* (Figure 7) [19, 56].

By looking at the the pyrolytic profiles of the EICs at m/z 57 registered for the *fresh* (a) and *dried-at-the-touch* (b) blended lacquers it is possible to notice an irregular shape. Between 10 and 18 minutes of RT the most abundant peak registered in A9. After 2 years of natural aging the same region (10-18 RT, A9-A12) assumes a bell-shape profile, with the A11 as the most intense peak of the group. A similar change

after 2 years of natural aging has been detected in both thitsi and urushi EICs at $m/z=57$, too. As already speculated in paragraph 5.1.4 and 5.2.4, this could be due to the shift of double bonds in *thitsiol* and *urushiol* side chain, due to the several nucleus-side chain and/or side chain-side chain couplings that occurs with polymerization. The pyrolytic fragmentation could, in this way, change its preferential positions along the side chain. The accelerated artificial daylight ageing did not influence any change in this chromatographic range.

Generally, for all recorded EICs at m/z 57 of thitsi-based model samples, the series of alkyl and alkenyl starts with heptane (A7) and ends with heptadecane (A17). The most abundant aliphatic hydrocarbon in all the EICs is pentadecane (A15) and followed by tridecane (A13) as the further most abundant alkanes. Comparing the alkenes series in the three blended lacquer types it is interesting to notice that, as observed for thitsi and urushi, in *fresh* and *dried-at-the-touch* 20:80 and 1:1 blended lacquer models the only alkene more abundant than the alkane counterpart is tetradecene (A14:1), which, however, becomes lower than A14 after 2 years of natural aged. For blended lacquer model with 10% oil the alkenes abundance is always lower than alkanes.

$m/z=91$ – alkyl and alkenyl benzenes

Extracted Ion Chromatograms (EIC) at $m/z=91$ of urushi added with thitsi filtered in a 20:80 ratio, urushi added with thitsi filtered in a 1:1 ratio and urushi added with thitsi filtered with 10% oil, are shown in Figure 85, 86 and 87, respectively.

Urushi/Thitsi blend EICs show alkyl ($m/z=92$ as base peak) and alkenyl ($m/z=91$ as base peak) benzene fragments which are the pyrolytic products produced by the cleavage at the benzylic position of the 3- and 4-alkylphenylcatechols in *thitsiol* (Figure 2) [56] and resulting from the dehydration of alkylphenols, intermediate compounds formed from catechols during pyrolysis, of both *thitsiol* and *urushiol* [19].

As observed for thitsi EICs at $m/z=91$, blended lacquer-base samples show a similar bell-shape profile in the same range of retention time (10-18 RT, peaks B3-B7, with B5 the most abundant of the group) which becomes more evident in the *2-year naturally aged* chromatogram.

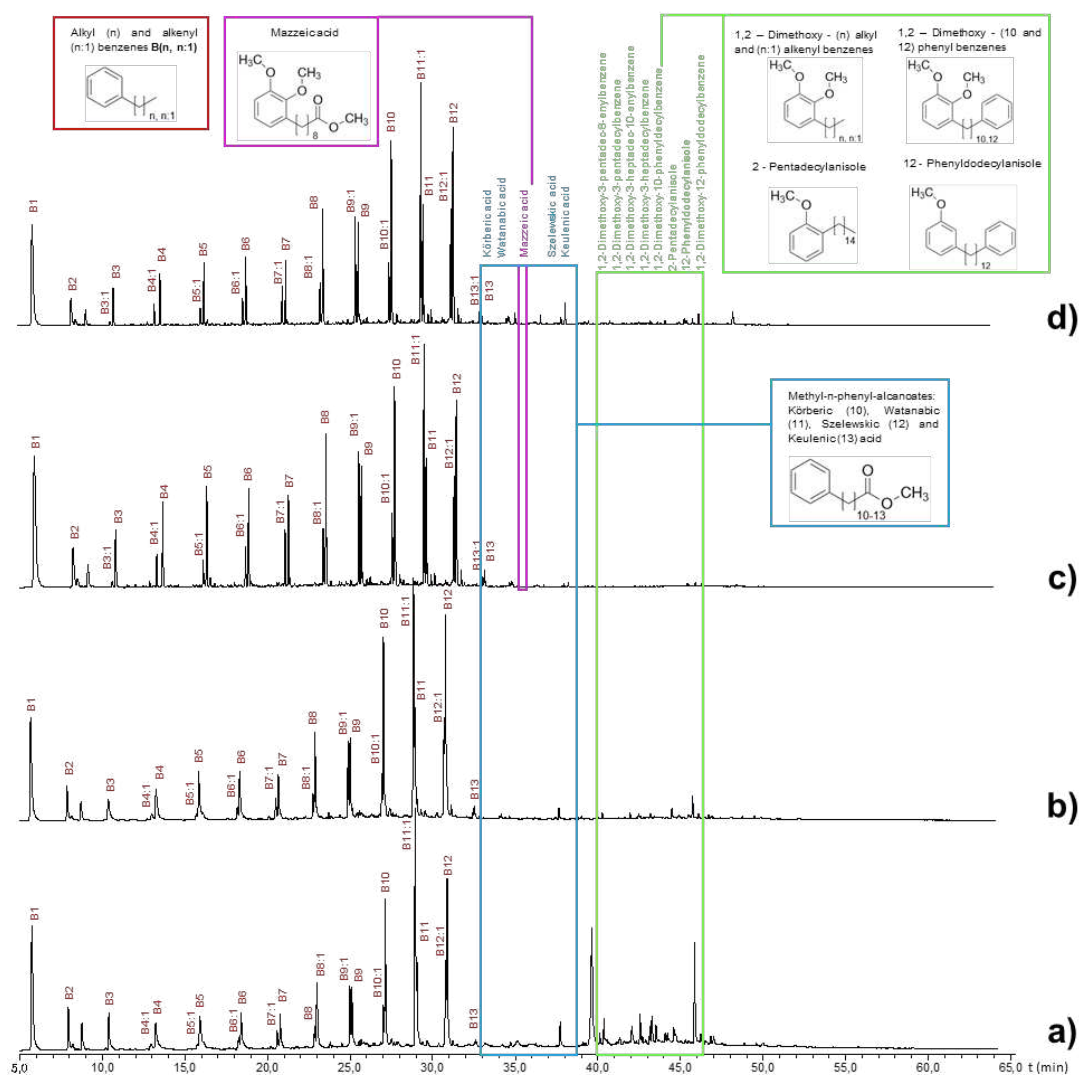


Figure 85. Extracted Ion Chromatograms (EIC) of urushi added with thitsi filtered in a 20:80 ratio acquired by THM-GC/MS and obtained by plotting single ion mass profile at $m/z=91$: **a)** fresh, **b)** dried at the touch (8 weeks), **c)** naturally aged (2 years) and **d)** accelerated artificial daylight aged (28 days, starting from the naturally aged samples set).

The EICs $m/z=91$ of urushi/thitsi blends show a first intense peak assigned to toluene (B1) and end with tridecyl benzene (B13), as detected for thitsi-based samples while urushi-based sample showed dodecyl benzene (B12) as the longest alkybenzene. Undecenyl benzene (B11:1) is the most intense peak of the series, commonly with thitsi, and it is formed during the cleavage at the benzylic position of 3- and 4-(12-phenyldodecyl) cathecols in the *thitsiol* polymer network [Tamburini 2015 and 2019]. The intensity of alkenyl benzenes is always lower than alkyl benzenes, except for the undecenyl and nonyl benzenes.

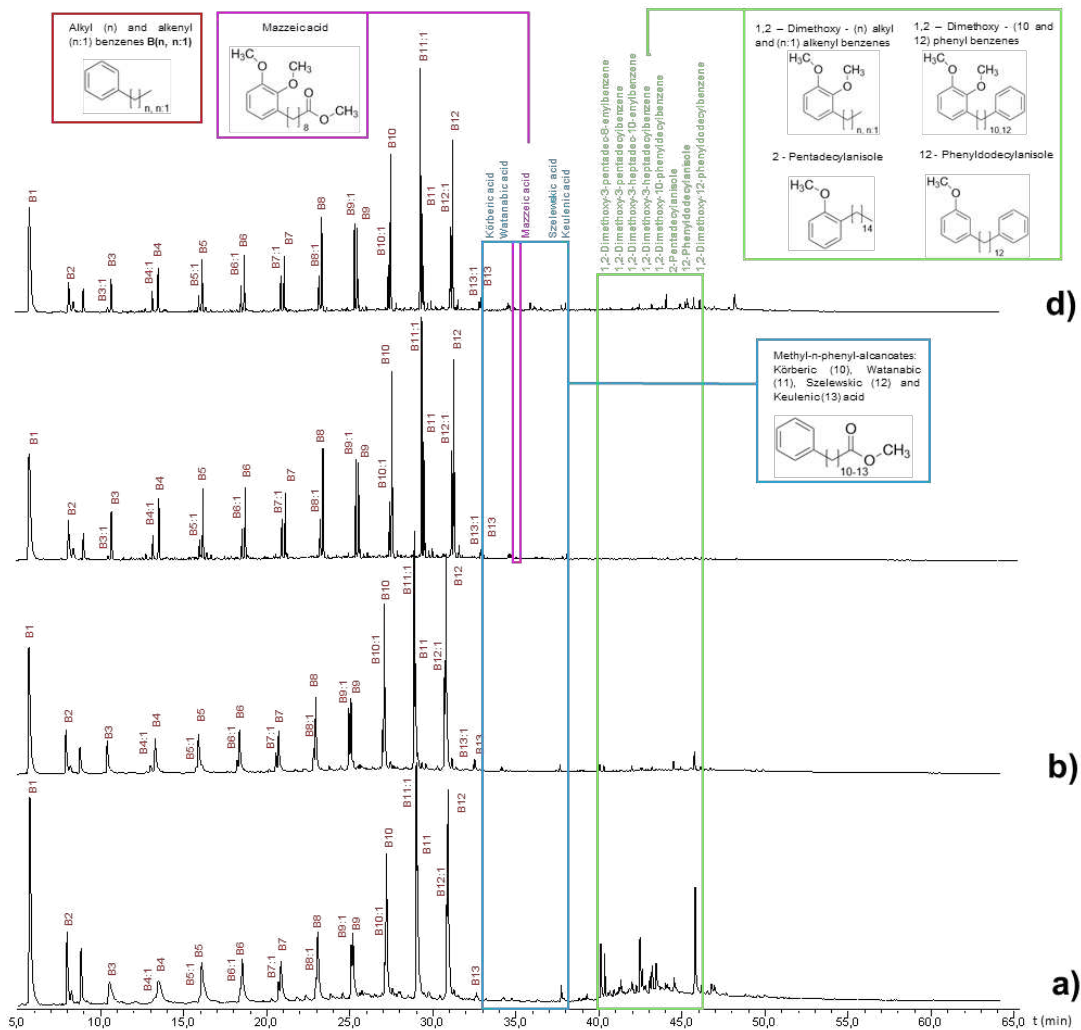


Figure 86. Extracted Ion Chromatograms (EIC) of urushi added with thitsi filtered in a 1:1 ratio acquired by THM-GC/MS and obtained by plotting single ion mass profile at $m/z=91$: **a)** fresh, **b)** dried at the touch (8 weeks), **c)** naturally aged (2 years) and **d)** accelerated artificially daylight aged (28 days, starting from the naturally aged samples set).

In this series of EICs between RT 41 and 48 minutes, alky/alkenyl (1,2-dimethoxy-3-pentadec-8-enylbenzene, base peak at $m/z=346$; 1,2-dimethoxy-3-pentadecylbenzene, base peak at $m/z=348$; 1,2-dimethoxy-3-heptadec-10-enylbenzene, base peak at $m/z=374$; 1,2-dimethoxy-3-heptadecylbenzene, base peak at $m/z=376$, highlighted in green) and phenyl benzenes (1,2-dimethoxy-10-phenyldodecylbenzene, base peak at $m/z=354$; 1,2-dimethoxy-12-phenyldodecylbenzene, base peak at $m/z=382$, highlighted in green) and alkyl and phenyl anisoles (2-pentadecylanisole, base peak at $m/z=122$; 12-phenyldodecylanisole, base peak at $m/z=122$, highlighted in green) were detected as

well in their methylated form. As explained before (paragraph 4.3), the use of TMAH as

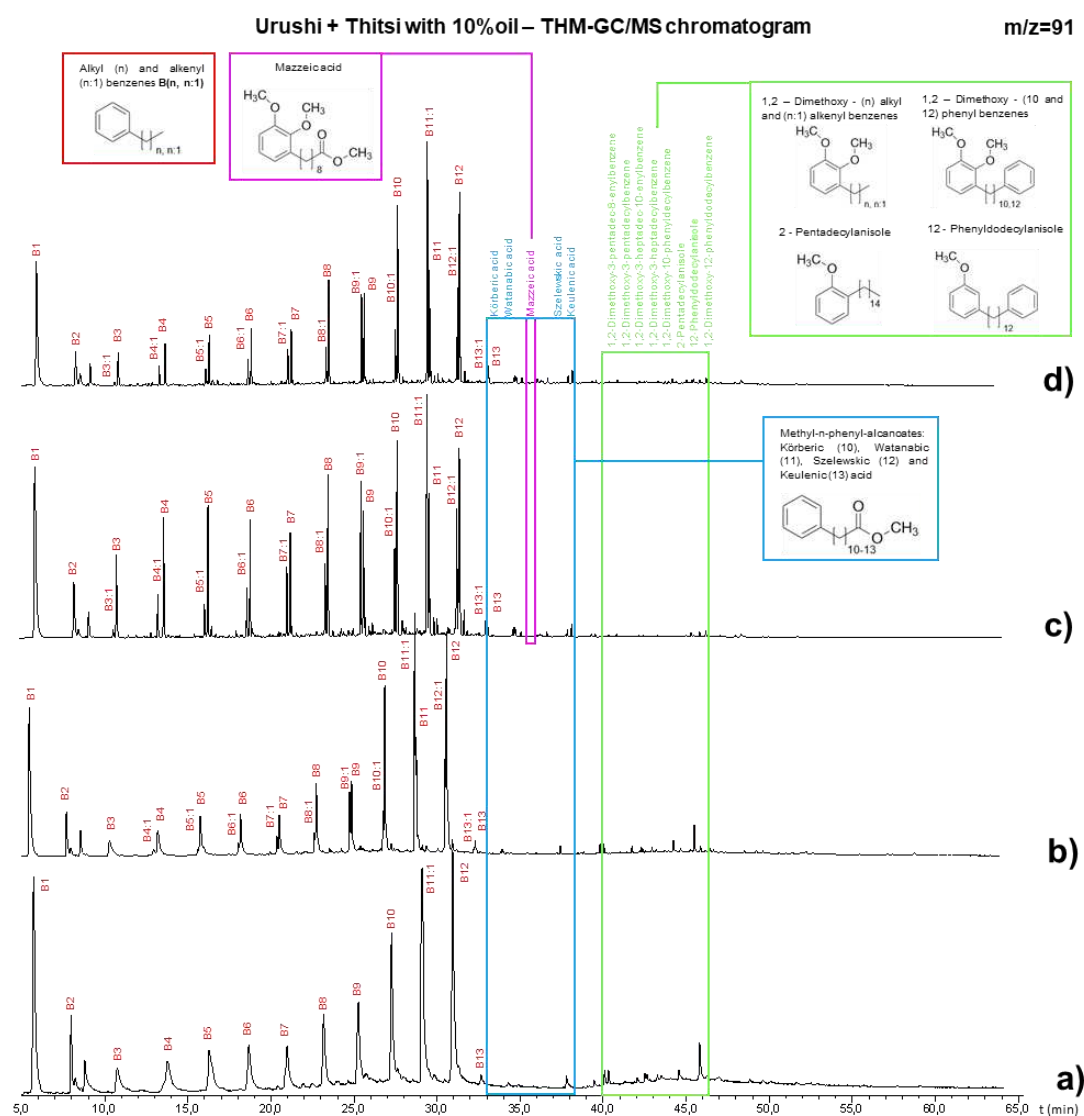


Figure 87. Extracted Ion Chromatograms (EIC) of urushi added with thitsi filtered with 10% oil acquired by THM-GC/MS and obtained by plotting single ion mass profile at $m/z=91$: **a)** fresh, **b)** dried at the touch (8 weeks), **c)** naturally aged (2 years) and **d)** accelerated artificially daylight aged (28 days, starting from the naturally aged samples set).

derivatizing reagent leads to the methylation of catechols and phenols which are registered at higher m/z values than those reported in the literature (m/z 108 and m/z 123, respectively) [24]. The addition of one and two methyl groups increases the m/z values of 14 to the phenols and 28 to the catechols, respectively. The result is a common base peak at m/z 122 for methylated phenols as anisoles and at m/z 151 for methylated catechols as dimethoxy benzenes. Furthermore, as already seen for thitsi, this series of fragments shows a gradually decrease of abundance after the 8-weeks

drying processes in climate chamber for all the three blended lacquer types, in particular for 20:80 and 1:1 blended lacquer type. As explained in paragraph 5.1.4, this could be due to the occurring of polymerization that involves catechol hydroxyl groups in the formation of polymerized network. As a consequence, less hydroxyl groups are available for the methylation with the passage of time.

Finally, one of the main advantages of using a derivatizing reagent such as TMAH for the investigation of Asian lacquers is shown by the detection of some methylated oxidation products between 31-38 minutes RT in all three urushi/thitsi blended lacquers. These are the catechol acids as methyl 8-(2,3-dimethoxyphenyl) octanoate also known Mazzeic acid (base peak at $m/z=136$, highlighted in blue) and the phenylalkanoic acids group as methyl phenyl alcanoates (base peak at $m/z=91$, highlighted in pink). The methyl phenyl alcanoates group includes methyl 10-phenyl-decanoate (körberic acid, MW= 262), methyl 11-phenyl-undecanoate (watanabic acid, MW=276), methyl 12-phenyl-dodecanoate (szelewskic acid, MW= 290), and methyl 13-phenyl-tridecanoate (keulenic acid, MW=304).

According to Tamburini [7] the phenylalkanoic acid as oxidation products are formed through a two-step mechanism in which phenyl catechol is subjected to the opening of catechol ring and finally oxidized to phenylalkanoic acid. The final step of the reaction mechanism shows in Figure 49, (Reaction mechanism 1) is the methylation with TMAH derivatizing reagent. One more oxidation step in Reaction mechanism 1 with the formation of *n*-oxo-phenylalkanoic acid has been proposed by Tamburini. However, nor this oxidation product nor its methylated counterpart has been detected.

It is deductible that reaction mechanisms for the formation of the detected oxidation products for urushi/thitsi blends are the same or similar to the ones proposed by Tamburini and presented for thitsi and urushi in paragraph 5.1.4 and 5.2.4 (Figure 49, Reaction mechanism 1 and Figure 53, Reaction mechanism 2), respectively. However, it is necessary to specify that no research have been conducted on blends of thitsi and urushi and no reaction mechanisms specific for them have proposed.

$m/z=120$

Extracted Ion Chromatograms (EIC) at $m/z=120$ of urushi added with thitsi filtered in a 20:80 ratio, urushi added with thitsi filtered in a 1:1 ratio and urushi added with thitsi filtered with 10% oil, are shown in Figure 88, 89 and 90, respectively.

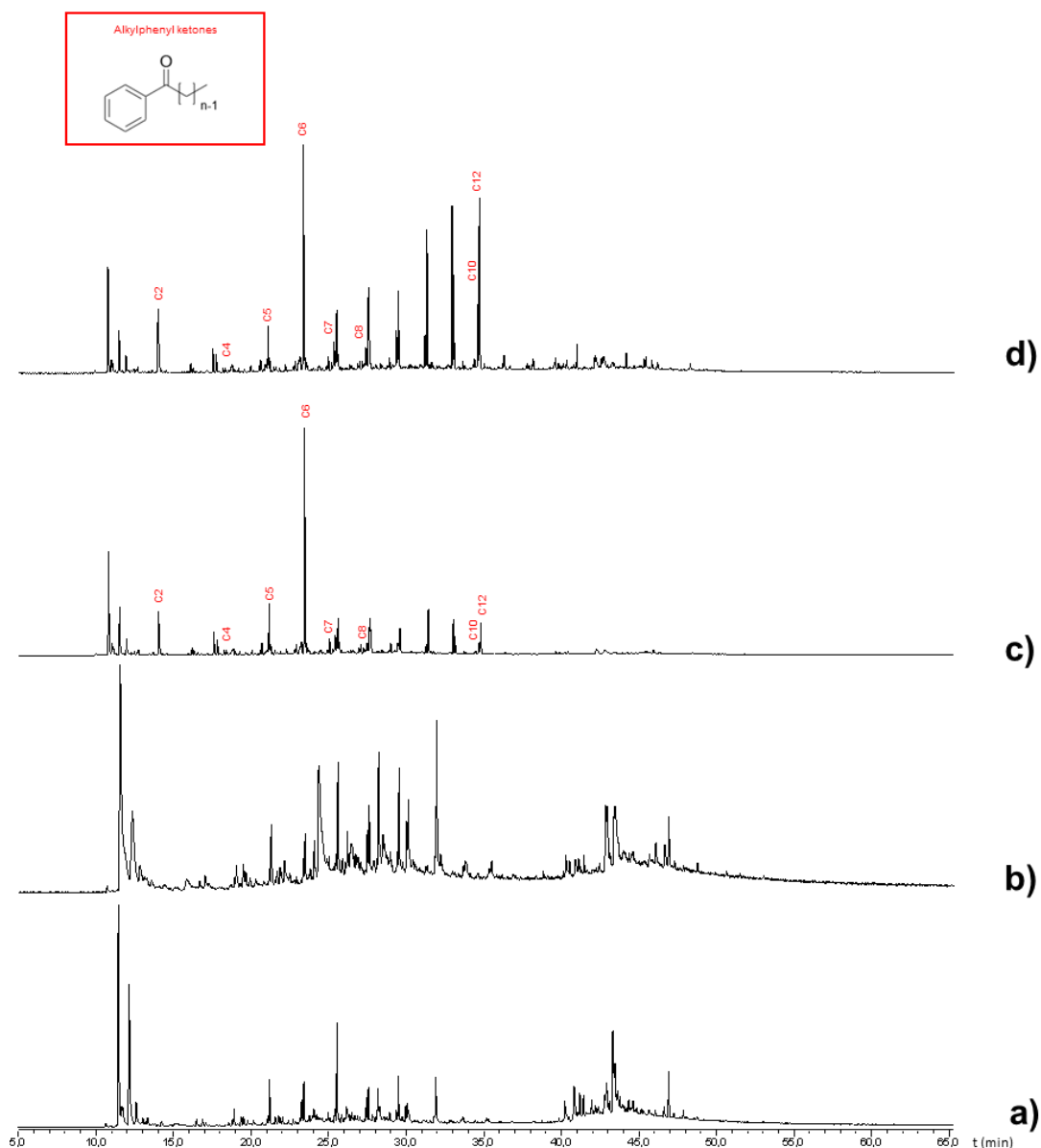


Figure 88. Extracted Ion Chromatograms (EIC) of urushi added with thitsi filtered in a 20:80 ratio acquired by THM-GC/MS and obtained by plotting single ion mass profile at $m/z=120$: a) fresh, b) dried at the touch (8 weeks), c) naturally aged (2 years) and d) accelerated artificially daylight aged (28 days, starting from the naturally aged samples set).

In all three urushi/thitsi blends the same alkyphenyl ketones detected for thitsi have been found. The series starts with acetophenone at 14 minutes RT and proceeds with phenylbutanone (C4, base peak at $m/z=105$), phenylpentanone (C5, base peak at $m/z=105$), phenylhexanone (C6, base peak at $m/z=105$) as the most abundant one, phenylheptanone (C7, base peak at $m/z=105$), phenyloctanone (C8, base peak at $m/z=105$), phenyldecanone (C10, base peak at $m/z=120$), and phenyldodecanone (C12, base peak at $m/z=120$).

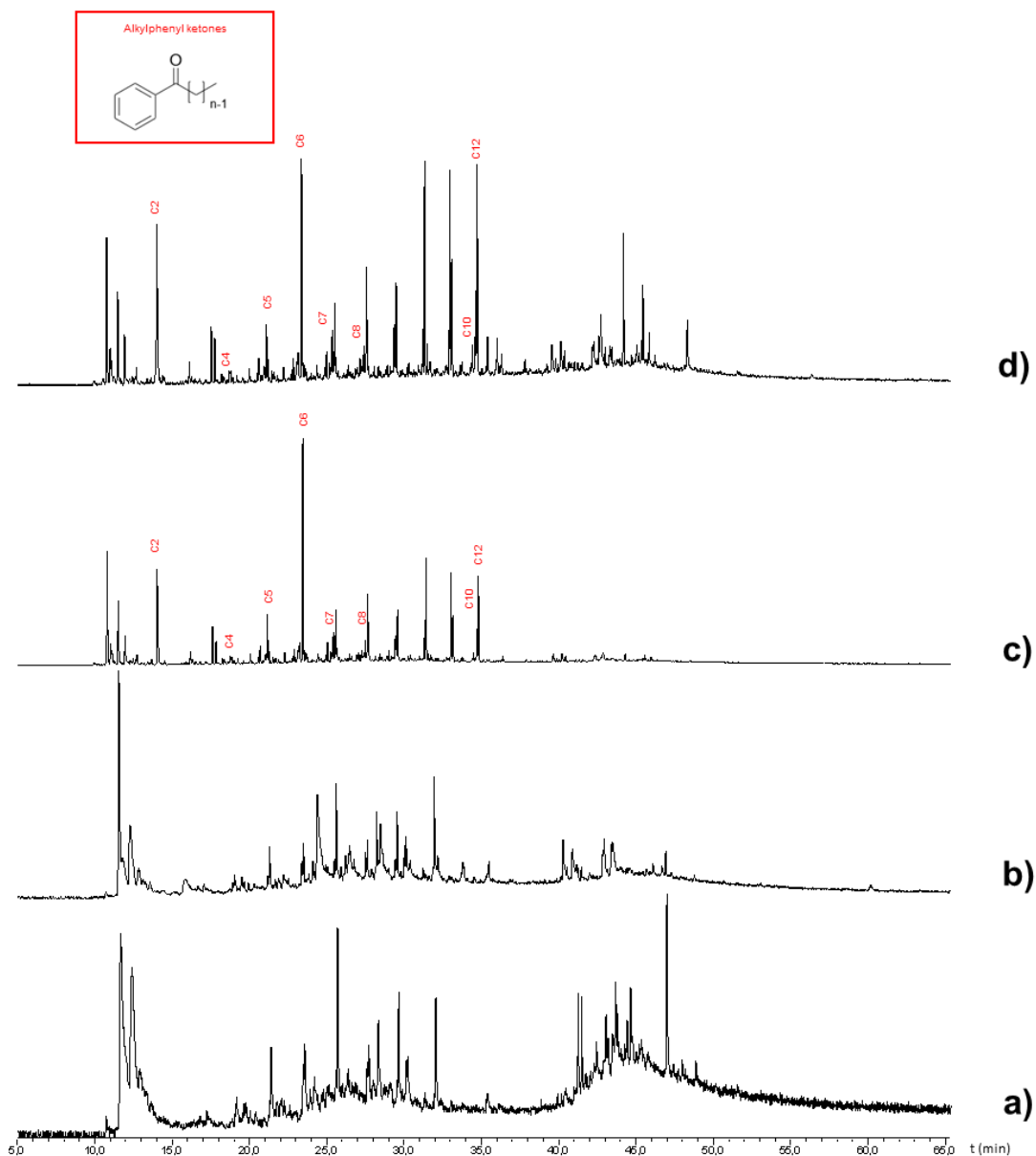


Figure 89. Extracted Ion Chromatograms (EIC) of urushi added with thitsi filtered in a 1:1 ratio acquired by THM-GC/MS and obtained by plotting single ion mass profile at $m/z=120$: **a)** fresh, **b)** dried at the touch (8 weeks), **c)** naturally aged (2 years) and **d)** accelerated artificially daylight aged (28 days, starting from the naturally aged samples set).

According to Tamburini, alkylphenyl ketones are the pyrolysis products of *n*-oxo-alkylphenyl catechols, as shown in Figure 49 (Reaction mechanism 1).

The appearance of this series of fragments in the EIC of the *2-year naturally aged* lacquer is complemented by the formation of Mazzeic acid, as mentioned before in

the paragraph for the m/z 91. The formation of the two groups of oxidation products

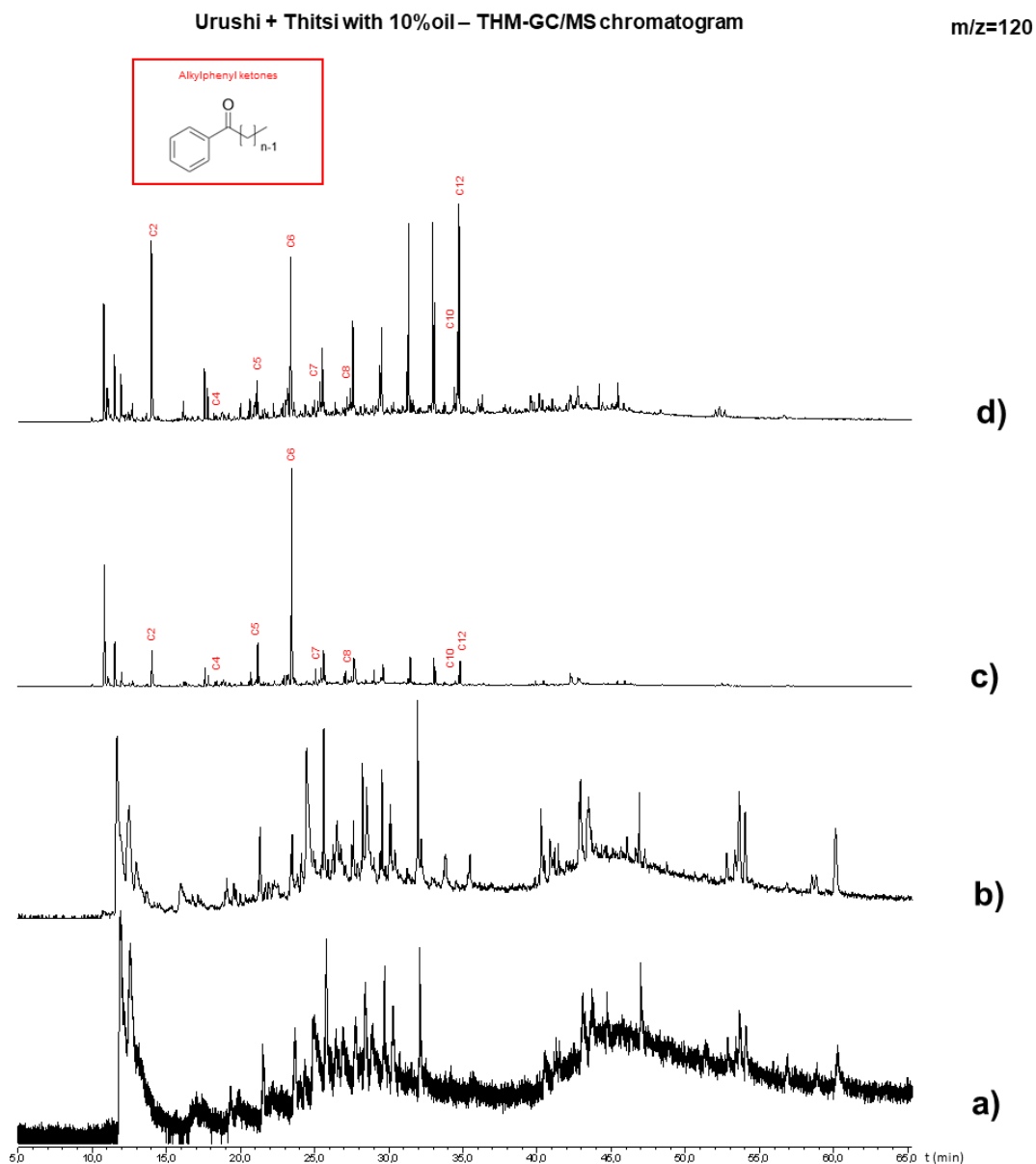


Figure 90. Extracted Ion Chromatograms (EIC) of urushi added with thitsi filtered with 10% oil acquired by THM-GC/MS and obtained by plotting single ion mass profile at $m/z=120$: **a)** fresh, **b)** dried at the touch (8 weeks), **c)** naturally aged (2 years) and **d)** accelerated artificial daylight aged (28 days, starting from the naturally aged samples set).

implies their production during the 2-year long period between the *dried-at-the-touch* state of the material and the *naturally aged* one. Furthermore, in the alkylphenyl ketones series, the abundance of C2, C10 and C12 fragments increases during the accelerated artificial daylight aging in all the three blended lacquer types. However, the great increase of acetophenone (C2) has been registered for 1:1 urushi/thitsi blended lacquer and for urushi/thitsi blended lacquer with 10%.

6. CONCLUSION AND OUTLOOK

Asian lacquers are important materials widely found in Cultural Heritage objects collected in indoor museums, particularly from the 17th century to today, which are suffering of a certain extent of degradation mainly due to their high sensitivity to daylight. The work performed within the frame of an Erasmus period at the Institute of Natural Sciences and Technology in the Arts, at the Academy of Fine Arts Vienna, allowed to study and understand for the first time the chemical and physical behaviour of the blend thitsiol/urshiol type of Asian lacquer, during the curing, natural ageing, as well as artificial accelerated daylight ageing process. Several important results were obtained thanks to the multi-analytical approach developed for this study and hereafter summarized in two main parts, as 1) optical and morphological observations and 2) chemical observations:

Optical and morphological observation by Digital Microscopy and Colorimetry

- ✓ First of all, the already known high sensitivity to the daylight of the thitsi but also of the urushi in minor extent was observed by using a Digital Microscope. Several microcracks were shown in a wide-spread and polygonal shape at the surface level of the artificially daylight aged thitsi but not urushi specimens, while it was possible to observe them for the first time in the blended thitsi/urushi, in an extent between the thitsi and urushi. This demonstrates the addition of urushi to the thitsi type of lacquer increases its light stability.
- ✓ A major shift in colour has been determined in the urushi-based sample ($\Delta E^*=24,3$) by colorimetric measurements. Among the thitsi-based samples and blended-based samples the greatest ΔE^* has been registered for thitsi with 10% oil ($\Delta E^*=12,1$) and urushi/thitsi with 10% oil ($\Delta E^*=13,4$), respectively. Thitsi pure and filtered registered a ΔE^* around 6 while urushi/thitsi blended lacquers in a 20:80 ratio and 1:1 ratio and registered a ΔE^* around 3.

Chemical observations by FTIR and THM-Py-GC/MS

- ✓ Since optically the distinction between the blended urushi/thitsi and the thitsi or urushi is not straightforward and almost impossible to determine because of their similarities in terms of final colour and appearance. FTIR and THM-Py-GC/MS results helped to distinguish the lacquer types by detecting the characteristic markers of thitsi and urushi and comparing those with blended lacquers, and by observing the characteristic vibration absorptions in their functional groups. First

of all, the presence of thitsi in the blended samples was shown by three peaks related to different substituted catechols (3- and 4-) in the region between 3000-3100 cm^{-1} , while the presence of urushi was suggested by the peak at 3010 cm^{-1} typical of urushi, which was shifted to 3024 cm^{-1} in thitsi. Then, blended lacquers shows a pyrolytic profile at $m/z=91$ (alkyl and alkenyl benzenes) more similar to the characteristic thitsi profile at $m/z=91$: both blended lacquers and thitsi show bell-shape between 10-18 RT and the undecenyl (B11:1) as the most abundant peak, while urushi has toluene (B1) as the most abundant peak. Furthermore, in blended lacquers have been found dimethoxy phenyl catechols and phenyl anisols fragments like in thitsi, due to the presence of thitsi in the blended lacquers.

- ✓ The polymerization and oxidation processes in blended urushi/thitsi lacquers were studied by the evaluation of FTIR and THM-Py-GC/MS data acquired during a 2-year long period. The increase of the carbonyl peak (C=O) and its shift at 1715 cm^{-1} , detected for all the lacquer types, proves the occurring of polymerization and oxidation process. Additionally, the decrease of the peak in the *fresh* and *dried-at-the-touch* lacquers assigned to C-H stretching of double bonds in the side chain of *thitsiol* and *urushiol*, suggests, together with the decrease of the peak assigned to C-OH stretching in phenols and catechols groups, that nucleus-side chain and side chain-side chain couplings have occurred during polymerization. In THM-Py-GC/MS data of blended lacquers the formation of oxidation products, such as Mazzeic acid, methyl-n-phenyl alcanoates, and alkylphenyl ketones have been found, proving that oxidation process occurred.

This work revealed for the first time unknown chemical and physical information about the curing, ageing, and photo-ageing processes of a very important typology of Asian lacquer such as blended urushi/thitsi. Nevertheless, further investigations would be necessary for achieving deeper chemical information, particularly by using chemometric methods for quantitative analyses. Finally, this study will also benefit of additional methodologies such as Nuclear Magnetic Resonance (NMR) for better understanding the chemical structures of monomers and dimers in Asian lacquers and their structural changes during polymerization, but also Optical Coherence Tomography (OCT) for highlight the thickness of the oxidized layer at the surface level and for measuring the depth of the microcrack formed during the exposure to the daylight.

7. REFERENCES

- [1] A.-S. Le Ho, C. Duhamel, C. Daher, L. Bellot-Gurlet, C. Paris, M. Regert, M. Sablier, G. Andr e, J.-P. Desroches e P. Dumas, «Alteration of Asian lacquer: in-depth insight using a physico-chemical multiscale approach,» *The Royal Society of Chemistry*, 2013.
- [2] G. Wilson e A. Heginbotham, French Rococo  b nisterie in the J. Paul Getty Museum, J. Paul Getty Trust, 2021.
- [3] «The influence of East Asian lacquer on European furniture,» Victoria and Albert Museum, [Online]. Available: <https://www.vam.ac.uk/articles/east-asian-lacquer-influence#:~:text=All%20over%20Europe%2C%20Japanese%20lacquer,and%20positioned%20against%20a%20wall..> [Consultato il giorno 23 11 2022].
- [4] C. Coueignoux, «Aqueous Cleaning of Photodegraded East Asian lacquer: a case study,» *Journal of the American Institute for Conservation*, vol. 48, pp. 51-67, 2009.
- [5] C. Coueignoux e S. Rivers, «Conservation of Photodegraded Asian lacquer surfaces: four case studies,» *Journal of the American Institute for Conservation*, vol. 54, pp. 14-18, 2015.
- [6] C. McSharry, R. Faulkner, S. Rivers, M. S. P. Shaffer e T. Welton, «The chemistry of East Asian lacquer: A review of the scientific literature,» *Studies in Conservation*, 2007.
- [7] D. Tamburini, G. Pescitelli, M. P. Colombini e I. Bonaducea, «The degradation of Burmese lacquer (thitsi) as observed in samples from two cultural artefacts,» *Journal of Analytical and Applied Pyrolysis*, 2017.
- [8] Y. Yamashita e S. Rivers, «Light-induced deterioration of urushi, maki-e and nashiji decoration,» in *East Asian Lacquer: Material Culture, Science and Conservation*, Archetype Publications Ltd, 2012, pp. 217-228.
- [9] R. Lu e T. Miyakoshi, *Lacquer Chemistry and Applications*, Elsevier, 2015.
- [1 J. Kumanotani, «Laccase-Catalyzed Polymerization of Urushiol in Precisely
0] Confined Japanese Lacquer System,» *Makromolekulare Chemistry*, vol. 179, pp. 47-61, 1978.
- [1 J. Kumanotani, «Urushi (oriental lacquer) - a natural aesthetic durable and future-
1] promising coating,» *Progress in Organic Coatings*, vol. 26, pp. 163-195, 1995.
- [1 N. Brommelle e P. Smith, *Urushi*, J. Paul Getty Trust, 1988.
2]
- [1 M. R. Schilling, A. Heginbotham, H. van Keulen e M. Szelewski, «Beyond the
3] basics: A systematic approach for comprehensive analysis of organic materials in Asian lacquers,» *Studies in Conservation*, vol. 61, pp. 3-27, 2016.

- [1 A. Heginbotham, H. Khanjian, R. Rivenc e M. Schilling, «A procedure for the efficient and simultaneous analysis of Asian and European lacquers in furniture of mixed origin,» in *ICOM COMMITTEE FOR CONSERVATION*, 2008.
- [1 J. Chasen, A. Heginbotham e M. Schilling, «The Analysis of East Asian and European Lacquer Surface on Rococo Furniture,» [Online]. Available: <https://www.getty.edu/publications/rococo/lacquer/>. [Consultato il giorno 23 11 2022].
- [1 «PHySICAL: sparking solutions for the cleaning of Asian lacquers,» KIK-IRPA 6] Royal Institute for Cultural Heritage, [Online]. Available: <https://www.kikirpa.be/en/projects/physical>. [Consultato il giorno 2022 11 2022].
- [1 T. Honda, R. Lu, N. Kitano, Y. Kamiya e T. Miyakoshi, «Applied Analysis and 7] Identification of Ancient Lacquer Based on Pyrolysis-Gas Chromatography/Mass Spectrometry,» *Journal of Applied Polymer Science*, vol. 118, pp. 897-901, 2010.
- [1 «Betel-Box,» Victoria and Albert Museum, [Online]. Available: 8] <https://collections.vam.ac.uk/item/O438440/betel-box/>. [Consultato il giorno 25 11 2022].
- [1 A.-S. Le Hô, M. Regert, O. Marescot, C. Duhamel, J. Langlois, T. Miyakoshi, C. 9] Genty e M. Sablier, «Molecular criteria for discriminating museum Asian lacquerware from different vegetal origins by pyrolysis gas chromatography/mass spectrometry,» *Analytica Chimica Acta*, vol. 710, pp. 9-16, 2012.
- [2 T. Honda, R. Lu, R. Sakai, T. Ishimura e T. Miyakoshi, «Characterization and 0] comparison of Asian lacquer saps,» *Progress in Organic Coatings*, vol. 61, pp. 68-75, 2008.
- [2 R. Lu, D. Kanamori e T. Miyakoshi, «Characterization of Thitsiol Dimer Structures 1] from Melanorrhoea usitata with Laccase Catalyst by NMR Spectroscopy,» *International Journal of Polymer Anal. Charact.*, vol. 16, pp. 86-94, 2011.
- [2 R. Lu, T. Honda e T. Miyakoshi, «Application of Pyrolysi-Gas 2] Chromatography/Mass Spectrometry to the Analysis of Lacquer Film,» in *Advanced Gas Chromatography – Progress in Agricultural, Biomedical and Industrial Applications*, Dr. Mustafa Ali Mohd, 2012.
- [2 R. Oshima, Y. Yamauchi, C. Watanabe e J. Kumanotani, «Enzymic Oxidative 3] Coupling of Urushiol in Sap of the Lac Tree, *Rhus vernicifera*,» *Journal of Organic Chemistry*, vol. 50, pp. 2613-2621, 1985.
- [2 X.-M. Ma, R. Lu e T. Miyakoshi, «Application of Pyrolysis Gas 4] Chromatography/Mass Spectrometry in Lacquer Research: A Review,» *Polymers*, vol. 6, pp. 132-144, 2014.
- [2 M. S. M. R. Webb e J. Chang, «The reproduction of realistic samples of Chinese 5] export lacquer for research,» *Studies in Conservation*, vol. 61, pp. 155-165, 2016.
- [2 A.-S. Le Hô, I. Fabre-Francke e C. Thiphavong, «Properties of Polymer- 6] Composite Used as Fills of Asian Lacquerware: Issues on Restoration Processes

- of Lacquered Objects from Cultural Heritage,» *International Journal of Polymer Science*, 2015.
- [2 T. Honda, X. Ma, R. Lu, D. Kanamori e T. Miyakoshi, «Preparation and
7] Characterization of a New Lacquer Based on Blending Urushiol with Thitsiol,»
Journal of Applied Polymer Science, vol. 121, p. 2734–2742, 2011.
- [2 H. H. Yu, J.-A. Lim, S. W. Ham, K.-B. Lee e Y. Lee, «Quantitative Analysis of
8] Blended Asian Lacquers Using ToF–SIMS, Py–GC/MS and HPLC,» *Polymers*,
vol. 13, n. 97, 2021.
- [2 G. Sluder e D. Wolf, *Digital Microscopy*, 3rd Edition, Academic Press, 2007.
9]
- [3 J. Ye, «Supereyes,» 8 09 2016. [Online]. Available: [https://www.supereyes-
0\] store.com/blogs/news/differences-between-traditional-microscope-and-digital-
microscope](https://www.supereyes-store.com/blogs/news/differences-between-traditional-microscope-and-digital-microscope). [Consultato il giorno 20 11 2022].
- [3 F. Mokobi, «Microbe Notes,» 10 05 2022. [Online]. Available:
1] <https://microbenotes.com/digital-microscope/>. [Consultato il giorno 20 11 2022].
- [3 J. Lindon, G. Tranter e D. Koppenaal, *Encyclopedia of spectroscopy and
2] spectrometry*, 2nd Edition, Academic Press, 2010.
- [3 J. Schanda, *COLORIMETRY Understanding the CIE System*, Wiley, 2007.
3]
- [3 D. Malacara, *Color Vision and Colorimetry THEORY and APPLICATIONS*, 2nd
4] Edition, Society of Photo-Optical Instrumentation Engineers (SPIE), 2011.
- [3 Z. Schuessler, «Delta E 101,» [Online]. Available:
5] <http://zschuessler.github.io/DeltaE/learn/>. [Consultato il giorno 20 11 2022].
- [3 M. Mahy, L. Van Eycken e A. Oosterlinck, «Evaluation of Uniform Color Spaces
6] Developed after the Adoption of CIELAB and CIELUV,» Wiley, 1994.
- [3 J. M. Thompson, *Infrared Spectroscopy*, Pan Stanford Publishing Pte, 2018.
7]
- [3 M. R. Derrick, D. Stulik e J. M. Landry, *Infrared Spectroscopy in Conservation
8] Science*, J. Paul Getty Trust, 1999.
- [3 B. Stuart, *Infrared Spectroscopy; Fundamentals and Applications*, Wiley, 2004.
9]
- [4 B. C. Smith, *Fundamentals of FOURIER TRANSFORM INFRARED
0] SPECTROSCOPY*, CRC Press, 2011.
- [4 J. C. Frade, M. I. Ribeiro, J. Graça e J. Rodrigues, «Applying pyrolysis-gas
1] chromatography/mass spectrometry to the identification of oriental lacquers:
study of two lacquered shields,» *Analytical and Bioanalytical Chemistry*, vol. 395,
p. 2167–2174, 2009.

- [4 V. Pitthard, S. Stanek, M. Griesser e T. Muxeneder, «Gas Chromatography-Mass Spectrometry of binding media from early 20th century paint samples from Arnold Schönberg's palette,» *Chromatographia*, vol. 62, pp. 175-182, 2005.
- [4 J. Challinor, « Review: the development and applications of thermally assisted hydrolysis and methylation reactions.,» *Journal of Analytical and Applied Pyrolysis* , vol. 61, pp. 3-34, 2001.
- [4 C. Poole, *Gas Chromatography*, Elsevier, 2012.
4]
- [4 V. Warren, *Gas Chromatography Analysis, Methods and Practises*, Nova Science Publishers, 2017.
5]
- [4 O. D. Parkman, Z. E. Penton e F. G. Kitson, *Gas Chromatography and Mass Spectrometry: A Practical Guide*, 2nd Edition, Elsevier, 2011.
6]
- [4 E. de Hoffmann e V. Stroobant, *Mass Spectrometry Principles and Applications*, 7] 3rd Edition, Wiley, 2007.
- [4 R. L. Feller, «Aspects of Chemical Research in Conservation: The Deterioration Process,» *Journal of the American Institute for Conservation*, pp. 91-99, 1994.
8]
- [4 R. L. Feller, *Accelerated Aging Photochemical and Thermal Aspects*, The J. Paul Getty Trust, 1994.
9]
- [5 D. R. Bauer, M. C. Paputa Peck e R. O. Carter III, «Evaluation of accelerated weathering tests for a polyester-urethane coating using photoacoustic infrared spectroscopy,» *Journal Coatings Technology*, vol. 59, pp. 103-109, 1987.
0]
- [5 H. A. Nelson, *Symposium on Correlation Between Accelerated Laboratory Tests and Service Tests on Protective Coatings*, Philadelphia: American Society for Testing and Materials, 1993.
1]
- [5 J. C. José Carlos Frade, I. Ribeiro, J. Grac, T. Vasconcelos e J. Rodrigues, «Chemotaxonomic application of Py-GC/MS: Identification of lacquer trees,» *Journal of Analytical and Applied Pyrolysis*, vol. 89, pp. 117-121, 2010.
2]
- [5 J. Lee, S. Jung, T. Terlier, K. Lee e Y. Lee, «Molecular identification of Asian lacquers from different trees using Py-GC/MS and ToF-SIMS,» *Surface and Interface Analysis*, vol. 50, pp. 696-704, 2018.
3]
- [5 R. Lu, Y. Kamiya, Y.-Y. Wan, T. Honda e T. Miyakoshi, «Synthesis of Rhus succedanea lacquer film and analysis by pyrolysis-gas chromatography/mass spectrometry,» *Journal of Analytical and Applied Pyrolysis*, vol. 78, pp. 117-124, 2007.
4]
- [5 N. Niimura, «Determination of the type of lacquer on East Asian lacquer ware,» *International Journal of Mass Spectrometry*, vol. 284, pp. 93-97, 2009.
5]
- [5 D. Tamburini, I. Bonaduce e M. P. Colombini, «Characterisation of oriental lacquers from Rhus succedanea and Melanorrhoea usitata using in situ
6]

- pyrolysis/silylation-gas chromatography mass spectrometry,» *Journal of Analytical and Applied Pyrolysis*, vol. 116, pp. 129-141, 2015.
- [5 D. Tamburini, V. Kotonski, A. Lluveras-Tenorio, M. P. Colombini e A. Green, «The evolution of the materials used in the yun technique for the decoration of Burmese objects: lacquer, binding media and pigments,» *Heritage Science*, pp. 7-28, 2019.
- [5 R. Lu, S. Harigaya, T. Ishimura, K. Nagase e T. Miyakoshi, «Development of a fast drying lacquer based on raw lacquer sap,» *Progress in Organic Coatings*, vol. 51, p. 238–243, 2004.
- [5 L. K. Cairns e P. C. B. Forbes, «Insight into the yellowing of drying oils using fluorescence spectroscopy,» *Heritage Science*, 2020.
- [6 H. Szczepanowska e R. Ploeger, «The chemical analysis of Southeast Asian lacquers collected from forests and workshops in Vietnam, Cambodia, and Myanmar,» *Journal of Cultural Heritage*, 2009.
- [6 R. Lu e T. Yoshida, «Structure and molecular weight of Asian lacquer polysaccharides,» *Carbohydrate Polymers*, vol. 54, p. 419–424, 2003.
- [6 J. Lee, M. J. Kim, M.-H. Kim, J.-M. Doh, H.-G. Hahn e Y. Lee, «Characterization of traditional Korean lacquers using surface analytical techniques,» *Surface and interface analysis*, vol. 47, p. 1180–1186, 2015.
- [6 M. Sung, R. Lu e T. Miyakoshi, «Analysis and Characterization of Korean Lacquer,» *International Journal of Polymer Analysis and Characterization*, vol. 20, p. 150–159, 2015.
- [6 X. Hao, H. Wu, Y. Zhao, T. Tong, X. Li, C. Yang, Y. Tang, X. Shen e H. Tong, «Analysis on the Composition/structure and Lacquering Techniques of the Coffin of Emperor Qianlong Excavated from the Eastern Imperial Tombs,» *Scientific Reports*, vol. 7, 2017.
- [6 J. Lee, J.-M. Doh, H.-G. Hahn, K.-B. Lee e Y. Lee, «Investigation of Asian lacquer films using ToF-SIMS and complementary analytical techniques,» *Surface and interface analysis*, 2016.
- [6 J. Kumanotani, T. Ii e A. Hikosaka, «Studies on Japanese Lacquer: Film Formation via o-Quinone and Enzymic Oxidation of Urushiol Homologues Catalyzed by Laccase,» *Journal of Polymer Science*, vol. 23, pp. 519-531, 1968.
- [6 T. Kato e J. Kumanotani, «Studies of Japanese Lacquer: Urushiol Dimerization by the Coupling Reaction between Urushiol Quinone and a Triolefinic Component of Urushiol,» *Journal of Polymer Science*, vol. 7, pp. 1455-1465, 1969.

